



Instituto
Nacional
de Tecnología
Industrial

Final Report

Key Comparison SIM.EM.RF-K5b.CL
Scattering Coefficients by Broad-Band Methods
2 GHz - 18 GHz - Type N Connector

H. Silva and G. Monasterios
RF & Microwaves Metrology Laboratory
Instituto Nacional de Tecnología Industrial
Argentina

September 13, 2016

Contents

1	Introduction	3
1.1	Motivations	3
1.2	Measured Quantities	3
1.3	Relation with CCEM.RF-K5b.CL	3
2	Traveling standards	4
2.1	Description of the standards	4
2.2	Details of the traveling standards	4
2.3	Photograph of traveling standards	4
3	Participants and organization	5
3.1	Participants	5
3.2	Schedule	7
4	Discussion about organization of the comparison	8
5	Measurement methods	8
6	Standards behavior	9
7	Treatment of measurement data from participants	9
7.1	Evaluation of results	9
7.2	Linking to CCEM.RF-K5b.CL	12
8	Conclusions	14
	Bibliography	16
	Annex A: Results	17
A.1	3 dB Attenuator	17
A.2	20 dB Attenuator	26
A.3	Matched load	36
A.4	Mismatched load	46
	Annex B: Uncertainty budget	53
B.1	INTI Uncertainty Budgets	53
B.2	NIST Uncertainty Budgets	60
B.3	NRC Uncertainty Budgets	67
B.4	CENAM Uncertainty Budgets	70
B.5	NPLI Uncertainty Budgets	82
	Annex C: Participants reports	88
C.1	INTI Report	88
C.2	NIST Report	89
C.3	NRC Report	90

C.4 CENAM Report	91
C.5 NPLI Report	98
Annex D: Pin Depth measurements	99
Annex E: Electrical stability of standards	101

1 Introduction

1.1 Motivations

This RMO key comparison is based on the responsibility of the Inter-American Metrology System (SIM) through the CIPM Mutual Recognition Agreement (MRA), to ensure the measurement capabilities of the National Metrology Institutes (NMIs) in America.

Through this key comparison, SIM demonstrates NMIs achievements in high frequency measurements by linking their results to key values resulting from previous CCEM-organized comparison. This link is provided by laboratories that participated in both comparisons.

INTI has proposed and piloted this first RF SIM comparison, which consists in S-parameter measurements in the frequency range from 2 GHz to 18 GHz in an unbalanced coaxial 50Ω system with Type N connector.

1.2 Measured Quantities

Scattering parameters of Type N connector devices were measured from 2 GHz to 18 GHz (inclusive) in 1 GHz steps.

For one-port devices (matched and mismatched loads) the measurand was the complex-valued reflection coefficient S_{11} . The matched load (VSWR=1.0) and mismatched load (VSWR=2.0) were chosen to perform reflection measurements at low and high magnitude values respectively.

For two-port devices (3 dB and 20 dB attenuators) the measurands were the four complex-valued S-parameters (S_{11} , S_{21} , S_{12} and S_{22}). The values of 3 dB and 20 dB were chosen to cover transmission coefficients at high and low magnitude values respectively.

The Technical Protocol [5] established that participants had to report S-parameters in the form:

$$S_{ab} = x + jy \tag{1}$$

where x and y are the real and imaginary parts of the reported S-parameter, subindex a corresponds to reflected or transmitted wave port and subindex b corresponds to incident wave port. Both the real and imaginary parts are expressed in linear units, and $j = \sqrt{-1}$ is the imaginary unit.

The uncertainty of each measured S-parameter was reported in the form of combined standard uncertainty of the real part $u(x)$, imaginary part $u(y)$ and correlation coefficient between them $r(x, y)$ (see section 7.1 for further details). For two-port devices, the male port was referred as port number 1 for the purposes of this report.

1.3 Relation with CCEM.RF-K5b.CL

The results of this regional key comparison were linked to those corresponding to the CCEM Key Comparison [3] through laboratories acting as “linking” [1] [2]. This enabled SIM laboratories’ results to be linked to both CCEM comparison key values and the results of laboratories that participated in that comparison. The traveling standards were chosen based on those used in the

CCEM comparison making possible to link both of them. The linking method is detailed in section 7.2.

2 Traveling standards

2.1 Description of the standards

The selected standards are commercially available devices covering low and high reflection and transmission coefficients. These standards are similar to those used in the CCEM Key Comparison [3]. They cover the most important cases that arise in the measurement of S-parameters. They were bought to be used specially for this comparison.

2.2 Details of the traveling standards

The specifications of the standards are given below:

Description	Nominal Value	Model	Serial Number	Connector
Attenuator	3 dB	HP 8491B(opt.003)	MY39266530	Male/Female
Attenuator	20 dB	HP 8491B(opt.020)	MY39266597	Male/Female
Matched Load	50 Ω (VSWR=1.0)	HP 909F	55719	Male
Mismatched Load	VSWR=2.0	Maury 2562G	9006	Male

Table 1: *Traveling standards*

2.3 Photograph of traveling standards



Figure 1: *One-port devices*

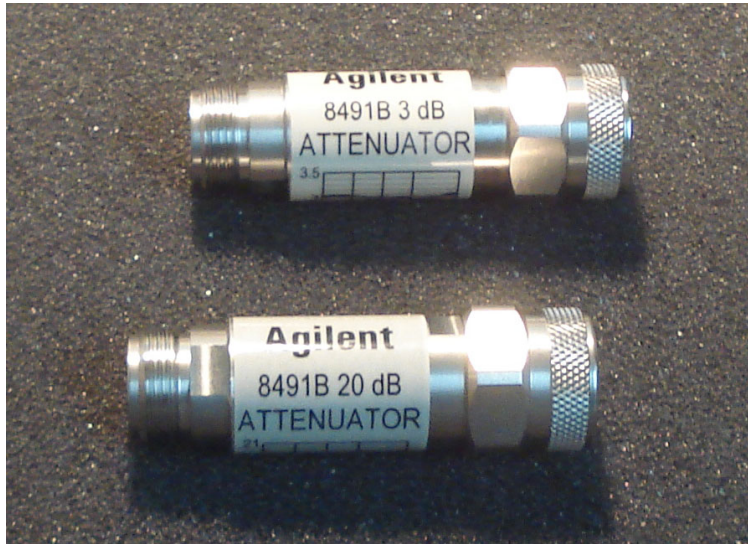


Figure 2: *Two-port devices*

3 Participants and organization

3.1 Participants

Hernando Silva / Guillermo Monasterios

Instituto Nacional de tecnología Industrial (**INTI**)

RF & Microwaves Laboratory

San Martín - Buenos Aires

ARGENTINA

Ronald Ginley

National Institute of Standards and Technology (**NIST**)

Radio Frequency Electronics Group (672.01)

Boulder - Colorado

UNITED STATES OF AMERICA

Alain Michaud

National Research Council (**NRC**)

Ottawa - Ontario

CANADA

Susana Padilla / Israel García

Centro Nacional de Metrología (**CENAM**)

Scattering Parameters Laboratory

El Marqués - Querétaro

MEXICO

Pramendra Singh Negi

National Physical Laboratory (**NPLI**)

LF & HF Voltage, Current and Microwave Standards

New Delhi

INDIA

Jin-seob Kang

Korea Research Institute of Standards and Science (**KRISS**)

Center for Electromagnetic Wave Division of Physical Metrology

Daejeon

SOUTH KOREA

3.2 Schedule

The original schedule proposed in September 2012 had to be modified for different reasons. Firstly, KRISS (Korea) and NPLI (India) asked the pilot laboratory if they could participate in this comparison. That request was submitted to SIM’s authorities, who allowed them to participate, so the total number of participants increased to six. Both KRISS and NPLI were scheduled to measure the comparison traveling standards at the end of the original participants list.

Secondly, CENAM had to postpone its participation for personal reasons, so they conducted their measurements after NIST and NRC instead of measuring the traveling standards before them. As a result, CENAM was the last NMI among SIM members to participate.

After SIM members made their measurements and because of long delays at this stage (see Section 4), the period allowed for the temporary exportation was coming to an end, so the pilot laboratory had to ask for the standards back to INTI (Argentina).

After a series of control measurements at the pilot laboratory, the traveling standards were sent to Asia. This is how the original concept of circulation for the standards like a “ring” became more like a “star”.

The following table depicts the resulting schedule, the dates on which each laboratory received and dispatched the traveling standards, and the date on which they sent the results to the pilot laboratory.

Laboratory	Arrival of standards	Dispatch of standards	Submitt of data
INTI (Argentina). 1st measurement	-	Nov. 2012	-
CENAM (Mexico)	Nov. 2012	Dec. 2012	(See 3.2)
NIST (USA)	Jan. 2013	Jun. 2013	Dec. 2013
NRC (Canada)	Jul. 2013	Nov. 2013	Aug. 2015
CENAM (Mexico)	Dec. 2013	Jan. 2014	May. 2014
INTI (Argentina) 1st control	Jan. 2014	Jun. 2014	-
NPLI (India)	Jul. 2014	Aug. 2014	Dec. 2014
KRISS (Korea)	Sep. 2014	Jan. 2015	-
INTI (Argentina) 2nd control	Feb. 2015	-	-

Table 2: *Participants’ measurement dates*

4 Discussion about organization of the comparison

In this section the pilot laboratory wants to remark some issues encountered during the process of managing this key comparison. It is written with the objective to make more dynamic the future comparisons that will take place within SIM.

After all the participants took their measurements, some of them did not send their data to the pilot to compute their results. After a request to meet a predefined deadline, the pilot did not have any other choice but to exclude KRISS from the comparison because they did not send their measurement results. This was agreed with SIM authorities, so an end was officially reached for the measurement stage. This caused a significant delay in the beginning of the redaction of the “Draft A Report”.

Regarding the pin-depth measurements, the necessity to get these values was to assure the mechanical stability of the standards after every shipment. This is why the pilot had to know these values when each laboratory received the traveling standards to avoid possible delays due to potentially damaged devices. Some participants sent this data together with the measurement results much later. Luckily the standards remained stable during all the comparison process.

Unlike other comparisons, there were no noticeable delays arising from customs issues in any country the traveling standards passed through.

5 Measurement methods

All participants performed their measurements with a VNA (Vector Network Analyzer) based system. In this key comparison, the 2-port devices were defined with the male port as port 1 and the female port as port 2. This was stated in the technical protocol [5].

Below are defined the methods each laboratory used to measure S-parameters. The complete report from each laboratory is included in Annex C.

Laboratory	Hardware	Calibration kit	Calibration method
INTI (Argentina)	VNA Rohde & Schwarz ZVK	Agilent 85054B/R&S ZV-Z21	SOLT (sliding)
NIST (USA)	VNA (model not specified)	5 air-lines	Multical LRL
NRC (Canada)	VNA Agilent PNA E8364C	HP 85054D + air-line	(not specified)
CENAM (Mexico)	VNA Agilent E8363C	HP 85054B	TRL ¹
NPLI (India)	VNA Wiltron 37247B	Anritsu 3653 + air-line	SOLT

Table 3: *Participants’ measurement methods*

¹CENAM performed its measurements with a VNA calibrated either with TRL and SOLT methods. CENAM has decided to include the TRL method results in this report.

6 Standards behavior

In order to check the mechanical stability of the traveling standards, participants were asked to provide pin-depth measurements of each device. In this manner, if a problem had arisen with any of the traveling standards during the shipping, the pilot laboratory could have found a solution or taken a decision about how to proceed.

Annex D shows pin-depth measurements of each participant. It does not show a significant variation of the inner conductor distance in relation to the reference plane (pin-depth). In addition, to help with the determination of a possible damage in the standards' inner conductor, the pilot assumed that each laboratory made visual inspection of each device before starting the measurements.

At the end of the comparison, the pilot laboratory did not find any damage to the connectors. Just a premature wearing of the threads of the male connectors was found after the first measurement loop took place. This does not have any influence in the electrical performance, but it demonstrates a degraded test port connector at one or more laboratory setups.

To ensure the electrical stability of the traveling standards, the pilot laboratory performed two control measurements after the first loop and at the end of the comparison (see table 2). The results of these measurements are summarized in Annex E. They show a good agreement taking into consideration the uncertainties of each measurement.

The differences in the uncertainties among different years are primary influenced by slight variations of the uncertainties pilot's budgets, and are not an indicator of a variation of the standards (e.g.: connector repeatability).

7 Treatment of measurement data from participants

7.1 Evaluation of results

The analysis of the results has been done for S_{11} (one-port devices) and S_{21} (two-port devices) at frequencies of 2 GHz, 9 GHz and 18 GHz. These measurands and frequencies were chosen to cover the low, medium and high frequency range in transmission and reflection measurements. In addition, this measurands match with those reported in [4], allowing the linking with CCEM Key Comparison.

As stated in section 1.2, each measured complex S-parameter should be reported in the form of a real part x plus its combined standard uncertainty $u(x)$, and an imaginary part y plus its combined standard uncertainty $u(y)$. If it is assumed that $u(x) = u(y)$, then only a single value of uncertainty needs to be given.

Additionally, the covariance $u(x, y)$ between the real and imaginary parts of S_{ab} should also be given (or, alternatively, the correlation coefficient $r(x, y)$). This value was assumed to be zero if it was not included in the laboratory report.

The uncertainties in the real and imaginary parts, $u(x)$ and $u(y)$, together with the covariance

coefficient $u(x, y)$, determine a 2×2 covariance matrix V_i associated to the complex-valued measurand [13]:

$$V_i = \begin{pmatrix} u^2(x) & u(x, y) \\ u(y, x) & u^2(y) \end{pmatrix} \quad (2)$$

or, in terms of the correlation coefficient:

$$V_i = \begin{pmatrix} u^2(x) & r(x, y)u(x)u(y) \\ r(y, x)u(x)u(y) & u^2(y) \end{pmatrix} \quad (3)$$

In the above matrices, $u(x, y) = u(y, x)$ and $r(x, y) = r(y, x)$, these matrices are symmetric. In order to evaluate and compare the data reported by laboratories taking part in this comparison exercise, the following quantities were calculated for each measurand in a similar way to [4], based on the guidelines in [1]:

7.1.1 Comparison reference value

The comparison reference value (CRV) is determined using an unweighted mean of the measurement results reported by the participants:

$$z_m = \frac{1}{N} \sum_{i=1}^N z_i \quad (4)$$

where z_m is the complex CRV, z_i is the complex value reported by laboratory i and N is the total number of participants in the comparison exercise.

Consistency test has not been applied in this comparison and all reported values contributed the same amount to the computation of the CRV.

The CRV uncertainties are determined by a 2×2 matrix covariance:

$$V_m = \begin{pmatrix} u^2(x_m) & u(x_m, y_m) \\ u(y_m, x_m) & u^2(y_m) \end{pmatrix} \quad (5)$$

where:

$$u^2(x_m) = \frac{1}{N(N-1)} \sum_{i=1}^N (x_i - x_m)^2 \quad (6)$$

$$u^2(y_m) = \frac{1}{N(N-1)} \sum_{i=1}^N (y_i - y_m)^2 \quad (7)$$

$$u(x_m, y_m) = \frac{1}{N(N-1)} \sum_{i=1}^N (x_i - x_m)(y_i - y_m) \quad (8)$$

In (6), (7) and (8), x_m and y_m are the real and imaginary parts of the CRV. x_i and y_i are the real and imaginary parts of the individual reported values.

7.1.2 Degrees of equivalence

7.1.2.1 With respect to the CRV

The degree of equivalence (DoE) d_i for laboratory i with respect to the CRV is given by:

$$d_i = z_i - z_m \quad (9)$$

The covariance matrix associated with this DoE for the unweighted mean CRV computation (as presented in section 7.1.1) is obtained by means of the expression in [10]:

$$V_{d_i} = V_m + \left(1 - \frac{2}{N}\right)V_i \quad (10)$$

where V_i is the covariance matrix (2) resulting from measurement uncertainties reported by the participants.

7.1.2.2 Bilateral DoE

The degree of equivalence d_{ij} between participants i and j , or bilateral DoE, is given by:

$$d_{ij} = z_i - z_j \quad (11)$$

where z_i and z_j are the measurement values reported by laboratories i and j , respectively. Assuming that z_i and z_j are uncorrelated, the covariance matrix of this bilateral DoE is simply obtained by:

$$V_{d_{ij}} = V_i + V_j \quad (12)$$

where V_i and V_j are the covariance matrices resulting from the measurement uncertainties reported by each laboratory.

7.1.2.3 Dimension reduction of DoE

The degrees of equivalence defined above are complex-valued magnitudes. Proper evaluation of the degrees of equivalence requires a reduction in the number of dimensions of these parameters. This is accomplished by means of the expressions detailed in [10]:

$$y = |d| \quad (13)$$

$$dy = |d| \sqrt{(d^T V_d^{-1} d)^{-1} k^2} \quad (14)$$

where d may be d_i for the degree of equivalence with respect to the CRV, or d_{ij} for the bilateral DoE.

The factor k is a suitable coverage factor chosen to give a 95% confidence level. Assuming that d follows a bivariate Gaussian distribution and the degrees of freedom are sufficient high [13], then $k = 2,45$.

In (14), dy is the distance from y to the confidence boundary through the origin of the coordinate system and is referred to as a confidence indicator.

7.2 Linking to CCEM.RF-K5b.CL

7.2.1 DoE respect to KCRV

The following methodology for linking the results of this SIM comparison with those from the CCEM.RF-K5b.CL was applied introducing a set of correction factors c_i :

$$c_i = d_{L_i,ccem} - d_{L_i,sim} \quad (15)$$

where:

- L_i refers to a laboratory i that participated in both CCEM and SIM comparisons, acting as a link between them.
- $d_{L_i,sim}$ is the degree of equivalence d_i (9) for the linking laboratory L_i .
- $d_{L_i,ccem}$ is the degree of equivalence respect to the KCRV for the linking laboratory L_i . This complex value is obtained from the data included in [4].

According to [11], the final correction factor between both comparisons c results from a weighted mean between the c_i factor of each linking laboratory. Additionally, its consistency has to be evaluated. Taking note that c_i are complex-valued magnitudes, the weighted mean c are obtained by means of the following expression [10]:

$$c = V_T^{-1} \sum_{i=1}^n V_{d_i}^{-1} c_i \quad (16)$$

Where V_{d_i} represents the 2×2 covariance matrix associated with the reproducibility (stability) of each linking laboratory and it is assumed to be the stated covariance matrix (2), n is the number of linking laboratories and V_T is obtained from the expression:

$$V_T = \sum_{i=1}^n V_{d_i}^{-1} \quad (17)$$

The covariance matrix V_c associated with c is:

$$V_c = V_T^{-1} \quad (18)$$

Consistency test over c is accomplished by means of the factor R_B^2 analog to the ‘‘Birge Ratio’’ [12, Appendix 2]:

$$R_B^2 = \frac{(Y - X.c)^T V^{-1} (Y - X.c)}{(2n - 2)} \quad (19)$$

where:

$$Y = \begin{bmatrix} c_1 \\ \vdots \\ c_n \end{bmatrix}_{2n \times 1} \quad X = \begin{bmatrix} I_1 \\ \vdots \\ I_n \end{bmatrix}_{2n \times 2} \quad V = \begin{bmatrix} V_{d_1} & \dots & 0 \\ \vdots & \ddots & \vdots \\ 0 & \dots & V_{d_n} \end{bmatrix}_{2n \times 2n}$$

$I_1 \dots I_n$ are 2×2 identity matrices. V is a matrix formed by V_{d_i} as sub-matrices in the diagonal and the off-diagonal components are all zero (i.e. is assumed the absent of any correlation among c_i of linking laboratories). Additionally V has to be a positive definite matrix.

Three laboratories participated in CCEM and SIM RMO key comparisons so there are three possible linking laboratories.

The weighted mean (16) was obtained taking into account only c_i of linking laboratories whose DoE respect to the KCRV (CCEM.RF-K5b.CL) and the CRV (SIM comparison) appear to be consistent. For this reason, to link the results of transmission coefficient of the 3 dB attenuator, only NIST and NPLI were used as linking laboratories. In the case of reflection coefficient of the matched load, only NRC and NIST data was used. Finally, to link the results of transmission coefficient of the 20 dB attenuator, all three linking laboratories might be used as links but only the data of SIM laboratories NRC and NIST was used.

If a bivariate normal distribution of c_i is assumed:

$$(2n-2)R_B^2 \sim \chi^2_{(2n-2)}$$

This property is used to test the consistency of weighted mean result by means of the hypothesis that “there is no significant difference between the observed variance and the variance deduced using the laboratories reproducibility estimates” [11].

If $(2n-2)R_B^2 > \chi^2_{(2n-2, 0,05)}$, then the hypothesis is rejected at 95 % of confidence level. If two linking laboratories are used, then $n = 2$ and $\chi^2_{(2, 0,05)} = 5,99$.

Finally, the condition not to reject the hypothesis is $R_B^2 < 2,995$.

This condition and the positive definite of V have been verified successfully in all measurands linked to the CCEM comparison: S_{21} of the 3 dB and 20 dB attenuator and S_{11} of the matched load at 2 GHz, 9 GHz and 18 GHz.

For a laboratory l_{sim} that participated only in this SIM comparison, its degree of equivalence $d_{l_{sim},KCRV}$ with respect to the KCRV from the CCEM comparison can be calculated as follows:

$$d_{l_{sim},KCRV} = d_{l_{sim}} + c \tag{20}$$

where $d_{l_{sim}}$ is the degree of equivalence of laboratory l_{sim} with respect to the CRV (9) from this SIM comparison.

The following expression represents the covariance matrix associated with $d_{l_{sim},KCRV}$:

$$V_{d_{l_{sim},KCRV}} = V_{l_{sim}} + V_{KCRV} + V_c \tag{21}$$

where:

- $V_{l_{sim}}$ is the laboratory l_{sim} covariance matrix (2).
- V_{KCRV} is the covariance matrix associated with the KCRV and is obtained from the data included in [4].

- V_c is the covariance matrix associated with c .

In addition, the expression (21) assumes the absence of any correlation between its terms as well as transfer uncertainties due to drift or instabilities associated to traveling devices.

The degrees of equivalence $d_{l_{sim},KCRV}$ also require a reduction in the number of dimensions. This is accomplished as explained in 7.1.2.3.

7.2.2 Bilateral DoE

Bilateral linking between laboratory l_{sim} , that only participated in SIM comparison, and laboratory k_{ccem} , that only participated in CCEM² comparison, was accomplished by the expression:

$$d_{l_{sim},k_{ccem}} = d_{l_{sim},KCRV} - d_{k,ccem} \quad (22)$$

where:

- $d_{l_{sim},KCRV}$ is the DoE with respect to KCRV of laboratory l_{sim} obtained in 7.2.1.
- $d_{k,ccem}$ is the DoE with respect to KCRV of laboratory k_{ccem} , obtained from the data included in [4].

The terms presented in (22) are correlated; for this reason it is necessary to take the correlation between its terms into account to find the covariance matrix associated with $d_{l_{sim},k_{ccem}}$. This is done by using the properties of covariance matrices detailed in [9]:

$$V_{d_{l_{sim},k_{ccem}}} = V_{d_{l_{sim},KCRV}} + V_{d_{k,ccem}} - 2 V_{KCRV} \quad (23)$$

where:

- $V_{d_{l_{sim},KCRV}}$ is taken from (21).
- $V_{d_{k,ccem}}$ is the covariance matrix associated with $d_{k,ccem}$ and is obtained from the data included in [4].
- V_{KCRV} is the covariance matrix associated with KCRV and is obtained from the data included in [4].

Finally, $d_{l_{sim},k_{ccem}}$ are reduced in the number of dimensions as explained in 7.1.2.3.

8 Conclusions

Degrees of equivalence with respect to reference values and bilateral DoE between participant laboratories have shown good consistency with the exceptions of NPLI in reflection measurements, and INTI for 3 dB attenuator S_{21} measurement at 18 GHz. Moreover, the linked DoE from SIM laboratories to key reference values from CCEM comparison, and the linked bilateral DoE from SIM laboratories with CCEM comparison participating laboratories, have also shown good consistency.

²Acronyms of CCEM participants have been kept as stated in the ‘‘CCEM Key Comparison Final Report’’ for ease of comparison.

A variety of VNA calibration methods have been applied by participants, allowing to test the performance of different type of S-parameter measurement systems based on vector network analyzers.

The purpose of this first SIM comparison in RF & microwave parameters was to show the ability of the region laboratories in this field. The authors encourage other SIM's laboratories to participate and pilot comparison exercises in high frequency parameters, which will enable them to test their methods and foster valuable exchange of information among colleagues.

References

- [1] Measurement comparisons in the context of the CIPM MRA. CIPM MRA-D-05, Version 1.5, March 2014.
- [2] CCEM guidelines for planning, organizing, conducting and reporting key, supplementary and pilot comparisons, 2007, 30 pp.
- [3] C.P.Eio; M.J.Maddock; N.M.Ridler; M.J.Salter, “CCEM.RF-K5b.CL Technical Protocol: Scattering Coefficients by Broad-Band Methods, 2-18 GHz - Type N Connector”, Version 1, August 2003.
- [4] C.P.Eio, “CCEM Key Comparison CCEM.RF-K5b.CL (GT-RF/92-3) Scattering Coefficients by Broad-Band Methods, 2-18 GHz - Type N Connector, Final Report of the Pilot Laboratory”, May 2010.
- [5] H.Silva, G. Monasterios “SIM.EM.RF-K5b.CL Technical Protocol: Scattering Coefficients by Broad-Band Methods 2-18 GHz - Type N Connector”, version 1, September 2012.
- [6] M.G.Cox, “The evaluation of key comparison data:An introduction”, Metrologia, 2002, 39, pp 587-588.
- [7] M.G.Cox, “The evaluation of key comparison data”, Metrologia, 2002, 39, pp 589-595.
- [8] K. Yhland, J. Stenarson, “A Simplified treatment of uncertainties in complex quantities”, CPEM 2004 Conference Digest, London, June 2004, pp 652-653.
- [9] M.Benjamin; H.Silva; G.Monasterios; N.Tempone, “Multivariate statistics applied to assess measurement uncertainty of complex reflection coefficient”, CPEM 2014 Conference Digest, R o de Janeiro, August 2014, pp 18-19.
- [10] M.Zeier, “On the analysis of multidimensional quantities in measurement comparison”, CPEM 2006 Conference Digest, Torino, July 2006, pp 458-459.
- [11] F.Delahaye; T.J.Witt, “Linking the results of 10 pF capacitance key comparisons CCEM-K4 and EUROMET 345”, BIPM key comparison database, CCEM-K4 Results.
- [12] R.Kacker; R.Datla; A.Parr, “Combined result and associated uncertainty from interlaboratory evaluations based on the ISO Guide”, Metrologia, 2002, 39, 279-293.
- [13] N.M.Riddler; M.J.Salter, “An approach to the treatment of uncertainty in complex S-parameter measurements”, Metrologia, 2002, 39, pp 295-302.
- [14] “EA Guidelines on the Evaluation of Vector Network Analysers (VNA)”. Euramet /cg-12/v 2.0, March 2011.

Annex A: Results

A.1 3 dB Attenuator

Lab i	Measurement and combined standard uncertainty S_{21} of 3 dB Attenuator at 2 GHz				
	$Re(S_{21})$	$u(Re(S_{21}))$ combined 1-sigma	$Im(S_{21})$	$u(Im(S_{21}))$ combined 1-sigma	$r(x, y)$
INTI	-0,64269	0,00029	-0,28534	0,00029	0,00
NIST	-0,64308	0,00191	-0,28578	0,00341	0,00
NRC	-0,64496	0,00250	-0,28618	0,00250	0,00
CENAM	-0,64255	0,00083	-0,28619	0,00145	-0,89
NPLI	-0,64459	0,00121	-0,28749	0,00121	0,07

Table 4

Reference Value (CRV) S_{21} of 3 dB Attenuator at 2 GHz				
$Re(x_i)$	$u(Re(x_i))$ combined 1-sigma	$Im(x_i)$	$u(Im(x_i))$ combined 1-sigma	$r(x,y)$
0,64357	0,00050	-0,28620	0,00036	0,63

Table 5

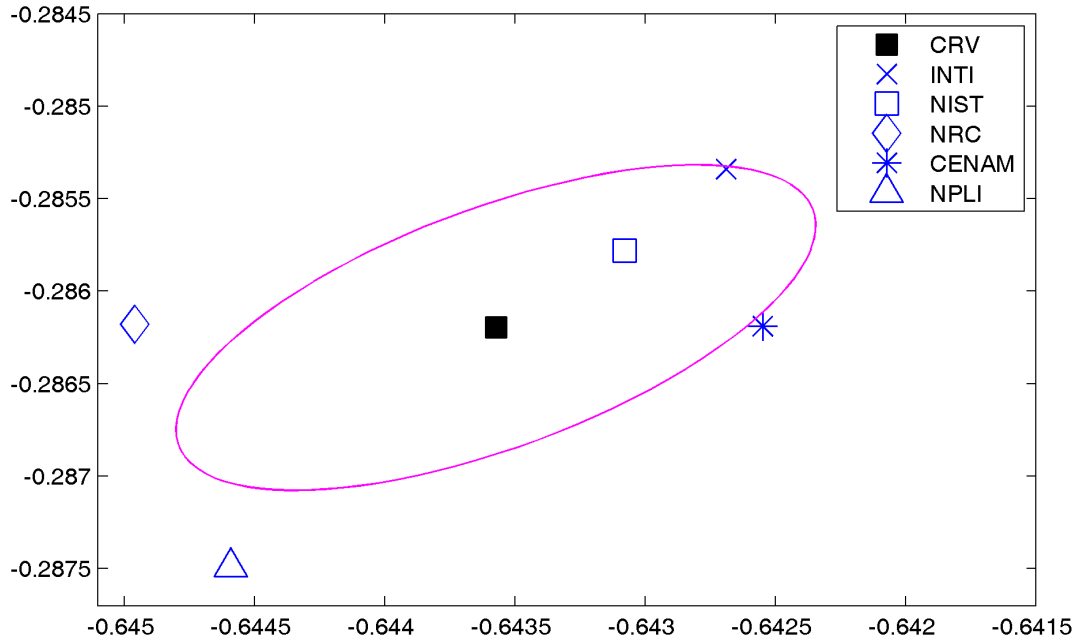


Figure 3: 3 dB Attenuator - Measurements of S_{21} along with CRV and its expanded uncertainty ($k = 2, 45$) at 2 GHz

	CRV		INTI		NIST	
	y	dy	y	dy	y	dy
INTI	0,0012	0,0014	-	-	0,0006	0,0060
NIST	0,0006	0,0045	0,0006	0,0060	-	-
NRC	0,0014	0,0049	0,0024	0,0062	0,0019	0,0078
CENAM	0,0010	0,0017	0,0009	0,0027	0,0007	0,0061
NPLI	0,0016	0,0027	0,0029	0,0032	0,0023	0,0069

Table 6: 3 dB Attenuator - DoE of S_{21} at 2 GHz

	NRC		CENAM		NPLI	
	y	dy	y	dy	y	dy
INTI	0,0024	0,0062	0,0009	0,0027	0,0029	0,0032
NIST	0,0019	0,0078	0,0007	0,0061	0,0023	0,0069
NRC	-	-	0,0024	0,0064	0,0014	0,0068
CENAM	0,0024	0,0064	-	-	0,0024	0,0032
NPLI	0,0014	0,0068	0,0024	0,0032	-	-

Table 7: 3 dB Attenuator - DoE of S_{21} at 2 GHz

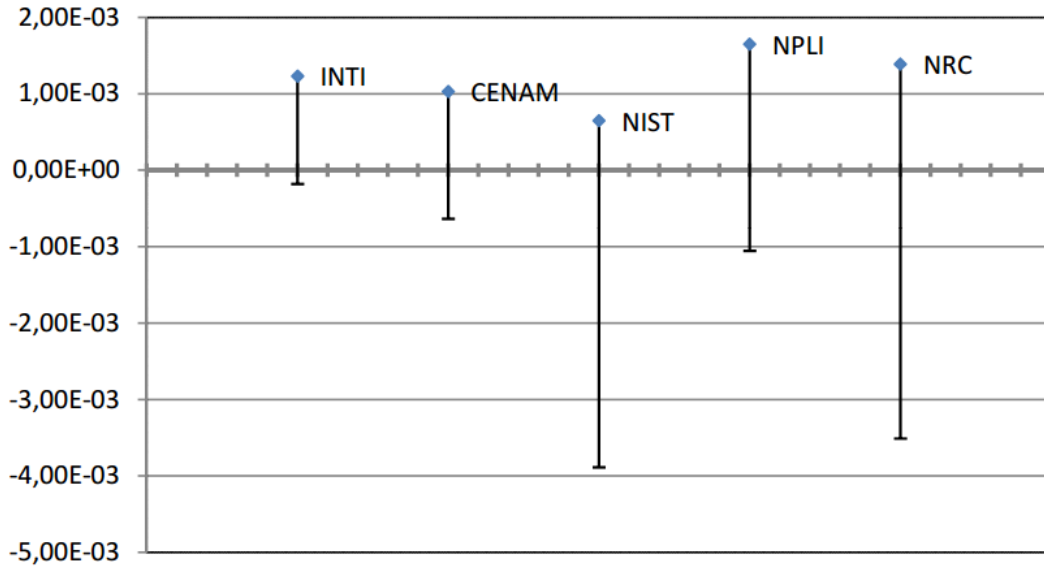


Figure 4: 3 dB Attenuator - DoE of S₂₁ respect to CRV at 2 GHz

	KCRV		NMIA		SPRING		SCL	
	y	dy	y	dy	y	dy	y	dy
INTI	0,0018	0,0032	0,0017	0,0034	0,0020	0,0048	0,0016	0,0173
CENAM	0,0012	0,0031	0,0010	0,0036	0,0012	0,0038	0,0010	0,0134

Table 8: 3 dB Attenuator - CCEM/SIM Linked DoE of S₂₁ at 2 GHz

	SNIIM		NIM		CSIR-NML		NMIJ	
	y	dy	y	dy	y	dy	y	dy
INTI	0,0033	0,0100	0,0045	0,0044	0,0021	0,0034	0,0021	0,0049
CENAM	0,0041	0,0106	0,0038	0,0049	0,0015	0,0034	0,0013	0,0055

Table 9: 3 dB Attenuator - CCEM/SIM Linked DoE of S₂₁ at 2 GHz

	SP		LNE		NPL	
	y	dy	y	dy	y	dy
INTI	0,0023	0,0051	0,0027	0,0031	0,0030	0,0029
CENAM	0,0015	0,0055	0,0019	0,0037	0,0021	0,0037

Table 10: 3 dB Attenuator - CCEM/SIM Linked DoE of S₂₁ at 2 GHz

Note: Since a step change in the 3 dB attenuator measurements was observed in the CCEM comparison, it had to be split into two different sub-comparisons, each one with its own KCRV [4, Section 5]. Given that linking laboratories belong to only one of these subsets, the 3 dB attenuator was linked to that particular subset.

Lab i	Measurement and combined standard uncertainty S_{21} of 3 dB Attenuator at 9 GHz				
	$Re(S_{21})$	$u(Re(S_{21}))$ combined 1-sigma	$Im(S_{21})$	$u(Im(S_{21}))$ combined 1-sigma	$r(x, y)$
INTI	0,70093	0,00076	0,14791	0,00076	0,00
NIST	0,69911	0,00404	0,15026	0,01137	0,00
NRC	0,70440	0,00250	0,14761	0,00250	0,00
CENAM	0,70330	0,00127	0,14710	0,00377	-0,33
NPLI	0,70035	0,00232	0,14899	0,00232	0,24

Table 11

Reference Value (CRV) S_{21} of 3 dB Attenuator at 9 GHz				
$Re(x_i)$	$u(Re(x_i))$ combined 1-sigma	$Im(x_i)$	$u(Im(x_i))$ combined 1-sigma	$r(x,y)$
0,70162	0,00097	0,14837	0,00056	-0,86

Table 12

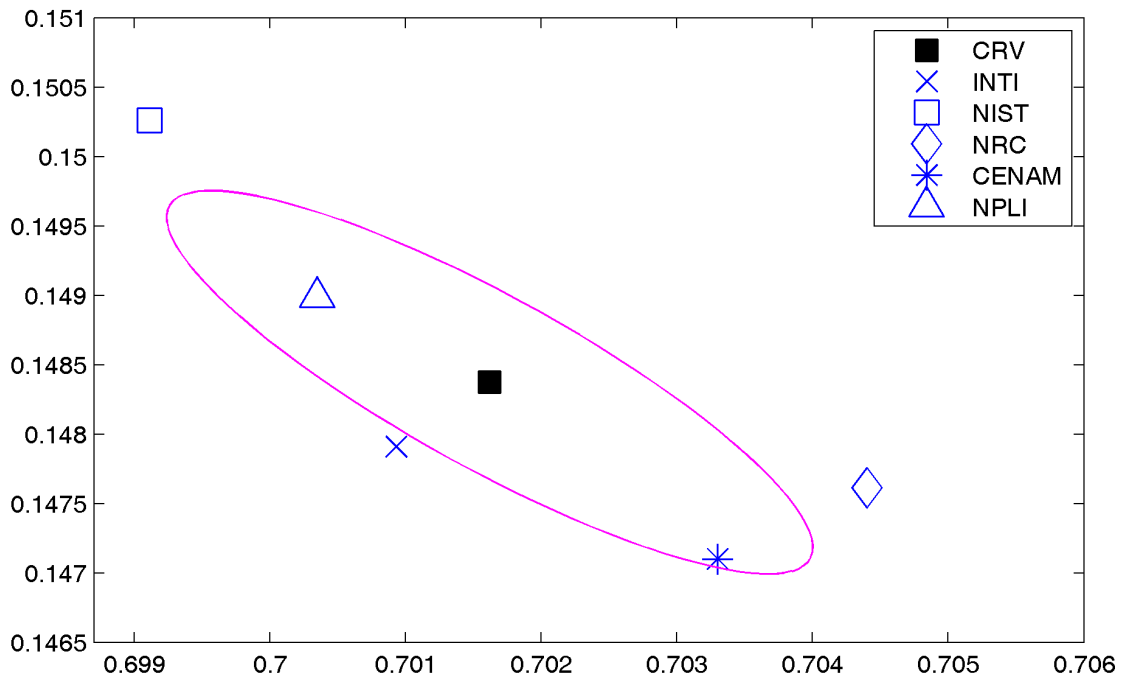


Figure 5: 3 dB Attenuator - Measurements of S_{21} along with CRV and its expanded uncertainty ($k = 2, 45$) at 9 GHz

	CRV		INTI		NIST	
	y	dy	y	dy	y	dy
INTI	0,0008	0,0017	-	-	0,0030	0,0149
NIST	0,0031	0,0097	0,0030	0,0149	-	-
NRC	0,0029	0,0054	0,0035	0,0064	0,0059	0,0128
CENAM	0,0021	0,0042	0,0025	0,0038	0,0052	0,0126
NPLI	0,0014	0,0048	0,0012	0,0054	0,0018	0,0150

Table 13: 3 dB Attenuator - DoE of S_{21} at 9 GHz

	NRC		CENAM		NPLI	
	y	dy	y	dy	y	dy
INTI	0,0035	0,0064	0,0025	0,0038	0,0012	0,0054
NIST	0,0059	0,0128	0,0052	0,0126	0,0018	0,0150
NRC	-	-	0,0012	0,0070	0,0043	0,0080
CENAM	0,0012	0,0070	-	-	0,0035	0,0072
NPLI	0,0043	0,0080	0,0035	0,0072	-	-

Table 14: 3 dB Attenuator - DoE of S_{21} at 9 GHz

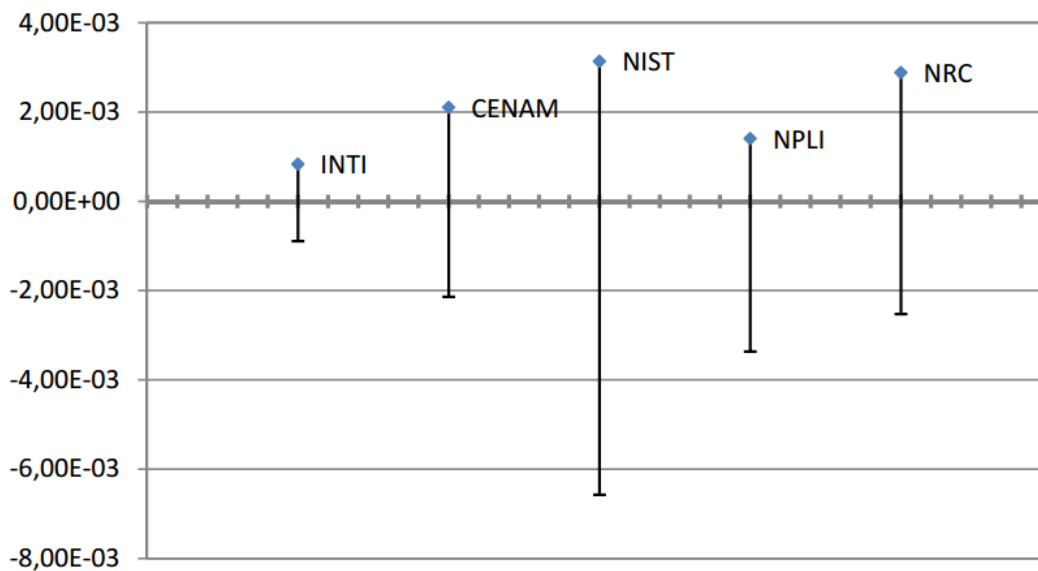


Figure 6: 3 dB Attenuator - DoE of S_{21} respect to CRV at 9 GHz

	KCRV		NMIA		SPRING		SCL	
	y	dy	y	dy	y	dy	y	dy
INTI	0,0035	0,0055	0,0051	0,0055	0,0049	0,0059	0,0053	0,0245
CENAM	0,0057	0,0072	0,0076	0,0071	0,0071	0,0066	0,0076	0,0230

Table 15: 3 dB Attenuator - CCEM/SIM Linked DoE of S_{21} at 9 GHz

	SNIIM		NIM		CSIR-NML		NMIJ	
	y	dy	y	dy	y	dy	y	dy
INTI	0,0012	0,0115	0,0065	0,0070	0,0040	0,0090	0,0048	0,0062
CENAM	0,0036	0,0118	0,0081	0,0102	0,0062	0,0107	0,0068	0,0086

Table 16: 3 dB Attenuator - CCEM/SIM Linked DoE of S_{21} at 9 GHz

	SP		LNE		NPL	
	y	dy	y	dy	y	dy
INTI	0,0057	0,0088	0,0050	0,0055	0,0076	0,0054
CENAM	0,0075	0,0113	0,0070	0,0080	0,0094	0,0084

Table 17: 3 dB Attenuator - CCEM/SIM Linked DoE of S_{21} at 9 GHz

Lab i	Measurement and combined standard uncertainty S_{21} of 3 dB Attenuator at 18 GHz				
	$Re(S_{21})$	$u(Re(S_{21}))$ combined 1-sigma	$Im(S_{21})$	$u(Im(S_{21}))$ combined 1-sigma	$r(x, y)$
INTI	0,67553	0,00125	-0,20365	0,00125	0,00
NIST	0,67825	0,00695	-0,19654	0,02156	0,00
NRC	0,67902	0,00250	-0,19898	0,00250	0,00
CENAM	0,68265	0,00349	-0,19027	0,00655	0,74
NPLI	0,68290	0,00352	-0,19898	0,00352	0,02

Table 18

Reference Value (CRV) S_{21} of 3 dB Attenuator at 18 GHz				
$Re(x_i)$	$u(Re(x_i))$ combined 1-sigma	$Im(x_i)$	$u(Im(x_i))$ combined 1-sigma	$r(x,y)$
0,67967	0,00139	-0,19768	0,00218	0,69

Table 19

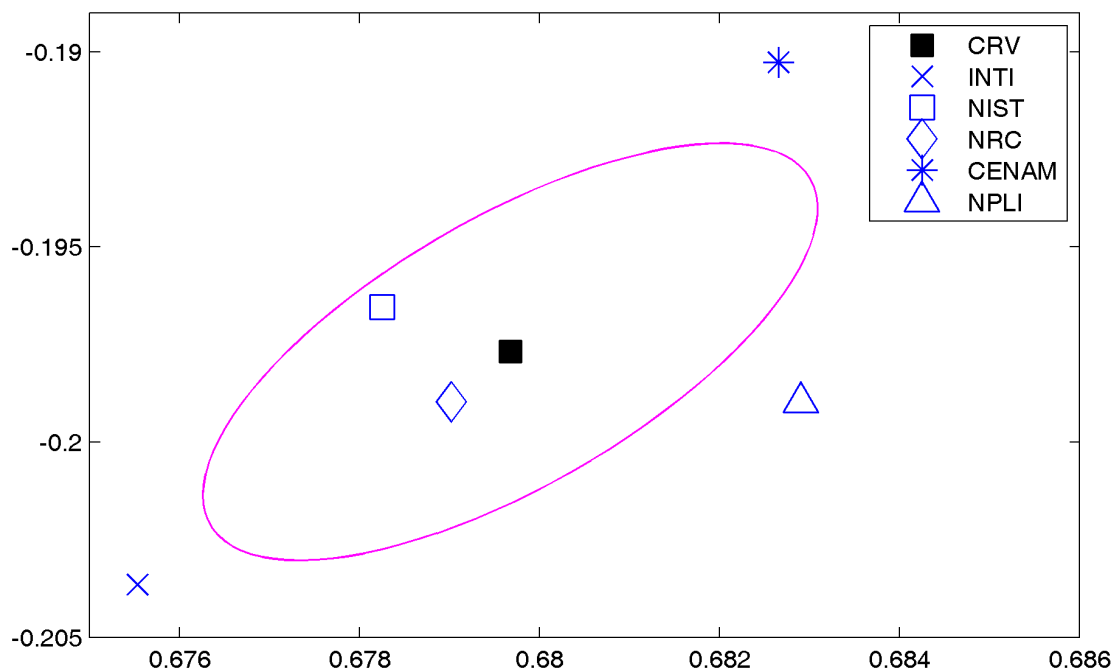


Figure 7: 3 dB Attenuator - Measurements of S_{21} along with CRV and its expanded uncertainty ($k = 2, 45$) at 18 GHz

	CRV		INTI		NIST	
	y	dy	y	dy	y	dy
INTI	0,0073	0,0063	-	-	0,0076	0,0368
NIST	0,0018	0,0168	0,0076	0,0368	-	-
NRC	0,0015	0,0076	0,0058	0,0068	0,0026	0,0410
CENAM	0,0080	0,0146	0,0152	0,0174	0,0077	0,0308
NPLI	0,0035	0,0070	0,0087	0,0092	0,0053	0,0212

Table 20: 3 dB Attenuator - DoE of S_{21} at 18 GHz

	NRC		CENAM		NPLI	
	y	dy	y	dy	y	dy
INTI	0,0058	0,0068	0,0152	0,0174	0,0087	0,0092
NIST	0,0026	0,0410	0,0077	0,0308	0,0053	0,0212
NRC	-	-	0,0094	0,0184	0,0039	0,0106
CENAM	0,0094	0,0184	-	-	0,0087	0,0158
NPLI	0,0039	0,0106	0,0087	0,0158	-	-

Table 21: 3 dB Attenuator - DoE of S_{21} at 18 GHz

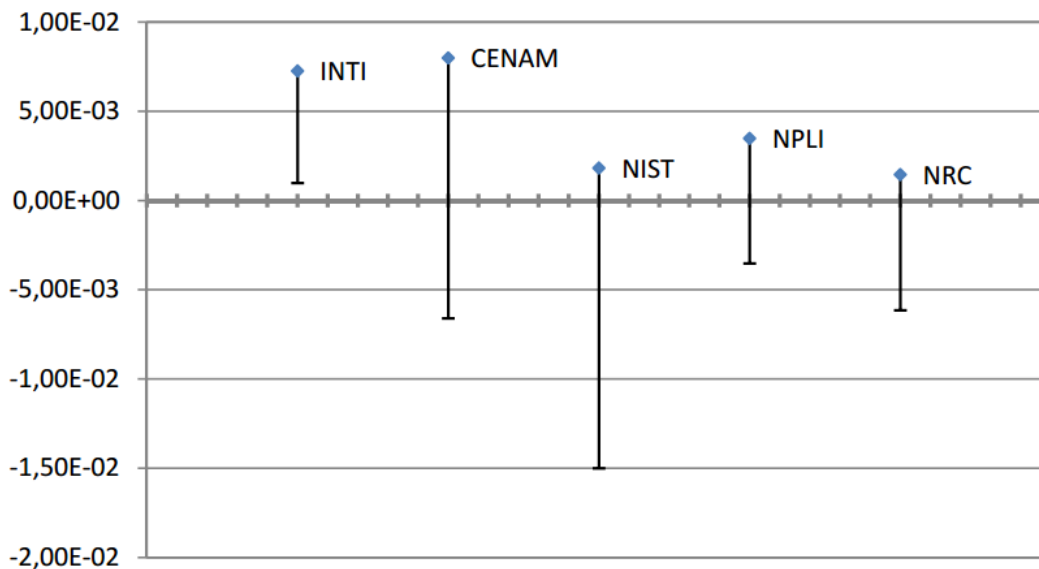


Figure 8: 3 dB Attenuator - DoE of S_{21} respect to CRV at 18 GHz

	KCRV		NMIA		SPRING		SCL	
	y	dy	y	dy	y	dy	y	dy
INTI	0,0093	0,0092	0,0129	0,0097	0,0181	0,0217	0,0138	0,0334
CENAM	0,0068	0,0175	0,0037	0,0117	0,0042	0,0256	0,0013	0,0325

Table 22: 3 dB Attenuator - CCEM/SIM Linked DoE of S_{21} at 18 GHz

	SNIIM		NIM		CSIR-NML		NMIJ	
	y	dy	y	dy	y	dy	y	dy
INTI	0,0088	0,0142	0,0132	0,0099	0,0091	0,0125	0,0106	0,0096
CENAM	0,0067	0,0207	0,0102	0,0124	0,0081	0,0187	0,0067	0,0150

Table 23: 3 dB Attenuator - CCEM/SIM Linked DoE of S_{21} at 18 GHz

	SP		LNE		NPL	
	y	dy	y	dy	y	dy
INTI	0,0108	0,0137	0,0091	0,0087	0,0116	0,0090
CENAM	0,0071	0,0181	0,0083	0,0153	0,0045	0,0150

Table 24: 3 dB Attenuator - CCEM/SIM Linked DoE of S_{21} at 18 GHz

A.2 20 dB Attenuator

Lab i	Measurement and combined standard uncertainty S_{21} of 20 dB Attenuator at 2 GHz				
	$Re(S_{21})$	$u(Re(S_{21}))$ combined 1-sigma	$Im(S_{21})$	$u(Im(S_{21}))$ combined 1-sigma	$r(x, y)$
INTI	-0,08619	0,00014	-0,05135	0,00014	0,00
NIST	-0,08639	0,00031	-0,05135	0,00046	0,00
NRC	-0,08700	0,00250	-0,05141	0,00250	0,00
CENAM	-0,08625	0,00013	-0,05133	0,00019	-0,96
NPLI	-0,08677	0,00037	-0,05159	0,00037	-0,14

Table 25

Reference Value (CRV) S_{21} of 20 dB Attenuator at 2 GHz				
$Re(x_i)$	$u(Re(x_i))$ combined 1-sigma	$Im(x_i)$	$u(Im(x_i))$ combined 1-sigma	$r(x,y)$
-0,08652	0,00016	-0,05141	0,00005	0,64

Table 26

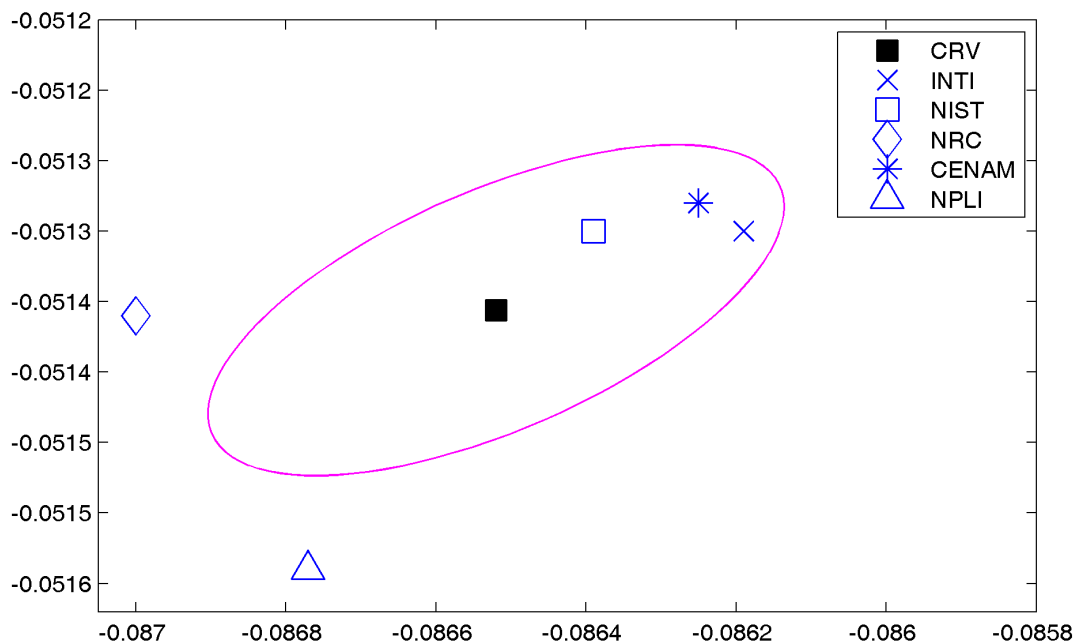


Figure 9: 20 dB Attenuator - Measurements of S_{21} along with CRV and its expanded uncertainty ($k = 2, 45$) at 2 GHz

	CRV		INTI		NIST	
	y	dy	y	dy	y	dy
INTI	0,0003	0,0005	-	-	0,0002	0,0008
NIST	0,0001	0,0007	0,0002	0,0008	-	-
NRC	0,0005	0,0048	0,0008	0,0061	0,0006	0,0062
CENAM	0,0003	0,0004	0,0001	0,0005	0,0001	0,0008
NPLI	0,0003	0,0007	0,0006	0,0009	0,0004	0,0012

Table 27: 20 dB Attenuator - DoE of S_{21} at 2 GHz

	NRC		CENAM		NPLI	
	y	dy	y	dy	y	dy
INTI	0,0008	0,0061	0,0001	0,0005	0,0006	0,0009
NIST	0,0006	0,0062	0,0001	0,0008	0,0004	0,0012
NRC	-	-	0,0008	0,0061	0,0003	0,0062
CENAM	0,0008	0,0061	-	-	0,0006	0,0009
NPLI	0,0003	0,0062	0,0006	0,0009	-	-

Table 28: 20 dB Attenuator - DoE of S_{21} at 2 GHz

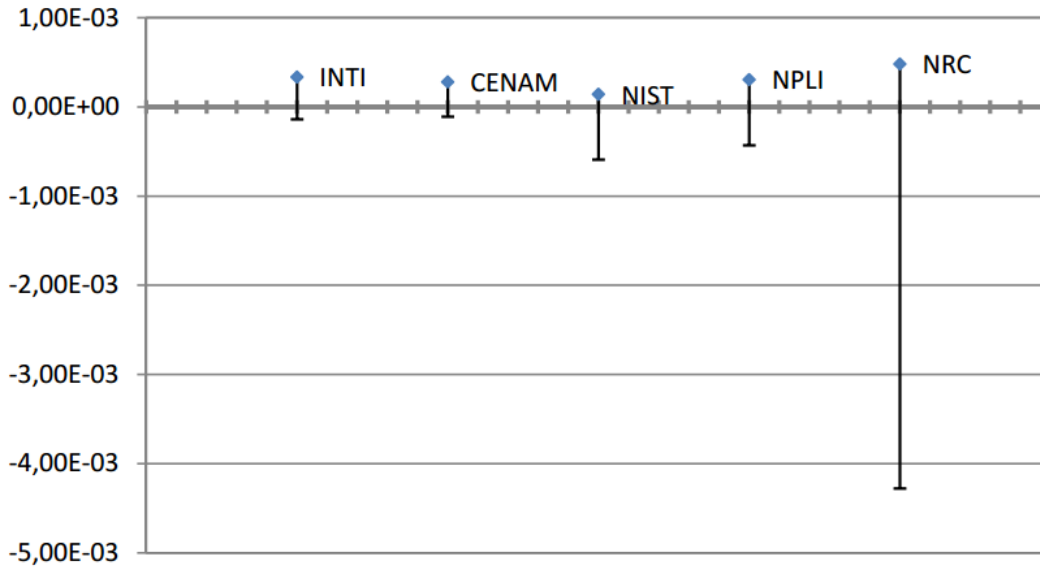


Figure 10: 20 dB Attenuator - DoE of S_{21} respect to CRV at 2 GHz

	KCRV		NPL		PTB		NMI-VSL	
	y	dy	y	dy	y	dy	y	dy
INTI	0,0002	0,0008	0,0002	0,0009	0,0001	0,0011	0,0002	0,0011
CENAM	0,0001	0,0008	0,0001	0,0009	0,0000	0,0014	0,0001	0,0011

Table 29: 20 dB Attenuator - CCEM/SIM Linked DoE of S_{21} at 2 GHz

	INRIM		METAS		CMI		UME	
	y	dy	y	dy	y	dy	y	dy
INTI	0,0002	0,0011	0,0001	0,0010	0,0002	0,0011	0,0003	0,0013
CENAM	0,0002	0,0012	0,0000	0,0011	0,0001	0,0011	0,0002	0,0013

Table 30: 20 dB Attenuator - CCEM/SIM Linked DoE of S_{21} at 2 GHz

	NMIA		SPRING		SCL		SNIIM	
	y	dy	y	dy	y	dy	y	dy
INTI	0,0001	0,0009	0,0002	0,0014	0,0002	0,0020	0,0005	0,0014
CENAM	0,0001	0,0011	0,0001	0,0014	0,0001	0,0021	0,0004	0,0015

Table 31: 20 dB Attenuator - CCEM/SIM Linked DoE of S_{21} at 2 GHz

	NIM		CSIR		NMIJ		SP	
	y	dy	y	dy	y	dy	y	dy
INTI	0,0003	0,0012	0,0003	0,0009	0,0002	0,0011	0,0001	0,0010
CENAM	0,0003	0,0012	0,0002	0,0009	0,0001	0,0012	0,0001	0,0010

Table 32: 20 dB Attenuator - CCEM/SIM Linked DoE of S_{21} at 2 GHz

	LNE	
	y	dy
INTI	0,0002	0,0011
CENAM	0,0001	0,0011

Table 33: 20 dB Attenuator - CCEM/SIM Linked DoE of S_{21} at 2 GHz

Lab i	Measurement and combined standard uncertainty S_{21} of 20 dB Attenuator at 9 GHz				
	$Re(S_{21})$	$u(Re(S_{21}))$ combined 1-sigma	$Im(S_{21})$	$u(Im(S_{21}))$ combined 1-sigma	$r(x, y)$
INTI	0,06970	0,00015	0,07181	0,00015	0,00
NIST	0,06965	0,00122	0,07165	0,00119	0,00
NRC	0,07135	0,00250	0,07177	0,00250	0,00
CENAM	0,07032	0,00036	0,07154	0,00036	-0,98
NPLI	0,07032	0,00098	0,07217	0,00098	-0,70

Table 34

Reference Value (CRV) S_{21} of 20 dB Attenuator at 9 GHz				
$Re(x_i)$	$u(Re(x_i))$ combined 1-sigma	$Im(x_i)$	$u(Im(x_i))$ combined 1-sigma	$r(x,y)$
0,07027	0,00031	0,07179	0,00011	0,10

Table 35

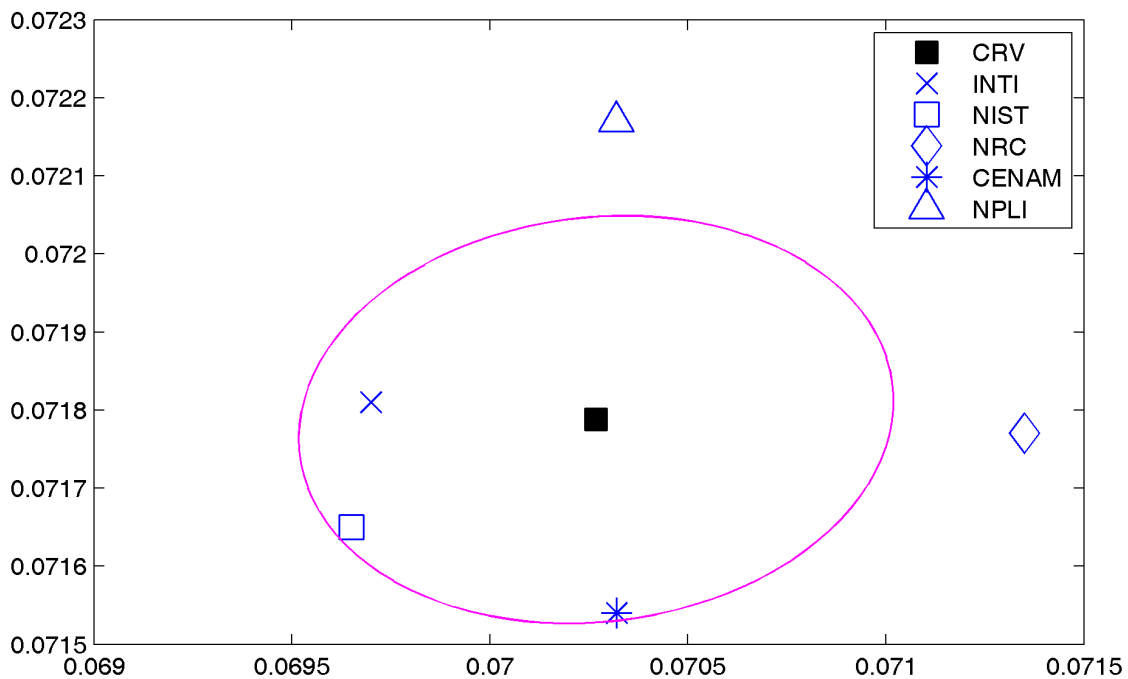


Figure 11: 20 dB Attenuator - Measurements of S_{21} along with CRV and its expanded uncertainty ($k = 2, 45$) at 9 GHz

	CRV		INTI		NIST	
	y	dy	y	dy	y	dy
INTI	0,0006	0,0008	-	-	0,0002	0,0029
NIST	0,0006	0,0024	0,0002	0,0029	-	-
NRC	0,0011	0,0048	0,0016	0,0061	0,0017	0,0068
CENAM	0,0002	0,0007	0,0007	0,0008	0,0007	0,0031
NPLI	0,0004	0,0013	0,0007	0,0014	0,0009	0,0032

Table 36: 20 dB Attenuator - DoE of S_{21} at 9 GHz

	NRC		CENAM		NPLI	
	y	dy	y	dy	y	dy
INTI	0,0016	0,0061	0,0007	0,0008	0,0007	0,0014
NIST	0,0017	0,0068	0,0007	0,0031	0,0009	0,0032
NRC	-	-	0,0011	0,0062	0,0011	0,0068
CENAM	0,0011	0,0062	-	-	0,0006	0,0017
NPLI	0,0011	0,0068	0,0006	0,0017	-	-

Table 37: 20 dB Attenuator - DoE of S_{21} at 9 GHz

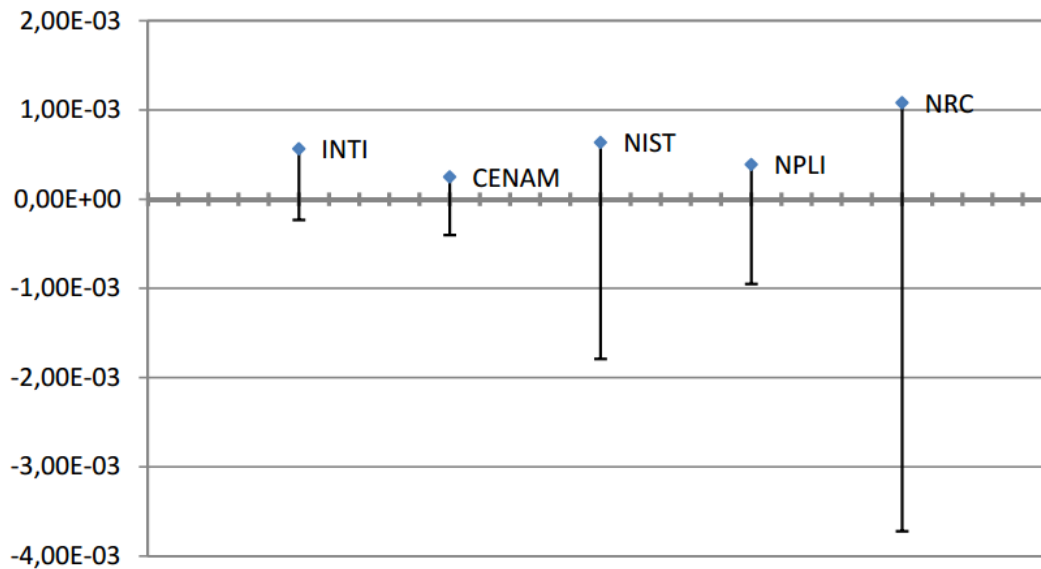


Figure 12: 20 dB Attenuator - DoE of S_{21} respect to CRV at 9 GHz

	KCRV		NPL		PTB		NMI-VSL	
	y	dy	y	dy	y	dy	y	dy
INTI	0,0005	0,0027	0,0005	0,0027	0,0004	0,0028	0,0004	0,0029
CENAM	0,0004	0,0027	0,0005	0,0027	0,0005	0,0028	0,0004	0,0028

Table 38: 20 dB Attenuator - CCEM/SIM Linked DoE of S_{21} at 9 GHz

	INRIM		METAS		CMI		UME	
	y	dy	y	dy	y	dy	y	dy
INTI	0,0009	0,0027	0,0005	0,0028	0,0004	0,0030	0,0006	0,0029
CENAM	0,0005	0,0027	0,0004	0,0029	0,0005	0,0030	0,0004	0,0028

Table 39: 20 dB Attenuator - CCEM/SIM Linked DoE of S_{21} at 9 GHz

	NMIA		SPRING		SCL		SNIIM	
	y	dy	y	dy	y	dy	y	dy
INTI	0,0005	0,0027	0,0002	0,0033	0,0007	0,0054	0,0001	0,0030
CENAM	0,0005	0,0028	0,0006	0,0035	0,0004	0,0054	0,0006	0,0032

Table 40: 20 dB Attenuator - CCEM/SIM Linked DoE of S_{21} at 9 GHz

	NIM		CSIR		NMIJ		SP	
	y	dy	y	dy	y	dy	y	dy
INTI	0,0002	0,0027	0,0006	0,0029	0,0006	0,0027	0,0004	0,0029
CENAM	0,0005	0,0029	0,0003	0,0029	0,0004	0,0027	0,0004	0,0029

Table 41: 20 dB Attenuator - CCEM/SIM Linked DoE of S_{21} at 9 GHz

	LNE	
	y	dy
INTI	0,0011	0,0030
CENAM	0,0010	0,0030

Table 42: 20 dB Attenuator - CCEM/SIM Linked DoE of S_{21} at 9 GHz

Lab i	Measurement and combined standard uncertainty S_{21} of 20 dB Attenuator at 18 GHz				
	$Re(S_{21})$	$u(Re(S_{21}))$ combined 1-sigma	$Im(S_{21})$	$u(Im(S_{21}))$ combined 1-sigma	$r(x, y)$
INTI	0,03707	0,00017	0,09130	0,00017	0,00
NIST	0,03670	0,00290	0,09125	0,00125	0,00
NRC	0,03688	0,00250	0,09148	0,00250	0,00
CENAM	0,03568	0,00085	0,09211	0,00041	-0,95
NPLI	0,03719	0,00377	0,09308	0,00377	-0,53

Table 43

Reference Value (CRV) S_{21} of 20 dB Attenuator at 18 GHz				
$Re(x_i)$	$u(Re(x_i))$ combined 1-sigma	$Im(x_i)$	$u(Im(x_i))$ combined 1-sigma	$r(x,y)$
0,03671	0,00027	0,09185	0,00034	0,04

Table 44

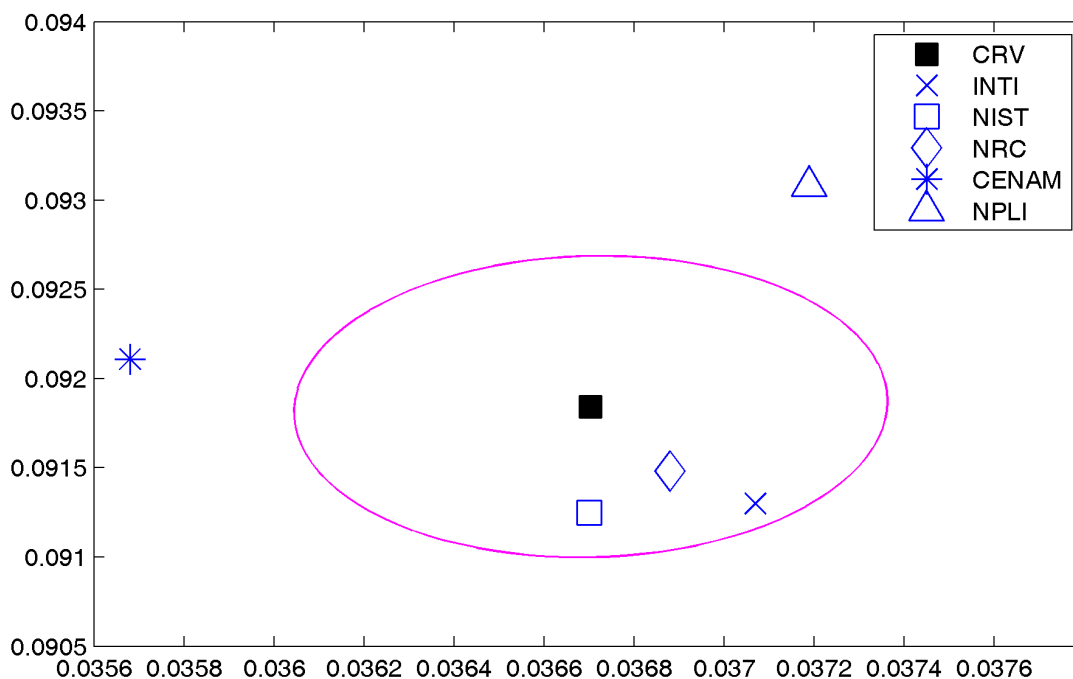


Figure 13: 20 dB Attenuator - Measurements of S_{21} along with CRV and its expanded uncertainty ($k = 2, 45$) at 18 GHz

	CRV		INTI		NIST	
	y	dy	y	dy	y	dy
INTI	0,0007	0,0008	-	-	0,0004	0,0068
NIST	0,0006	0,0025	0,0004	0,0068	-	-
NRC	0,0004	0,0048	0,0003	0,0061	0,0003	0,0076
CENAM	0,0011	0,0017	0,0016	0,0022	0,0013	0,0046
NPLI	0,0013	0,0053	0,0018	0,0076	0,0019	0,0083

Table 45: 20 dB Attenuator - DoE of S_{21} at 18 GHz

	NRC		CENAM		NPLI	
	y	dy	y	dy	y	dy
INTI	0,0003	0,0061	0,0016	0,0022	0,0018	0,0076
NIST	0,0003	0,0076	0,0013	0,0046	0,0019	0,0083
NRC	-	-	0,0014	0,0065	0,0016	0,0097
CENAM	0,0014	0,0065	-	-	0,0018	0,0065
NPLI	0,0016	0,0097	0,0018	0,0065	-	-

Table 46: 20 dB Attenuator - DoE of S_{21} at 18 GHz

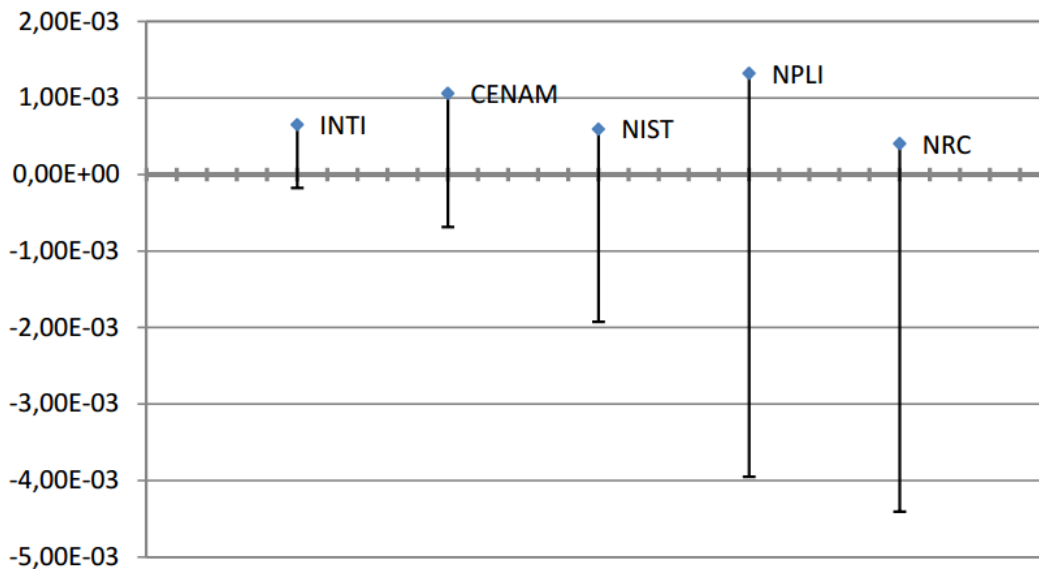


Figure 14: 20 dB Attenuator - DoE of S_{21} respect to CRV at 18 GHz

	KCRV		NPL		PTB		NMI-VSL	
	y	dy	y	dy	y	dy	y	dy
INTI	0,0004	0,0042	0,0004	0,0046	0,0005	0,0044	0,0004	0,0044
CENAM	0,0021	0,0045	0,0019	0,0047	0,0021	0,0047	0,0020	0,0047

Table 47: 20 dB Attenuator - CCEM/SIM Linked DoE of S_{21} at 18 GHz

	INRIM		METAS		CMI		UME	
	y	dy	y	dy	y	dy	y	dy
INTI	0,0013	0,0042	0,0004	0,0045	0,0001	0,0056	0,0009	0,0053
CENAM	0,0029	0,0046	0,0020	0,0047	0,0017	0,0052	0,0025	0,0057

Table 48: 20 dB Attenuator - CCEM/SIM Linked DoE of S_{21} at 18 GHz

	NMIA		SPRING		SCL		SNIIM	
	y	dy	y	dy	y	dy	y	dy
INTI	0,0004	0,0035	0,0004	0,0052	0,0012	0,0097	0,0007	0,0040
CENAM	0,0020	0,0043	0,0014	0,0052	0,0028	0,0087	0,0009	0,0049

Table 49: 20 dB Attenuator - CCEM/SIM Linked DoE of S_{21} at 18 GHz

	NIM		CSIR		NMIJ		SP	
	y	dy	y	dy	y	dy	y	dy
INTI	0,0011	0,0045	0,0014	0,0046	0,0004	0,0041	0,0003	0,0039
CENAM	0,0025	0,0051	0,0030	0,0049	0,0020	0,0045	0,0019	0,0047

Table 50: 20 dB Attenuator - CCEM/SIM Linked DoE of S_{21} at 18 GHz

	LNE	
	y	dy
INTI	0,0007	0,0032
CENAM	0,0023	0,0042

Table 51: 20 dB Attenuator - CCEM/SIM Linked DoE of S_{21} at 18 GHz

A.3 Matched load

Lab i	Measurement and combined standard uncertainty S_{11} of Matched load at 2 GHz				
	$Re(S_{11})$	$u(Re(S_{11}))$ combined 1-sigma	$Im(S_{11})$	$u(Im(S_{11}))$ combined 1-sigma	$r(x, y)$
INTI	-0,00037	0,00248	-0,00088	0,00248	0,00
NIST	-0,00067	0,00234	-0,00134	0,00333	0,00
NRC	0,00051	0,00520	-0,00098	0,00520	0,00
CENAM	0,00119	0,00091	-0,00106	0,00133	0,05
NPLI	0,00278	0,00333	-0,00543	0,00333	0,85

Table 52

Reference Value (CRV) S_{11} of Matched load at 2 GHz				
$Re(x_i)$	$u(Re(x_i))$ combined 1-sigma	$Im(x_i)$	$u(Im(x_i))$ combined 1-sigma	$r(x,y)$
0,00069	0,00062	-0,00194	0,00088	-0,83

Table 53

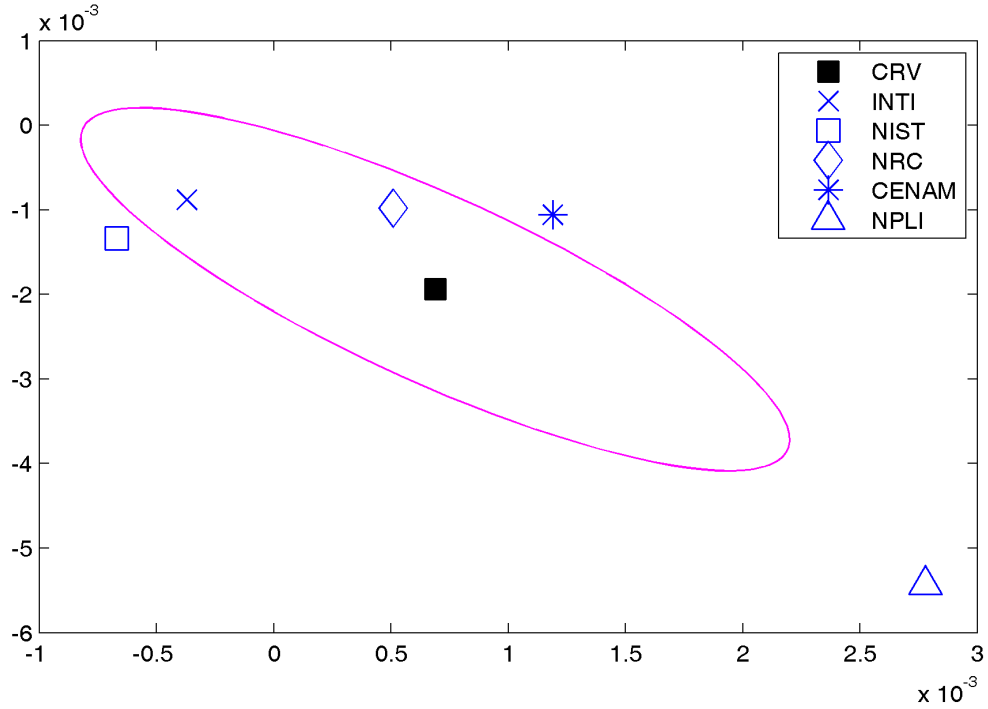


Figure 15: Matched load - Measurements of S_{11} along with CRV and its expanded uncertainty ($k = 2, 45$) at 2 GHz

	CRV		INTI		NIST	
	y	dy	y	dy	y	dy
INTI	0,0015	0,0053	-	-	0,0006	0,0095
NIST	0,0015	0,0050	0,0006	0,0095	-	-
NRC	0,0010	0,0101	0,0009	0,0141	0,0012	0,0141
CENAM	0,0010	0,0024	0,0016	0,0065	0,0019	0,0062
NPLI	0,0041	0,0036	0,0055	0,0069	0,0053	0,0077

Table 54: Matched load - DoE of S_{11} at 2 GHz

	NRC		CENAM		NPLI	
	y	dy	y	dy	y	dy
INTI	0,0009	0,0141	0,0016	0,0065	0,0055	0,0069
NIST	0,0012	0,0141	0,0019	0,0062	0,0053	0,0077
NRC	-	-	0,0007	0,0129	0,0050	0,0134
CENAM	0,0007	0,0129	-	-	0,0046	0,0046
NPLI	0,0050	0,0134	0,0046	0,0046	-	-

Table 55: Matched load - DoE of S_{11} at 2 GHz

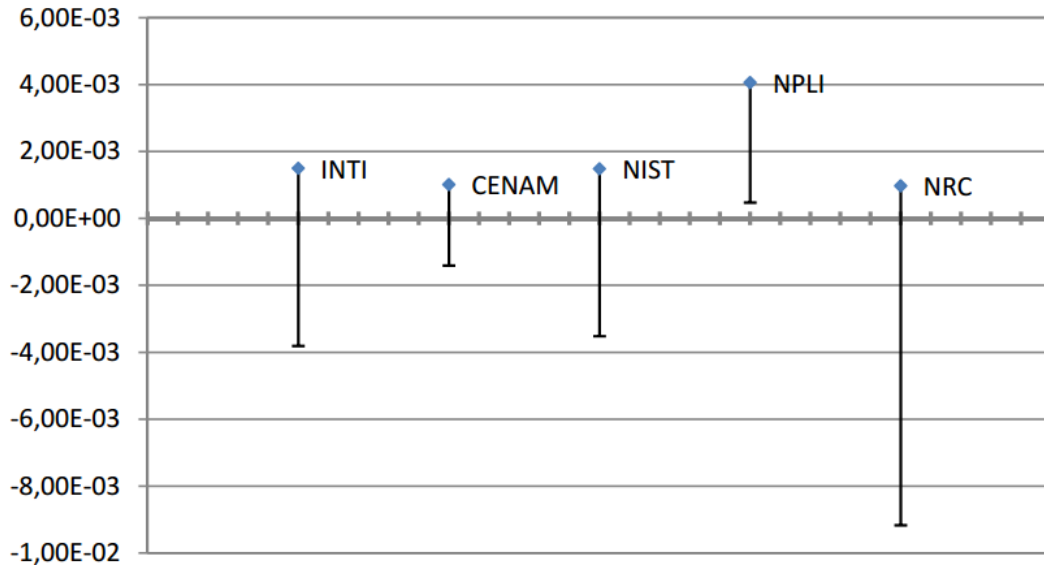


Figure 16: Matched load - DoE of S₁₁ respect to CRV at 2 GHz

	KCRV		NPL		PTB		NMI-VSL	
	y	dy	y	dy	y	dy	y	dy
INTI	0,0006	0,0080	0,0010	0,0084	0,0009	0,0089	0,0025	0,0104
CENAM	0,0009	0,0057	0,0006	0,0063	0,0023	0,0065	0,0026	0,0117

Table 56: Matched load - CCEM/SIM Linked DoE of S₁₁ at 2 GHz

	INRIM		METAS		CMI		UME	
	y	dy	y	dy	y	dy	y	dy
INTI	0,0028	0,0153	0,0011	0,0093	0,0004	0,0141	0,0018	0,0159
CENAM	0,0019	0,0147	0,0005	0,0075	0,0013	0,0126	0,0014	0,0151

Table 57: Matched load - CCEM/SIM Linked DoE of S₁₁ at 2 GHz

	NMIA		SPRING		SCL		SNIIM	
	y	dy	y	dy	y	dy	y	dy
INTI	0,0009	0,0095	0,0018	0,0164	0,0010	0,0122	0,0021	0,0094
CENAM	0,0013	0,0068	0,0014	0,0121	0,0018	0,0103	0,0017	0,0085

Table 58: Matched load - CCEM/SIM Linked DoE of S₁₁ at 2 GHz

	NIM		CSIR		NMIJ		SP	
	y	dy	y	dy	y	dy	y	dy
INTI	0,0005	0,0082	0,0006	0,0100	0,0005	0,0086	0,0007	0,0103
CENAM	0,0011	0,0060	0,0011	0,0082	0,0012	0,0064	0,0015	0,0079

Table 59: Matched load - CCEM/SIM Linked DoE of S_{11} at 2 GHz

	LNE	
	y	dy
INTI	0,0004	0,0132
CENAM	0,0019	0,0114

Table 60: Matched load - CCEM/SIM Linked DoE of S_{11} at 2 GHz

Lab i	Measurement and combined standard uncertainty S_{11} of Matched load at 9 GHz				
	$Re(S_{11})$	$u(Re(S_{11}))$ combined 1-sigma	$Im(S_{11})$	$u(Im(S_{11}))$ combined 1-sigma	$r(x, y)$
INTI	-0,00403	0,00284	0,01550	0,00284	0,00
NIST	-0,00264	0,00349	0,01770	0,00438	0,00
NRC	-0,00119	0,00600	0,02339	0,00600	0,00
CENAM	-0,00404	0,00222	0,01643	0,00151	-0,74
NPLI	-0,01441	0,00551	0,02265	0,00551	-0,51

Table 61

Reference Value (CRV) S_{11} of Matched load at 9 GHz				
$Re(x_i)$	$u(Re(x_i))$ combined 1-sigma	$Im(x_i)$	$u(Im(x_i))$ combined 1-sigma	$r(x,y)$
-0,00526	0,00235	0,01913	0,00163	-0,35

Table 62

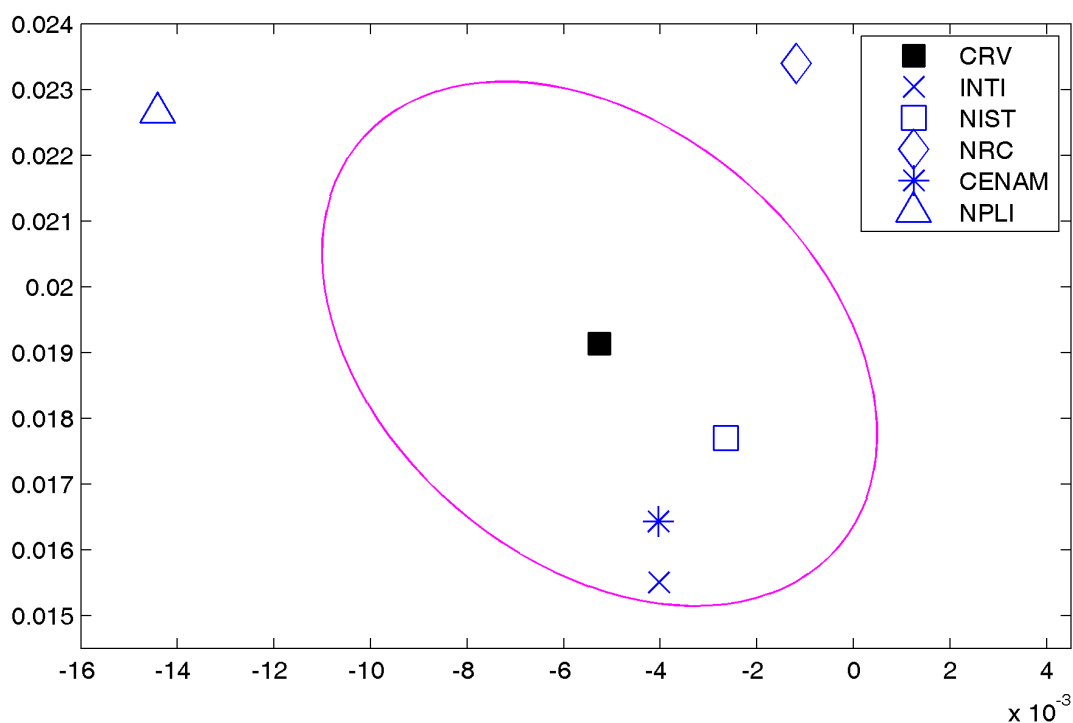


Figure 17: Matched load - Measurements of S_{11} along with CRV and its expanded uncertainty ($k = 2, 45$) at 9 GHz

	CRV		INTI		NIST	
	y	dy	y	dy	y	dy
INTI	0,0038	0,0070	-	-	0,0026	0,0122
NIST	0,0030	0,0092	0,0026	0,0122	-	-
NRC	0,0059	0,0121	0,0084	0,0163	0,0059	0,0181
CENAM	0,0030	0,0053	0,0009	0,0077	0,0019	0,0099
NPLI	0,0098	0,0127	0,0126	0,0176	0,0128	0,0173

Table 63: Matched load - DoE of S_{11} at 9 GHz

	NRC		CENAM		NPLI	
	y	dy	y	dy	y	dy
INTI	0,0084	0,0163	0,0009	0,0077	0,0126	0,0176
NIST	0,0059	0,0181	0,0019	0,0099	0,0128	0,0173
NRC	-	-	0,0075	0,0149	0,0132	0,0192
CENAM	0,0075	0,0149	-	-	0,0121	0,0169
NPLI	0,0132	0,0192	0,0121	0,0169	-	-

Table 64: Matched load - DoE of S_{11} at 9 GHz

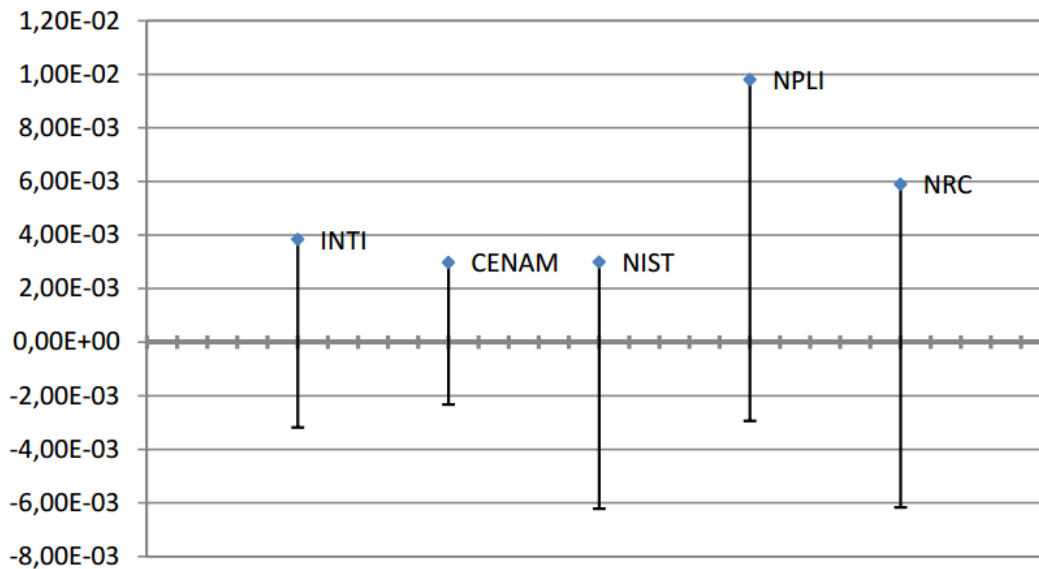


Figure 18: Matched load - DoE of S_{11} respect to CRV at 9 GHz

	KCRV		NPL		PTB		NMI-VSL	
	y	dy	y	dy	y	dy	y	dy
INTI	0,0042	0,0111	0,0032	0,0113	0,0068	0,0115	0,0046	0,0224
CENAM	0,0034	0,0089	0,0023	0,0090	0,0059	0,0096	0,0037	0,0217

Table 65: Matched load - CCEM/SIM Linked DoE of S_{11} at 9 GHz

	INRIM		METAS		CMI		UME	
	y	dy	y	dy	y	dy	y	dy
INTI	0,0055	0,0166	0,0057	0,0142	0,0058	0,0159	0,0048	0,0200
CENAM	0,0047	0,0159	0,0048	0,0135	0,0049	0,0152	0,0040	0,0199

Table 66: Matched load - CCEM/SIM Linked DoE of S_{11} at 9 GHz

	NMIA		SPRING		SCL		SNIIM	
	y	dy	y	dy	y	dy	y	dy
INTI	0,0053	0,0121	0,0037	0,0187	0,0043	0,0268	0,0051	0,0112
CENAM	0,0044	0,0109	0,0028	0,0179	0,0035	0,0265	0,0047	0,0096

Table 67: Matched load - CCEM/SIM Linked DoE of S_{11} at 9 GHz

	NIM		CSIR		NMIJ		SP	
	y	dy	y	dy	y	dy	y	dy
INTI	0,0061	0,0110	0,0037	0,0125	0,0044	0,0106	0,0047	0,0126
CENAM	0,0059	0,0098	0,0028	0,0111	0,0042	0,0094	0,0046	0,0118

Table 68: Matched load - CCEM/SIM Linked DoE of S_{11} at 9 GHz

	LNE	
	y	dy
INTI	0,0032	0,0155
CENAM	0,0027	0,0142

Table 69: Matched load - CCEM/SIM Linked DoE of S_{11} at 9 GHz

Lab i	Measurement and combined standard uncertainty S_{11} of Matched load at 18 GHz				
	$Re(S_{11})$	$u(Re(S_{11}))$ combined 1-sigma	$Im(S_{11})$	$u(Im(S_{11}))$ combined 1-sigma	$r(x, y)$
INTI	0,02690	0,00341	0,05679	0,00341	0,00
NIST	0,02616	0,00473	0,05333	0,00685	0,00
NRC	0,03261	0,00800	0,06458	0,00800	0,00
CENAM	0,02836	0,00263	0,05670	0,00174	0,31
NPLI	0,01336	0,00601	0,06596	0,00601	0,76

Table 70

Reference Value (CRV) S_{11} of Matched load at 18 GHz				
$Re(x_i)$	$u(Re(x_i))$ combined 1-sigma	$Im(x_i)$	$u(Im(x_i))$ combined 1-sigma	$r(x,y)$
0,02548	0,00323	0,05947	0,00246	-0,37

Table 71

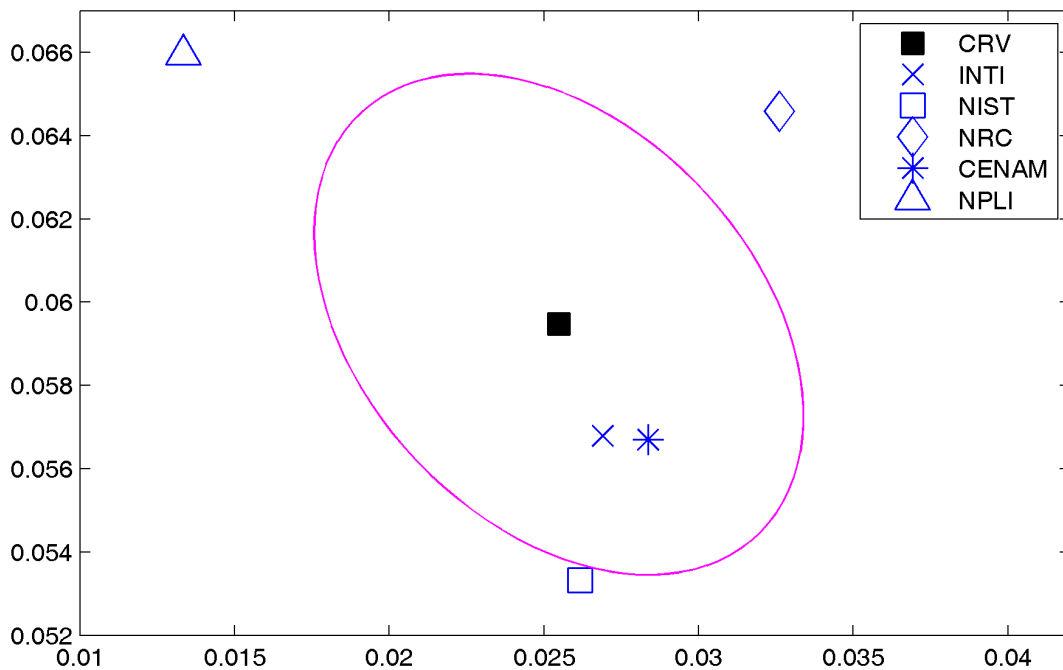


Figure 19: Matched load - Measurements of S_{11} along with CRV and its expanded uncertainty ($k = 2, 45$) at 18 GHz

	CRV		INTI		NIST	
	y	dy	y	dy	y	dy
INTI	0,0030	0,0097	-	-	0,0035	0,0185
NIST	0,0062	0,0144	0,0035	0,0185	-	-
NRC	0,0088	0,0163	0,0097	0,0213	0,0130	0,0249
CENAM	0,0040	0,0086	0,0015	0,0104	0,0040	0,0160
NPLI	0,0137	0,0103	0,0163	0,0112	0,0180	0,0158

Table 72: Matched load - DoE of S_{11} at 18 GHz

	NRC		CENAM		NPLI	
	y	dy	y	dy	y	dy
INTI	0,0097	0,0213	0,0015	0,0104	0,0163	0,0112
NIST	0,0130	0,0249	0,0040	0,0160	0,0180	0,0158
NRC	-	-	0,0090	0,0204	0,0193	0,0231
CENAM	0,0090	0,0204	-	-	0,0176	0,0088
NPLI	0,0193	0,0231	0,0176	0,0088	-	-

Table 73: Matched load - DoE of S_{11} at 18 GHz

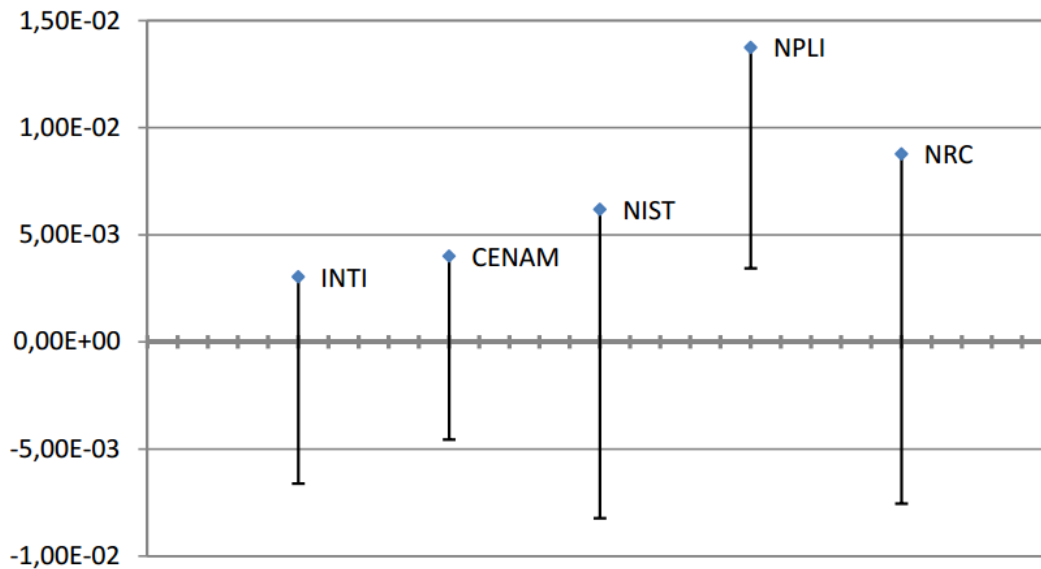


Figure 20: Matched load - DoE of S_{11} respect to CRV at 18 GHz

	KCRV		NPL		PTB		NMI-VSL	
	y	dy	y	dy	y	dy	y	dy
INTI	0,0022	0,0133	0,0038	0,0138	0,0036	0,0134	0,0049	0,0193
CENAM	0,0037	0,0120	0,0053	0,0128	0,0051	0,0123	0,0064	0,0186

Table 74: Matched load - CCEM/SIM Linked DoE of S_{11} at 18 GHz

	INRIM		METAS		CMI		UME	
	y	dy	y	dy	y	dy	y	dy
INTI	0,0041	0,0186	0,0027	0,0170	0,0022	0,0190	0,0032	0,0219
CENAM	0,0054	0,0173	0,0039	0,0151	0,0031	0,0170	0,0042	0,0203

Table 75: Matched load - CCEM/SIM Linked DoE of S_{11} at 18 GHz

	NMIA		SPRING		SCL		SNIIM	
	y	dy	y	dy	y	dy	y	dy
INTI	0,0006	0,0165	0,0011	0,0212	0,0022	0,0278	0,0062	0,0144
CENAM	0,0014	0,0138	0,0018	0,0155	0,0036	0,0272	0,0075	0,0134

Table 76: Matched load - CCEM/SIM Linked DoE of S_{11} at 18 GHz

	NIM		CSIR		NMIJ		SP	
	y	dy	y	dy	y	dy	y	dy
INTI	0,0058	0,0137	0,0066	0,0171	0,0045	0,0152	0,0028	0,0185
CENAM	0,0073	0,0126	0,0066	0,0155	0,0041	0,0138	0,0028	0,0172

Table 77: Matched load - CCEM/SIM Linked DoE of S_{11} at 18 GHz

	LNE	
	y	dy
INTI	0,0033	0,0195
CENAM	0,0019	0,0187

Table 78: Matched load - CCEM/SIM Linked DoE of S_{11} at 18 GHz

A.4 Mismatched load

Lab i	Measurement and combined standard uncertainty S_{11} of Mismatched load at 2 GHz				
	$Re(S_{11})$	$u(Re(S_{11}))$ combined 1-sigma	$Im(S_{11})$	$u(Im(S_{11}))$ combined 1-sigma	$r(x, y)$
INTI	0,31844	0,00300	0,08359	0,00300	0,00
NIST	0,31613	0,00359	0,08477	0,00344	0,00
NRC	0,31924	0,00520	0,08498	0,00520	0,00
CENAM	0,31774	0,00109	0,08620	0,00160	0,42
NPLI	0,32436	0,00582	0,08470	0,00582	-0,44

Table 79

Reference Value (CRV) S_{11} of Mismatched load at 2 GHz				
$Re(x_i)$	$u(Re(x_i))$ combined 1-sigma	$Im(x_i)$	$u(Im(x_i))$ combined 1-sigma	$r(x,y)$
0,31918	0,00139	0,08485	0,00041	-0,13

Table 80

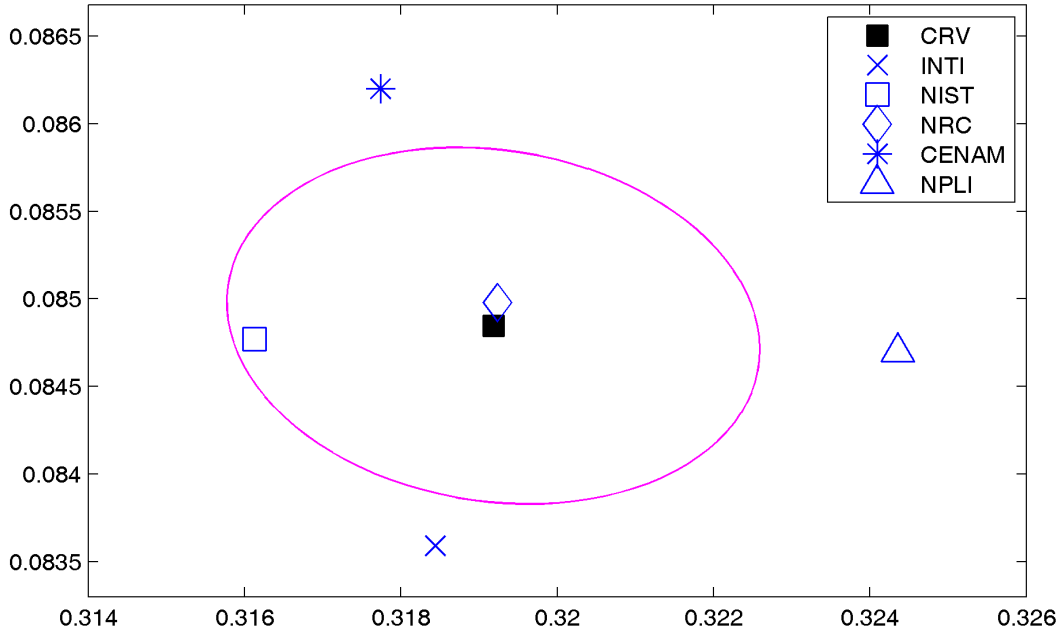


Figure 21: Mismatched load - Measurements of S_{11} along with CRV and its expanded uncertainty ($k = 2, 45$) at 2 GHz

	CRV		INTI		NIST	
	y	dy	y	dy	y	dy
INTI	0,0015	0,0059	-	-	0,0026	0,0114
NIST	0,0031	0,0076	0,0026	0,0114	-	-
NRC	0,0001	0,0100	0,0016	0,0147	0,0031	0,0155
CENAM	0,0020	0,0032	0,0027	0,0081	0,0021	0,0095
NPLI	0,0052	0,0106	0,0060	0,0142	0,0082	0,0159

Table 81: Mismatched load - DoE of S_{11} at 2 GHz

	NRC		CENAM		NPLI	
	y	dy	y	dy	y	dy
INTI	0,0016	0,0147	0,0027	0,0081	0,0060	0,0142
NIST	0,0031	0,0155	0,0021	0,0095	0,0082	0,0159
NRC	-	-	0,0019	0,0130	0,0051	0,0188
CENAM	0,0019	0,0130	-	-	0,0068	0,0146
NPLI	0,0051	0,0188	0,0068	0,0146	-	-

Table 82: Mismatched load - DoE of S_{11} at 2 GHz

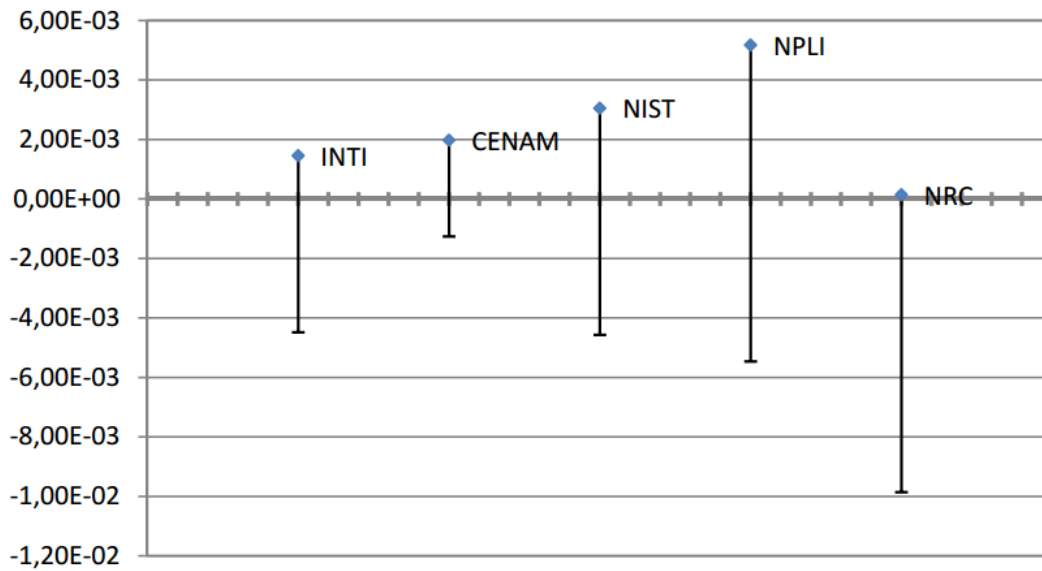


Figure 22: Mismatched load - DoE of S_{11} respect to CRV at 2 GHz

Lab i	Measurement and combined standard uncertainty S_{11} of Mismatched load at 9 GHz				
	$Re(S_{11})$	$u(Re(S_{11}))$ combined 1-sigma	$Im(S_{11})$	$u(Im(S_{11}))$ combined 1-sigma	$r(x, y)$
INTI	-0,31298	0,00455	0,15726	0,00455	0,00
NIST	-0,31491	0,00434	0,15502	0,00416	0,00
NRC	-0,31733	0,00800	0,16852	0,00800	0,00
CENAM	-0,31458	0,00274	0,15565	0,00148	0,58
NPLI	-0,32919	0,00881	0,16247	0,00881	-0,53

Table 83

Reference Value (CRV) S_{11} of Mismatched load at 9 GHz				
$Re(x_i)$	$u(Re(x_i))$ combined 1-sigma	$Im(x_i)$	$u(Im(x_i))$ combined 1-sigma	$r(x,y)$
-0,31780	0,00293	0,15978	0,00255	-0,44

Table 84

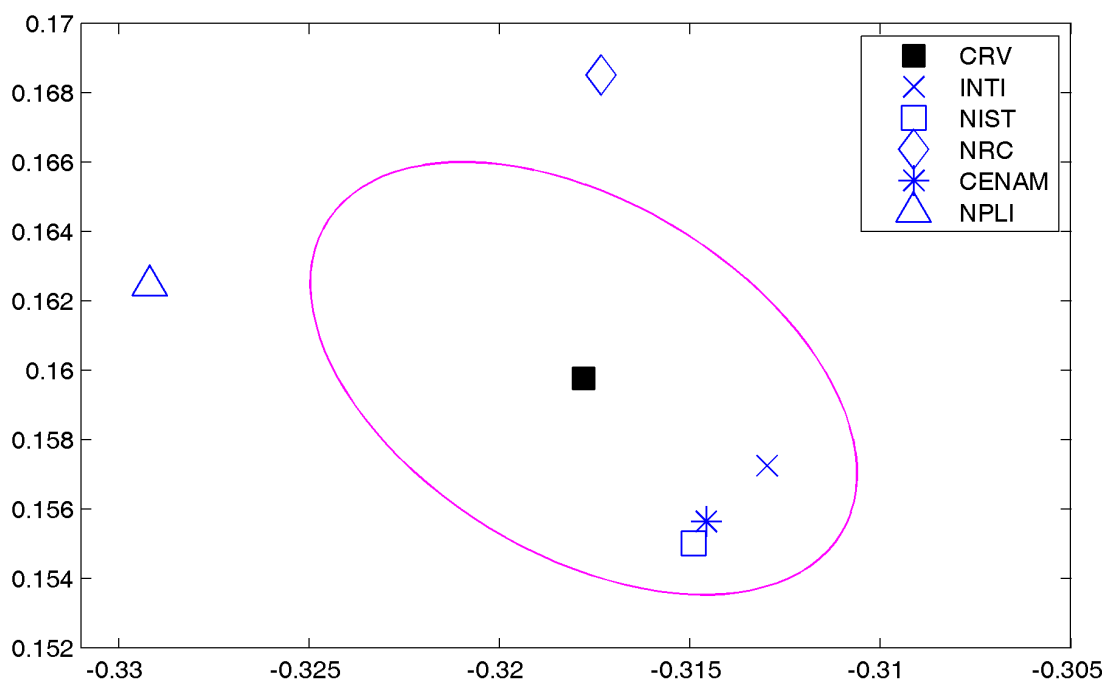


Figure 23: Mismatched load - Measurements of S_{11} along with CRV and its expanded uncertainty ($k = 2, 45$) at 9 GHz

	CRV		INTI		NIST	
	y	dy	y	dy	y	dy
INTI	0,0054	0,0118	-	-	0,0030	0,0152
NIST	0,0056	0,0110	0,0030	0,0152	-	-
NRC	0,0087	0,0163	0,0121	0,0226	0,0137	0,0221
CENAM	0,0052	0,0080	0,0023	0,0129	0,0007	0,0116
NPLI	0,0117	0,0178	0,0170	0,0254	0,0161	0,0270

Table 85: Mismatched load - DoE of S_{11} at 9 GHz

	NRC		CENAM		NPLI	
	y	dy	y	dy	y	dy
INTI	0,0121	0,0226	0,0023	0,0129	0,0170	0,0254
NIST	0,0137	0,0221	0,0007	0,0116	0,0161	0,0270
NRC	-	-	0,0132	0,0198	0,0133	0,0251
CENAM	0,0132	0,0198	-	-	0,0161	0,0249
NPLI	0,0133	0,0251	0,0161	0,0249	-	-

Table 86: Mismatched load - DoE of S_{11} at 9 GHz

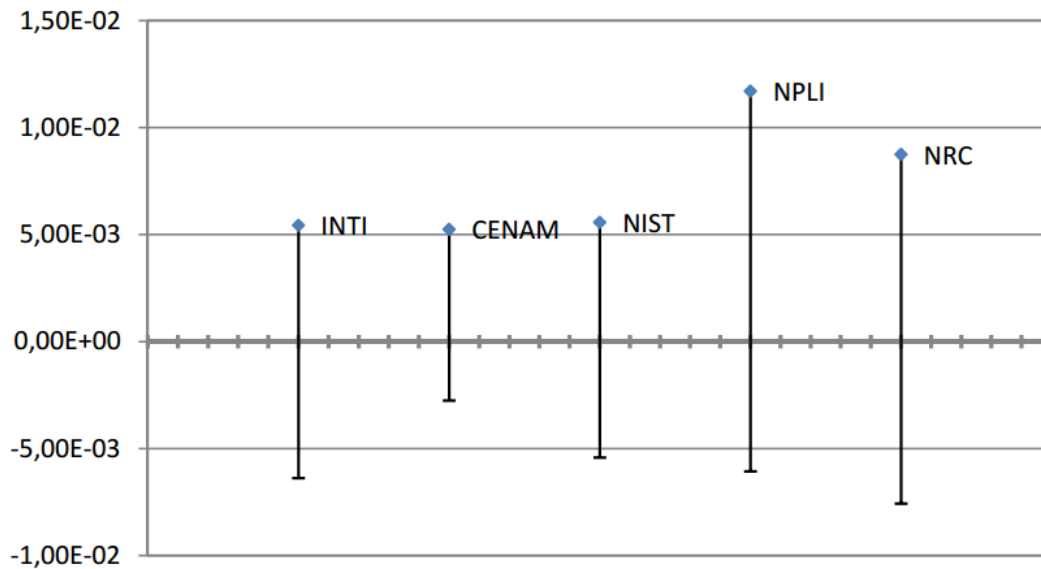


Figure 24: Mismatched load - DoE of S_{11} respect to CRV at 9 GHz

Lab i	Measurement and combined standard uncertainty S_{11} of Mismatched load at 18 GHz				
	$Re(S_{11})$	$u(Re(S_{11}))$ combined 1-sigma	$Im(S_{11})$	$u(Im(S_{11}))$ combined 1-sigma	$r(x, y)$
INTI	0,00093	0,00660	0,29499	0,00660	0,00
NIST	-0,00211	0,00521	0,29549	0,00740	0,00
NRC	0,00409	0,01000	0,30607	0,01000	0,00
CENAM	-0,00329	0,00257	0,29595	0,00244	-0,83
NPLI	-0,01595	0,00881	0,31020	0,00881	0,62

Table 87

Reference Value (CRV) S_{11} of Mismatched load at 18 GHz				
$Re(x_i)$	$u(Re(x_i))$ combined 1-sigma	$Im(x_i)$	$u(Im(x_i))$ combined 1-sigma	$r(x,y)$
-0,00326	0,00342	0,30054	0,00317	-0,51

Table 88

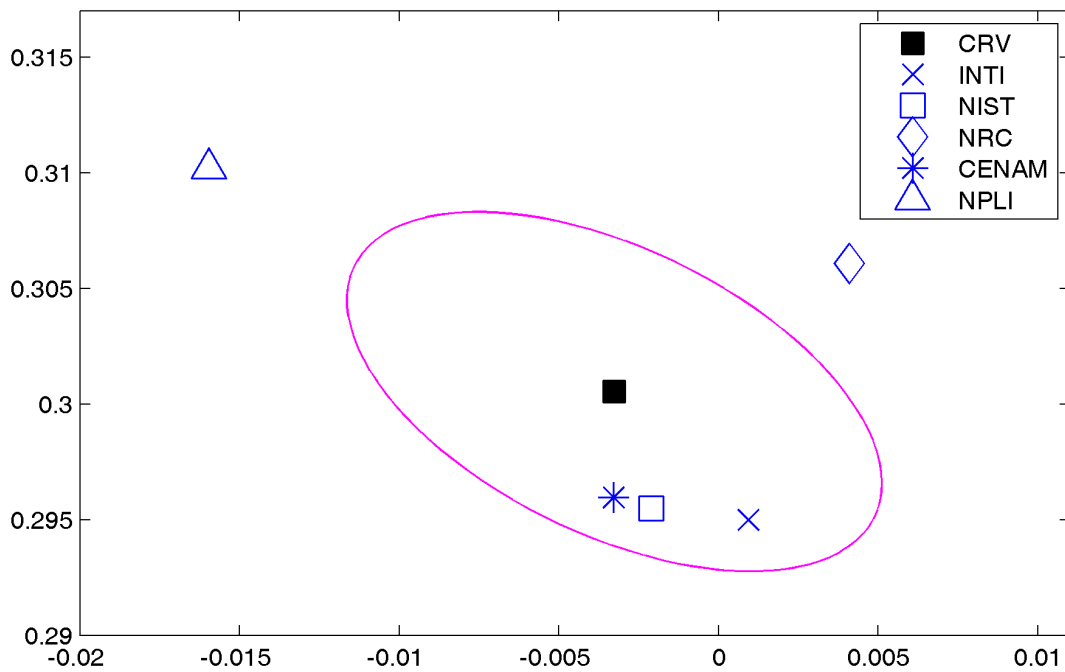


Figure 25: Mismatched load - Measurements of S_{11} along with CRV and its expanded uncertainty ($k = 2, 45$) at 18 GHz

	CRV		INTI		NIST	
	y	dy	y	dy	y	dy
INTI	0,0070	0,0159	-	-	0,0031	0,0207
NIST	0,0052	0,0163	0,0031	0,0207	-	-
NRC	0,0092	0,0199	0,0115	0,0294	0,0123	0,0297
CENAM	0,0046	0,0073	0,0043	0,0177	0,0013	0,0150
NPLI	0,0159	0,0144	0,0227	0,0209	0,0202	0,0204

Table 89: Mismatched load - DoE of S_{11} at 18 GHz

	NRC		CENAM		NPLI	
	y	dy	y	dy	y	dy
INTI	0,0115	0,0294	0,0043	0,0177	0,0227	0,0209
NIST	0,0123	0,0297	0,0013	0,0150	0,0202	0,0204
NRC	-	-	0,0125	0,0246	0,0205	0,0298
CENAM	0,0125	0,0246	-	-	0,0191	0,0156
NPLI	0,0205	0,0298	0,0191	0,0156	-	-

Table 90: Mismatched load - DoE of S_{11} at 18 GHz

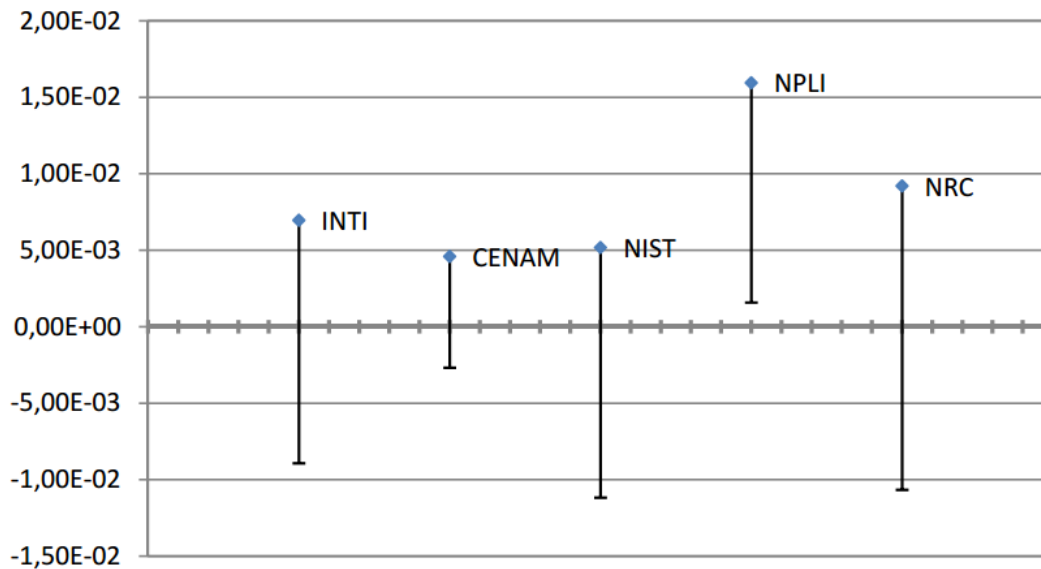


Figure 26: Mismatched load - DoE of S_{11} respect to CRV at 18 GHz

Annex B: Uncertainty budget

B.1 INTI Uncertainty Budgets

B.1.1 Reflection measurements

Uncertainty region of complex input quantities was considered circular, that is:

$$u(x_i) = u(re(x_i)) = u(im(x_i)) \text{ and } cov(re(x_i), im(x_i)) = 0.$$

According to [8], if the uncertainty region of the input quantities satisfies these properties, the uncertainty region of the measurand will satisfy the same properties, namely:

$$u(s_{11}) = u(re(s_{11})) = u(im(s_{11})) \text{ and } cov(re(s_{11}), im(s_{11})) = 0.$$

For this reason, the real and imaginary uncertainty components are identical.

Due to the correlation between effective directivity and effective source match [14], real and imaginary standard deviation (square root of variances) of their distributions were linearly added to get a worst case circular uncertainty region (see [9] for further details).

Quantity	Standard Uncertainty $u(x_i)$	Probability distribution (Bidimensional)	Sensitivity coefficient c_i	Uncertainty contribution $c_i u(x_i)$
Eff. Directivity	0,00248	Ring	1	0,00248
Eff. Test p. match	0,00290	Ring	$ \Gamma_m ^2$	0,00000
Linear sum				0,00248
Linearity	0,00000	Ring	1	0,00000
Repeatability	0,00007	$u_{rep} = \sqrt{u_{rep}^2(re(x_i)) + u_{rep}^2(im(x_i))}$	1	0,00007
			u_{total}	0,00248

Matched load at 2 GHz

Quantity	Standard Uncertainty $u(x_i)$	Probability distribution (Bidimensional)	Sensitivity coefficient c_i	Uncertainty contribution $c_i u(x_i)$
Eff. Directivity	0,00283	Ring	1	0,00283
Eff. Test p. match	0,00198	Ring	$ \Gamma_m ^2$	0,00000
Linear sum				0,00283
Linearity	0,00003	Ring	1	0,00003
Repeatability	0,00025	$u_{rep} = \sqrt{u_{rep}^2(re(x_i)) + u_{rep}^2(im(x_i))}$	1	0,00025
u_{total}				0,00284

Matched load at 9 GHz

Quantity	Standard Uncertainty $u(x_i)$	Probability distribution (Bidimensional)	Sensitivity coefficient c_i	Uncertainty contribution $c_i u(x_i)$
Eff. Directivity	0,00332	Ring	1	0,00332
Eff. Test p. match	0,00820	Ring	$ \Gamma_m ^2$	0,00003
Linear sum				0,00336
Linearity	0,00003	Ring	1	0,00003
Repeatability	0,00058	$u_{rep} = \sqrt{u_{rep}^2(re(x_i)) + u_{rep}^2(im(x_i))}$	1	0,00058
u_{total}				0,00341

Matched load at 18 GHz

Quantity	Standard Uncertainty $u(x_i)$	Probability distribution (Bidimensional)	Sensitivity coefficient c_i	Uncertainty contribution $c_i u(x_i)$
Eff. Directivity	0,00262	Ring	1	0,00262
Eff. Test p. match	0,00339	Ring	$ \Gamma_m ^2$	0,00037
Linear sum				0,02985
Tracking	0,00050	Disc	$ \Gamma_m $	0,00016
Linearity	0,00000	Ring	1	0,00000
Repeatability	0,00018	$u_{rep} = \sqrt{u_{rep}^2(re(x_i)) + u_{rep}^2(im(x_i))}$	1	0,00018
			u_{total}	0,00300

Mismatched load at 2 GHz

Quantity	Standard Uncertainty $u(x_i)$	Probability distribution (Bidimensional)	Sensitivity coefficient c_i	Uncertainty contribution $c_i u(x_i)$
Eff. Directivity	0,00431	Ring	1	0,00431
Eff. Test p. match	0,00184	Ring	$ \Gamma_m ^2$	0,00023
Linear sum				0,00454
Tracking	0,00050	Disc	$ \Gamma_m $	0,00018
Linearity	0,00000	Ring	1	0,00000
Repeatability	0,00031	$u_{rep} = \sqrt{u_{rep}^2(re(x_i)) + u_{rep}^2(im(x_i))}$	1	0,00031
			u_{total}	0,00455

Mismatched load at 9 GHz

Quantity	Standard Uncertainty $u(x_i)$	Probability distribution (Bidimensional)	Sensitivity coefficient c_i	Uncertainty contribution $c_i u(x_i)$
Eff. Directivity	0,00566	Ring	1	0,00566
Eff. Test p. match	0,01054	Ring	$ \Gamma_m ^2$	0,00092
Linear sum				0,00657
Tracking	0,00050	Disc	$ \Gamma_m $	0,00015
Linearity	0,00023	Ring	1	0,00023
Repeatability	0,00054	$u_{rep} = \sqrt{u_{rep}^2(re(x_i)) + u_{rep}^2(im(x_i))}$	1	0,00054
			u_{total}	0,00660

Mismatched load at 18 GHz

B.1.2 Transmission measurements

Uncertainty estimation in transmission measurement was performed considering only the magnitude of measurand. If the condition $u(|S_{21}|) \ll |S_{21}|$ is fulfilled, we can assume a circular uncertainty region of the measurand, where $u(|S_{21}|) = u(\text{re}(S_{21})) = u(\text{im}(S_{21}))$ and $\text{cov}(\text{re}(S_{21}), \text{im}(S_{21})) = 0$.

Quantity	Standard Uncertainty $u(x_i)$	Probability distribution	Sensitivity coefficient c_i	Uncertainty contribution $c_i u(x_i)$	
Mtm	0,00020	Σ U-type	8,686	0,00174 dB	
Linearity	0,00168 dB	Rectangular	1	0,00168 dB	
Stability	0,00100 dB	Gaussian	1	0,00100 dB	
Cable flex	0,00172 dB	Gaussian	1	0,00172 dB	
Repeatability	0,00181 dB	u_{rep}	1	0,00181 dB	
				$u(S_{21})_{total}$	0,00362 dB
				$u(S_{21})_{total}$	0,00029

3 dB Attenuator S_{21} at 2 GHz

Quantity	Standard Uncertainty $u(x_i)$	Probability distribution	Sensitivity coefficient c_i	Uncertainty contribution $c_i u(x_i)$	
Mtm	0,00039	Σ U-type	8,686	0,00335 dB	
Linearity	0,00613 dB	Rectangular	1	0,00613 dB	
Stability	0,00100 dB	Gaussian	1	0,00100 dB	
Cable flex	0,00298 dB	Gaussian	1	0,00298 dB	
Repeatability	0,00522 dB	u_{rep}	1	0,00522 dB	
				$u(S_{21})_{total}$	0,00926 dB
				$u(S_{21})_{total}$	0,00076

3 dB Attenuator S_{21} at 9 GHz

Quantity	Standard Uncertainty $u(x_i)$	Probability distribution	Sensitivity coefficient c_i	Uncertainty contribution $c_i u(x_i)$	
Mtm	0,00129	Σ U-type	8,686	0,01122 dB	
Linearity	0,00168 dB	Rectangular	1	0,00168 dB	
Stability	0,00200 dB	Gaussian	1	0,00200 dB	
Cable flex	0,00083 dB	Gaussian	1	0,00083 dB	
Repeatability	0,01013 dB	u_{rep}	1	0,01013 dB	
				$u(S_{21})_{total}$	0,01536 dB
				$u(S_{21})_{total}$	0,00125

3 dB Attenuator S_{21} at 18 GHz

Quantity	Standard Uncertainty $u(x_i)$	Probability distribution	Sensitivity coefficient c_i	Uncertainty contribution $c_i u(x_i)$	
Mtm	0,00003	Σ U-type	8,686	0,00022 dB	
Linearity	0,01162 dB	Rectangular	1	0,01162 dB	
Stability	0,00100 dB	Gaussian	1	0,00100 dB	
Cable flex	0,00172 dB	Gaussian	1	0,00172 dB	
Isolation	0,00088 dB	Gaussian	1	0,00088 dB	
Repeatability	0,00183 dB	u_{rep}	1	0,00183 dB	
				$u(S_{21})_{total}$	0,01196 dB
				$u(S_{21})_{total}$	0,00014

20 dB Attenuator S_{21} at 2 GHz

Quantity	Standard Uncertainty $u(x_i)$	Probability distribution	Sensitivity coefficient c_i	Uncertainty contribution $c_i u(x_i)$	
Mtm	0,00018	Σ U-type	8,686	0,00156 dB	
Linearity	0,01162 dB	Rectangular	1	0,01162 dB	
Stability	0,00100 dB	Gaussian	1	0,00100 dB	
Cable flex	0,00298 dB	Gaussian	1	0,00298 dB	
Isolation	0,00100 dB	Gaussian	1	0,00100 dB	
Repeatability	0,00434 dB	u_{rep}	1	0,00434 dB	
				$u(S_{21})_{total}$	0,01293 dB
				$u(S_{21})_{total}$	0,00015

20 dB Attenuator S_{21} at 9 GHz

Quantity	Standard Uncertainty $u(x_i)$	Probability distribution	Sensitivity coefficient c_i	Uncertainty contribution $c_i u(x_i)$	
Mtm	0,00093	Σ U-type	8,686	0,00804 dB	
Linearity	0,00751 dB	Rectangular	1	0,00751 dB	
Stability	0,00200 dB	Gaussian	1	0,00200 dB	
Cable flex	0,00083 dB	Gaussian	1	0,00083 dB	
Isolation	0,00525 dB	Gaussian	1	0,00525 dB	
Repeatability	0,00890 dB	u_{rep}	1	0,00890 dB	
				$u(S_{21})_{total}$	0,01524 dB
				$u(S_{21})_{total}$	0,00017

20 dB Attenuator S_{21} at 18 GHz

B.2 NIST Uncertainty Budgets

Uncertainties were obtained for magnitude and phase coordinates of measurand, then the uncertainties for real and imaginary components were obtained through a proper coordinates transformation.

B.2.1 Reflection measurements

Uncertainty contribution	Estimated value	
Type B - due to imperfections in air line standards and test ports (1 sigma)	0,0017	magnitude
Type A - due to connector variability, long term system variations, power meter resolution, and system noise during calibration (1 sigma)	0,0006	magnitude
Type A - evaluated from repeat measurements of the device under test (1 sigma)	0,0001	magnitude
Type B - due to imperfections in air line standards and test ports (1 sigma)	36,35	phase (deg)
Type A - due to connector variability, long term system variations, power meter resolution, and system noise during calibration (1 sigma)	0,03	phase (deg)
Type A - evaluated from repeat measurements of the device under test (1 sigma)	2,45	phase (deg)
Expanded Unc. Magnitude	0,0036	
Expanded Unc. Phase	72,74	(deg)

Matched load at 2 GHz

Uncertainty contribution	Estimated value	
Type B - due to imperfections in air line standards and test ports (1 sigma)	0,0018	magnitude
Type A - due to connector variability, long term system variations, power meter resolution, and system noise during calibration (1 sigma)	0,0012	magnitude
Type A - evaluated from repeat measurements of the device under test (1 sigma)	0,0005	magnitude
Type B - due to imperfections in air line standards and test ports (1 sigma)	5,55	phase (deg)
Type A - due to connector variability, long term system variations, power meter resolution, and system noise during calibration (1 sigma)	0,07	phase (deg)
Type A - evaluated from repeat measurements of the device under test (1 sigma)	0,87	phase (deg)
Expanded Unc. Magnitude	0,0044	
Expanded Unc. Phase	11,11	(deg)

Matched load at 9 GHz

Uncertainty contribution	Estimated value	
Type B - due to imperfections in air line standards and test ports (1 sigma)	0,0019	magnitude
Type A - due to connector variability, long term system variations, power meter resolution, and system noise during calibration (1 sigma)	0,0032	magnitude
Type A - evaluated from repeat measurements of the device under test (1 sigma)	0,0004	magnitude
Type B - due to imperfections in air line standards and test ports (1 sigma)	1,77	phase (deg)
Type A - due to connector variability, long term system variations, power meter resolution, and system noise during calibration (1 sigma)	0,18	phase (deg)
Type A - evaluated from repeat measurements of the device under test (1 sigma)	1,18	phase (deg)
Expanded Unc. Magnitude	0,0074	
Expanded Unc. Phase	3,68	(deg)

Matched load 18 GHz

Uncertainty contribution	Estimated value	
Type B - due to imperfections in air line standards and test ports (1 sigma)	0,0017	magnitude
Type A - due to connector variability, long term system variations, power meter resolution, and system noise during calibration (1 sigma)	0,0006	magnitude
Type A - evaluated from repeat measurements of the device under test (1 sigma)	0,0000	magnitude
Type B - due to imperfections in air line standards and test ports (1 sigma)	0,30	phase (deg)
Type A - due to connector variability, long term system variations, power meter resolution, and system noise during calibration (1 sigma)	0,03	phase (deg)
Type A - evaluated from repeat measurements of the device under test (1 sigma)	0	phase (deg)
Expanded Unc. Magnitude	0,0036	
Expanded Unc. Phase	0,6	(deg)

Mismatched load at 2 GHz

Uncertainty contribution	Estimated value	
Type B - due to imperfections in air line standards and test ports (1 sigma)	0,0018	magnitude
Type A - due to connector variability, long term system variations, power meter resolution, and system noise during calibration (1 sigma)	0,0012	magnitude
Type A - evaluated from repeat measurements of the device under test (1 sigma)	0,0001	magnitude
Type B - due to imperfections in air line standards and test ports (1 sigma)	0,33	phase (deg)
Type A - due to connector variability, long term system variations, power meter resolution, and system noise during calibration (1 sigma)	0,07	phase (deg)
Type A - evaluated from repeat measurements of the device under test (1 sigma)	0,01	phase (deg)
Expanded Unc. Magnitude	0,0044	
Expanded Unc. Phase	0,67	(deg)

Mismatched load at 9 GHz

Uncertainty contribution	Estimated value	
Type B - due to imperfections in air line standards and test ports (1 sigma)	0,0019	magnitude
Type A - due to connector variability, long term system variations, power meter resolution, and system noise during calibration (1 sigma)	0,0032	magnitude
Type A - evaluated from repeat measurements of the device under test (1 sigma)	0,0001	magnitude
Type B - due to imperfections in air line standards and test ports (1 sigma)	0,47	phase (deg)
Type A - due to connector variability, long term system variations, power meter resolution, and system noise during calibration (1 sigma)	0,18	phase (deg)
Type A - evaluated from repeat measurements of the device under test (1 sigma)	0,03	phase (deg)
Expanded Unc. Magnitude	0,0074	
Expanded Unc. Phase	1,01	(deg)

Mismatched load at 18 GHz

B.2.2 Transmission measurements

Uncertainty contribution	Estimated value	
Type B - due to imperfections in air line standards and test ports (1 sigma)	0,0020	magnitude(dB)
Type A - due to connector variability, long term system variations, power meter resolution, and system noise during calibration (1 sigma)	0,0080	magnitude(dB)
Type A - evaluated from repeat measurements of the device under test (1 sigma)	0,0030	magnitude(dB)
Type B - due to imperfections in air line standards and test ports (1 sigma)	0,12	phase (deg)
Type A - due to connector variability, long term system variations, power meter resolution, and system noise during calibration (1 sigma)	0,08	phase (deg)
Type A - evaluated from repeat measurements of the device under test (1 sigma)	0,05	phase (deg)
Expanded Unc. Magnitude	0,016	(dB)
Expanded Unc. Phase	0,30	(deg)

3 dB Attenuator S_{21} at 2 GHz

Uncertainty contribution	Estimated value	
Type B - due to imperfections in air line standards and test ports (1 sigma)	0,0040	magnitude(dB)
Type A - due to connector variability, long term system variations, power meter resolution, and system noise during calibration (1 sigma)	0,0110	magnitude(dB)
Type A - evaluated from repeat measurements of the device under test (1 sigma)	0,0400	magnitude(dB)
Type B - due to imperfections in air line standards and test ports (1 sigma)	0,44	phase (deg)
Type A - due to connector variability, long term system variations, power meter resolution, and system noise during calibration (1 sigma)	0,14	phase (deg)
Type A - evaluated from repeat measurements of the device under test (1 sigma)	0,08	phase (deg)
Expanded Unc. Magnitude	0,04	(dB)
Expanded Unc. Phase	0,93	(deg)

3 dB Attenuator S_{21} at 9 GHz

Uncertainty contribution	Estimated value	
Type B - due to imperfections in air line standards and test ports (1 sigma)	0,0060	magnitude(dB)
Type A - due to connector variability, long term system variations, power meter resolution, and system noise during calibration (1 sigma)	0,0180	magnitude(dB)
Type A - evaluated from repeat measurements of the device under test (1 sigma)	0,0090	magnitude(dB)
Type B - due to imperfections in air line standards and test ports (1 sigma)	0,87	phase (deg)
Type A - due to connector variability, long term system variations, power meter resolution, and system noise during calibration (1 sigma)	0,27	phase (deg)
Type A - evaluated from repeat measurements of the device under test (1 sigma)	0,09	phase (deg)
Expanded Unc. Magnitude	0,039	(dB)
Expanded Unc. Phase	1,82	(deg)

3 dB Attenuator S_{21} at 18 GHz

Uncertainty contribution	Estimated value	
Type B - due to imperfections in air line standards and test ports (1 sigma)	0,0020	magnitude(dB)
Type A - due to connector variability, long term system variations, power meter resolution, and system noise during calibration (1 sigma)	0,0080	magnitude(dB)
Type A - evaluated from repeat measurements of the device under test (1 sigma)	0,0010	magnitude(dB)
Type B - due to imperfections in air line standards and test ports (1 sigma)	0,12	phase (deg)
Type A - due to connector variability, long term system variations, power meter resolution, and system noise during calibration (1 sigma)	0,08	phase (deg)
Type A - evaluated from repeat measurements of the device under test (1 sigma)	0,05	phase (deg)
Expanded Unc. Magnitude	0,016	(dB)
Expanded Unc. Phase	0,30	(deg)

20 dB Attenuator S_{21} at 2 GHz

Uncertainty contribution	Estimated value	
Type B - due to imperfections in air line standards and test ports (1 sigma)	0,0040	magnitude(dB)
Type A - due to connector variability, long term system variations, power meter resolution, and system noise during calibration (1 sigma)	0,0110	magnitude(dB)
Type A - evaluated from repeat measurements of the device under test (1 sigma)	0,0470	magnitude(dB)
Type B - due to imperfections in air line standards and test ports (1 sigma)	0,44	phase (deg)
Type A - due to connector variability, long term system variations, power meter resolution, and system noise during calibration (1 sigma)	0,14	phase (deg)
Type A - evaluated from repeat measurements of the device under test (1 sigma)	0,06	phase (deg)
Expanded Unc. Magnitude	0,047	(dB)
Expanded Unc. Phase	0,93	(deg)

20 dB Attenuator S_{21} at 9 GHz

Uncertainty contribution	Estimated value	
Type B - due to imperfections in air line standards and test ports (1 sigma)	0,0060	magnitude(dB)
Type A - due to connector variability, long term system variations, power meter resolution, and system noise during calibration (1 sigma)	0,0180	magnitude(dB)
Type A - evaluated from repeat measurements of the device under test (1 sigma)	0,0210	magnitude(dB)
Type B - due to imperfections in air line standards and test ports (1 sigma)	0,87	phase (deg)
Type A - due to connector variability, long term system variations, power meter resolution, and system noise during calibration (1 sigma)	0,27	phase (deg)
Type A - evaluated from repeat measurements of the device under test (1 sigma)	0,02	phase (deg)
Expanded Unc. Magnitude	0,042	(dB)
Expanded Unc. Phase	1,82	(deg)

20 dB Attenuator S_{21} at 18 GHz

B.3 NRC Uncertainty Budgets

B.3.1 Small reflection coefficient

The next tables give the error budget for the well matched terminations. There is no phase, and the uncertainty on both components (Re,Im) are equal and assumed to be not correlated. This condition applies in the case of the termination **#55719** at **2, 9, and 18 GHz** respectively.

Matched termination **#55719** uncertainty at 2 GHz

Airlines standards	0,005	rect
Connector Repeatability	0,001	Gauss
Combined Uncertainty	0,0052	k=1

Matched termination **#55719** uncertainty at 9 GHz

Airlines standards	0,005	rect
Connector Repeatability	0,002	Gauss
Combined Uncertainty	0,006	k=1

Matched termination **#55719** uncertainty at 18 GHz

Airlines standards	0,005	rect
Connector Repeatability	0,004	Gauss
Combined Uncertainty	0,008	k=1

B.3.2 Large reflection coefficient

When the reflection coefficient is large, then the phase of the reflection coefficient becomes more important. It is linked to the length of the calibration standards. We have performed many calibrations/measurements cycles with different experimental configurations, and we find that the phase varies for the high frequencies. The standard deviation for the phase of the mismatch termination is about one degree (N=7). We include this uncertainty component that we call “length of short/lines”.

The next tables give the error budget in the case of the **mismatched termination #9006** at **2, 9, and 18 GHz** respectively.

Mismatch termination **#9006** uncertainty at 2 GHz

Airlines standards	0,005	rect
Connector Repeatability	0,001	Gauss
Combined Uncertainty	0,0052	k=1

Mismatch termination **#9006** uncertainty at 9 GHz

Airlines standards	0,005	rect
Connector Repeatability	0,002	Gauss
Length of short/lines	0,004	rect
Combined Uncertainty	0,008	k=1

Mismatch termination **#9006** uncertainty at 18 GHz

Airlines standards	0,005	rect
Connector Repeatability	0,004	Gauss
Length of short/lines	0,008	rect
Combined Uncertainty	0,010	k=1

B.3.3 Large transmission coefficient

In the case of the transmission, the uncertainty is largely due to the connector repeatability. The system is characterized by comparison to a similar measurement using a matched source and matched receiver. This uncertainty can also be compared to the deviation of a single connector during a power factor calibration. Also a THRU measurement can be performed before and after the measurement and give an idea of the performance of the cables, etc... The measurements that appear “stable” are sometimes difficult to reproduce.

The next tables give the uncertainty for the transmission coefficients of the 3 dB attenuator **#66530** and 20 dB attenuator **#66597** at **2, 9, and 18 GHz**.

Transmission uncertainty at 2 GHz for (3 dB) att. **#66530**

Connector Repeatability	0,0025	Gauss
Combined Uncertainty	0,0025	k=1

Transmission uncertainty at 9 GHz for (3 dB) att. **#66530**

Connector Repeatability	0,0025	Gauss
Combined Uncertainty	0,0025	k=1

Transmission uncertainty at 18 GHz for (3 dB) att. **#66530**

Connector Repeatability	0,0025	Gauss
Combined Uncertainty	0,0025	k=1

Transmission uncertainty at 2 GHz for (20 dB) att. **#66597**

Connector Repeatability	0,0025	Gauss
Combined Uncertainty	0,0025	k=1

Transmission uncertainty at 9 GHz for (20 dB) att. **#66597**

Connector Repeatability	0,0025	Gauss
Combined Uncertainty	0,0025	k=1

Transmission uncertainty at 18 GHz for (20 dB) att. **#66597**

Connector Repeatability	0,0025	Gauss
Combined Uncertainty	0,0025	k=1

B.4 CENAM Uncertainty Budgets

B.4.1 Reflection measurements (TRL -METHOD)

Quantity	Standard Uncertainty Mag[$u(x_i)$]	Probability Distribution	Sensitivity Coefficient c_i	Uncertainty contribution Mag[$c_i u(x_i)$]
Effective Directivity	0,0009005	U-shaped	1	0,0009005
Effective Test Port Match	0,0015293	U-shaped	0,000003	0,000000004
Linear sum of the directivity and test port match		U-shaped		0,0009005
Reflection Tracking	0,0011547	Rectangular	0,0016	0,000002
Linearity	0,0002228	Rectangular	0,0016	0,000000
System Repeatability	0,0001155	Rectangular	1	0,000115
Connector Repeatability	0,0000385	Gaussian	1	0,000038
Ambient Conditions	0,0002659	Rectangular	1	0,000266
Reference Line	0,0005245	Rectangular	1	0,000524
Repeat measurements	0,0000260	Gaussian	1	0,000026
Magnitude combined uncertainty (k = 1):				0,00108

Matched load at 2 GHz

Quantity	Standard Uncertainty Phase[$u(x_i)$] [Degrees]	Probability Distribution	Sensitivity Coefficient c_i	Uncertainty contribution Phase[$c_i u(x_i)$] [Degrees]
Magnitude of reflection coefficient 0.0016 at 2 GHz	42,37	Gaussian	1	42,37
Thermal coefficient in phase	0,12	Rectangular	1	0,12
Repeat measurements	0,81	Gaussian	1	0,81
Phase combined uncertainty (k = 1):				42,38
Real component combined uncertainty (k = 1):				0,0009
Imaginary component combined uncertainty (k = 1):				0,0013

Matched load at 2 GHz

Quantity	Standard Uncertainty Mag[$u(x_i)$]	Probability Distribution	Sensitivity Coefficient c_i	Uncertainty contribution Mag[$c_i u(x_i)$]
Effective Directivity	0,0017967	U-shaped	1	0,0017967
Effective Test Port Match	0,0018175	U-shaped	0,000286	0,000000520
Linear sum of the directivity and test port match		U-shaped		0,0017973
Reflection Tracking	0,0011547	Rectangular	0,0169	0,000020
Linearity	0,0001413	Rectangular	0,0169	0,000002
System Repeatability	0,0001155	Rectangular	1	0,000115
Connector Repeatability	0,0000427	Gaussian	1	0,000043
Ambient Conditions	0,0002659	Rectangular	1	0,000266
Reference Line	0,0005245	Rectangular	1	0,000524
Repeat measurements	0,0000546	Gaussian	1	0,000055
Magnitude combined uncertainty (k = 1):				0,00190

Matched load at 9 GHz

Quantity	Standard Uncertainty Phase[$u(x_i)$] [Degrees]	Probability Distribution	Sensitivity Coefficient c_i	Uncertainty contribution Phase[$c_i u(x_i)$] [Degrees]
Magnitude of reflection coefficient 0.0169 at 9 GHz	6,43	Gaussian	1	6,43
Thermal coefficient in phase	0,12	Rectangular	1	0,12
Repeat measurements	0,16	Gaussian	1	0,16
Phase combined uncertainty (k = 1):				6,44
Real component combined uncertainty (k = 1):				0,0022
Imaginary component combined uncertainty (k = 1):				0,0015

Matched load at 9 GHz

Quantity	Standard Uncertainty Mag[$u(x_i)$]	Probability Distribution	Sensitivity Coefficient c_i	Uncertainty contribution Mag[$c_i u(x_i)$]
Effective Directivity	0,0020393	U-shaped	1	0,0020393
Effective Test Port Match	0,0024802	U-shaped	0,004021	0,000009972
Linear sum of the directivity and test port match		U-shaped		0,0020493
Reflection Tracking	0,0017321	Rectangular	0,0634	0,000110
Linearity	0,0005094	Rectangular	0,0634	0,000032
System Repeatability	0,0005196	Rectangular	1	0,000520
Connector Repeatability	0,0000796	Gaussian	1	0,000080
Ambient Conditions	0,0003989	Rectangular	1	0,000399
Reference Line	0,0005245	Rectangular	1	0,000524
Repeat measurements	0,0001171	Gaussian	1	0,000117
Magnitude combined uncertainty (k = 1):				0,00222

Matched load at 18 GHz

Quantity	Standard Uncertainty Phase[$u(x_i)$] [Degrees]	Probability Distribution	Sensitivity Coefficient c_i	Uncertainty contribution Phase[$c_i u(x_i)$] [Degrees]
Magnitude of reflection coefficient 0.0634 at 18 GHz	2,01	Gaussian	1	2,01
Thermal coefficient in phase	0,12	Rectangular	1	0,12
Repeat measurements	0,14	Gaussian	1	0,14
Phase combined uncertainty (k = 1):				2,02
Real component combined uncertainty (k = 1):				0,0026
Imaginary component combined uncertainty (k = 1):				0,0017

Matched load at 18 GHz

Quantity	Standard Uncertainty Mag[$u(x_i)$]	Probability Distribution	Sensitivity Coefficient c_i	Uncertainty contribution Mag[$c_i u(x_i)$]
Effective Directivity	0,0009005	U-shaped	1	0,0009005
Effective Test Port Match	0,0015293	U-shaped	0,108386	0,000165752
Linear sum of the directivity and test port match		U-shaped		0,0010663
Reflection Tracking	0,0011547	Rectangular	0,3292	0,000380
Linearity	0,0000385	Rectangular	0,3292	0,000013
System Repeatability	0,0001155	Rectangular	1	0,000115
Connector Repeatability	0,0000385	Gaussian	1	0,000038
Ambient Conditions	0,0002659	Rectangular	1	0,000266
Reference Line	0,0005245	Rectangular	1	0,000524
Repeat measurements	0,0000283	Gaussian	1	0,000028
Magnitude combined uncertainty (k = 1):				0,00128

Mismatched load at 2 GHz

Quantity	Standard Uncertainty Phase[$u(x_i)$] [Degrees]	Probability Distribution	Sensitivity Coefficient c_i	Uncertainty contribution Phase[$c_i u(x_i)$] [Degrees]
Magnitude of reflection coefficient 0.0016 at 2 GHz	0,223	Gaussian	1	0,223
Thermal coefficient in phase	0,115	Rectangular	1	0,115
Repeat measurements	0,005	Gaussian	1	0,005
Phase combined uncertainty (k = 1):				0,251
Real component combined uncertainty (k = 1):				0,0011
Imaginary component combined uncertainty (k = 1):				0,0016

Mismatched load at 2 GHz

Quantity	Standard Uncertainty Mag[$u(x_i)$]	Probability Distribution	Sensitivity Coefficient c_i	Uncertainty contribution Mag[$c_i u(x_i)$]
Effective Directivity	0,0017967	U-shaped	1	0,0017967
Effective Test Port Match	0,0018175	U-shaped	0,123184	0,000223893
Linear sum of the directivity and test port match		U-shaped		0,0020206
Reflection Tracking	0,0011547	Rectangular	0,3510	0,000405
Linearity	0,0000363	Rectangular	0,3510	0,000013
System Repeatability	0,0001155	Rectangular	1	0,000115
Connector Repeatability	0,0000427	Gaussian	1	0,000043
Ambient Conditions	0,0002659	Rectangular	1	0,000266
Reference Line	0,0005245	Rectangular	1	0,000524
Repeat measurements	0,0000334	Gaussian	1	0,000033
Magnitude combined uncertainty (k = 1):				0,00215

Mismatched load at 9 GHz

Quantity	Standard Uncertainty Phase[$u(x_i)$] [Degrees]	Probability Distribution	Sensitivity Coefficient c_i	Uncertainty contribution Phase[$c_i u(x_i)$] [Degrees]
Magnitude of reflection coefficient 0.0169 at 9 GHz	0,350	Gaussian	1	0,350
Thermal coefficient in phase	0,115	Rectangular	1	0,115
Repeat measurements	0,018	Gaussian	1	0,018
Phase combined uncertainty (k = 1):				0,369
Real component combined uncertainty (k = 1):				0,0027
Imaginary component combined uncertainty (k = 1):				0,0015

Mismatched load at 9 GHz

Quantity	Standard Uncertainty Mag[$u(x_i)$]	Probability Distribution	Sensitivity Coefficient c_i	Uncertainty contribution Mag[$c_i u(x_i)$]
Effective Directivity	0,0020393	U-shaped	1	0,0020393
Effective Test Port Match	0,0024802	U-shaped	0,087601	0,000217268
Linear sum of the directivity and test port match		U-shaped		0,0022566
Reflection Tracking	0,0017321	Rectangular	0,2960	0,000513
Linearity	0,0002249	Rectangular	0,2960	0,000067
System Repeatability	0,0005196	Rectangular	1	0,000520
Connector Repeatability	0,0000796	Gaussian	1	0,000080
Ambient Conditions	0,0003989	Rectangular	1	0,000399
Reference Line	0,0005245	Rectangular	1	0,000524
Repeat measurements	0,0000789	Gaussian	1	0,000079
Magnitude combined uncertainty (k = 1):				0,00246

Mismatched load at 18 GHz

Quantity	Standard Uncertainty Phase[$u(x_i)$] [Degrees]	Probability Distribution	Sensitivity Coefficient c_i	Uncertainty contribution Phase[$c_i u(x_i)$] [Degrees]
Magnitude of reflection coefficient 0.0634 at 18 GHz	0,477	Gaussian	1	0,477
Thermal coefficient in phase	0,115	Rectangular	1	0,115
Repeat measurements	0,051	Gaussian	1	0,051
Phase combined uncertainty (k = 1):				0,494
Real component combined uncertainty (k = 1):				0,0026
Imaginary component combined uncertainty (k = 1):				0,0024

Mismatched load at 18 GHz

B.4.2 Transmission measurements (TRL -METHOD)

Quantity	Standard Uncertainty Mag[$u(x_i)$] [dB]	Probability Distribution	Sensitivity Coefficient c_i	Uncertainty contribution Mag[$c_i u(x_i)$] [dB]
Linearity	0.0000346 dB/dB	Rectangular	3,06	0,000106
Mismatch calculated	0,0007110	U-shaped	1	0,000711
Cross-talk	0,0000566	Rectangular	1	0,000057
Transmission Tracking	0,0035281	Rectangular	1	0,003528
System Repeatability	0,0006087	Gaussian	1	0,000609
Connector Repeatability	0,0003757	Gaussian	1	0,000376
Cable flexure	0,0008660	Rectangular	1	0,000866
Ambient Conditions	0,0023094	Rectangular	1	0,002309
Repeat measurements	0,0002662	Gaussian	1	0,000266
Magnitude combined uncertainty (k = 1):				0,00443

3 dB Attenuator S_{21} at 2 GHz

Quantity	Standard Uncertainty Phase[$u(x_i)$] [Degrees]	Probability Distribution	Sensitivity Coefficient c_i	Uncertainty contribution Phase[$c_i u(x_i)$] [Degrees]
Magnitude of transmission coefficient	0,029	Gaussian	1	0,029
Thermal coefficient in phase	0,115	Rectangular	1	0,115
Uncertainty in phase standard	0,0010	Gaussian	1	0,001
Stability of the cable	0,058	Rectangular	1	0,058
Repeat measurements	0,003	Gaussian	1	0,003
Phase combined uncertainty (k = 1):				0,132
Real component combined uncertainty (k = 1):				0,0008
Imaginary component combined uncertainty (k = 1):				0,0014

3 dB Attenuator S_{21} at 2 GHz

Quantity	Standard Uncertainty Mag[$u(x_i)$] [dB]	Probability Distribution	Sensitivity Coefficient c_i	Uncertainty contribution Mag[$c_i u(x_i)$] [dB]
Linearity	0.0000346 dB/dB	Rectangular	2,87	0,000099
Mismatch calculated	0,0013700	U-shaped	1	0,001370
Cross-talk	0,0000554	Rectangular	1	0,000055
Transmission Tracking	0,0144250	Rectangular	1	0,014425
System Repeatability	0,0019679	Gaussian	1	0,001968
Connector Repeatability	0,0005112	Gaussian	1	0,000511
Cable flexure	0,0008660	Rectangular	1	0,000866
Ambient Conditions	0,0023094	Rectangular	1	0,002309
Repeat measurements	0,0003702	Gaussian	1	0,000370
Magnitude combined uncertainty (k = 1):				0,01484

3 dB Attenuator S_{21} at 9 GHz

Quantity	Standard Uncertainty Phase[$u(x_i)$] [Degrees]	Probability Distribution	Sensitivity Coefficient c_i	Uncertainty contribution Phase[$c_i u(x_i)$] [Degrees]
Magnitude of transmission coefficient	0,098	Gaussian	1	0,098
Thermal coefficient in phase	0,115	Rectangular	1	0,115
Uncertainty in phase standard	0,004	Gaussian	1	0,004
Stability of the cable	0,260	Rectangular	1	0,260
Repeat measurements	0,024	Gaussian	1	0,024
Phase combined uncertainty (k = 1):				0,302
Real component combined uncertainty (k = 1):				0,0013
Imaginary component combined uncertainty (k = 1):				0,0038

3 dB Attenuator S_{21} at 9 GHz

Quantity	Standard Uncertainty Mag[$u(x_i)$] [dB]	Probability Distribution	Sensitivity Coefficient c_i	Uncertainty contribution Mag[$c_i u(x_i)$] [dB]
Linearity	0.0001848 dB/dB	Rectangular	2,99	0,000553
Mismatch calculated	0,0030026	U-shaped	1	0,003003
Cross-talk	0,0000562	Rectangular	1	0,000056
Transmission Tracking	0,0266956	Rectangular	1	0,026696
System Repeatability	0,0098988	Gaussian	1	0,009899
Connector Repeatability	0,0006047	Gaussian	1	0,000605
Cable flexure	0,0017321	Rectangular	1	0,001732
Ambient Conditions	0,0034641	Rectangular	1	0,003464
Repeat measurements	0,0002906	Gaussian	1	0,000291
Magnitude combined uncertainty (k = 1):				0,02890

3 dB Attenuator S_{21} at 18 GHz

Quantity	Standard Uncertainty Phase[$u(x_i)$] [Degrees]	Probability Distribution	Sensitivity Coefficient c_i	Uncertainty contribution Phase[$c_i u(x_i)$] [Degrees]
Magnitude of transmission coefficient	0,191	Gaussian	1	0,191
Thermal coefficient in phase	0,115	Rectangular	1	0,115
Uncertainty in phase standard	0,009	Gaussian	1	0,009
Stability of the cable	0,520	Rectangular	1	0,520
Repeat measurements	0,062	Gaussian	1	0,062
Phase combined uncertainty (k = 1):				0,569
Real component combined uncertainty (k = 1):				0,0035
Imaginary component combined uncertainty (k = 1):				0,0066

3 dB Attenuator S_{21} at 18 GHz

Quantity	Standard Uncertainty Mag[$u(x_i)$] [dB]	Probability Distribution	Sensitivity Coefficient c_i	Uncertainty contribution Mag[$c_i u(x_i)$] [dB]
Linearity	0.000346 dB/dB	Rectangular	19,97	0,000691
Mismatch calculated	0,0001208	U-shaped	1	0,000121
Cross-talk	0,0003969	Rectangular	1	0,000397
Transmission Tracking	0,0005033	Rectangular	1	0,000503
System Repeatability	0,0006087	Gaussian	1	0,000609
Connector Repeatability	0,0003757	Gaussian	1	0,000376
Cable flexure	0,0008660	Rectangular	1	0,000866
Ambient Conditions	0,0023094	Rectangular	1	0,002309
Repeat measurements	0,0003259	Gaussian	1	0,000326
Magnitude combined uncertainty (k = 1):				0,00276

20 dB Attenuator S_{21} at 2 GHz

Quantity	Standard Uncertainty Phase[$u(x_i)$] [Degrees]	Probability Distribution	Sensitivity Coefficient c_i	Uncertainty contribution Phase[$c_i u(x_i)$] [Degrees]
Magnitude of transmission coefficient	0,018	Gaussian	1	0,018
Thermal coefficient in phase	0,115	Rectangular	1	0,115
Uncertainty in phase standard	0,0010	Gaussian	1	0,001
Stability of the cable	0,058	Rectangular	1	0,058
Repeat measurements	0,004	Gaussian	1	0,004
Phase combined uncertainty (k = 1):				0,130
Real component combined uncertainty (k = 1):				0,00013
Imaginary component combined uncertainty (k = 1):				0,00019

20 dB Attenuator S_{21} at 2 GHz

Quantity	Standard Uncertainty Mag[$u(x_i)$] [dB]	Probability Distribution	Sensitivity Coefficient c_i	Uncertainty contribution Mag[$c_i u(x_i)$] [dB]
Linearity	0.0000346 dB/dB	Rectangular	19,97	0,000691
Mismatch calculated	0,0006583	U-shaped	1	0,000658
Cross-talk	0,0003971	Rectangular	1	0,000397
Transmission Tracking	0,0020125	Rectangular	1	0,002013
System Repeatability	0,0019679	Gaussian	1	0,001968
Connector Repeatability	0,0005112	Gaussian	1	0,000511
Cable flexure	0,0008660	Rectangular	1	0,000866
Ambient Conditions	0,0023094	Rectangular	1	0,002309
Repeat measurements	0,0005102	Gaussian	1	0,000510
Magnitude combined uncertainty (k = 1):				0,00395

20 dB Attenuator S_{21} at 9 GHz

Quantity	Standard Uncertainty Phase[$u(x_i)$] [Degrees]	Probability Distribution	Sensitivity Coefficient c_i	Uncertainty contribution Phase[$c_i u(x_i)$] [Degrees]
Magnitude of transmission coefficient	0,026	Gaussian	1	0,026
Thermal coefficient in phase	0,115	Rectangular	1	0,115
Uncertainty in phase standard	0,004	Gaussian	1	0,004
Stability of the cable	0,260	Rectangular	1	0,260
Repeat measurements	0,022	Gaussian	1	0,022
Phase combined uncertainty (k = 1):				0,286
Real component combined uncertainty (k = 1):				0,00036
Imaginary component combined uncertainty (k = 1):				0,00036

20 dB Attenuator S_{21} at 9 GHz

Quantity	Standard Uncertainty Mag[$u(x_i)$] [dB]	Probability Distribution	Sensitivity Coefficient c_i	Uncertainty contribution Mag[$c_i u(x_i)$] [dB]
Linearity	0.0001848 dB/dB	Rectangular	20,11	0,003716
Mismatch calculated	0,0022239	U-shaped	1	0,002224
Cross-talk	0,0004032	Rectangular	1	0,000403
Transmission Tracking	0,0037161	Rectangular	1	0,003716
System Repeatability	0,0098988	Gaussian	1	0,009899
Connector Repeatability	0,0006047	Gaussian	1	0,000605
Cable flexure	0,0017321	Rectangular	1	0,001732
Ambient Conditions	0,0034641	Rectangular	1	0,003464
Repeat measurements	0,0007994	Gaussian	1	0,000799
Magnitude combined uncertainty (k = 1):				0,01211

20 dB Attenuator S_{21} at 18 GHz

Quantity	Standard Uncertainty Phase[$u(x_i)$] [Degrees]	Probability Distribution	Sensitivity Coefficient c_i	Uncertainty contribution Phase[$c_i u(x_i)$] [Degrees]
Magnitude of transmission coefficient	0,080	Gaussian	1	0,080
Thermal coefficient in phase	0,115	Rectangular	1	0,115
Uncertainty in phase standard	0,009	Gaussian	1	0,009
Stability of the cable	0,520	Rectangular	1	0,520
Repeat measurements	0,055	Gaussian	1	0,055
Phase combined uncertainty (k = 1):				0,541
Real component combined uncertainty (k = 1):				0,00085
Imaginary component combined uncertainty (k = 1):				0,00041

20 dB Attenuator S_{21} at 18 GHz

B.5 NPLI Uncertainty Budgets

Both in reflection and transmission s-parameters measurement, the real and imaginary components are considered to have the same uncertainty $u(re(s_{ab})) = u(im(s_{ab}))$.

B.5.1 Reflection measurements

Contribution	Estimate	Uncertainty	Distribution	Divisor	Std. Unc.
Effective Dir.	0,004687	0,004687	U	1,414	
Eff.TPmtch	0,0312	1,16E-06	U	1,414	
Sum Corr.Qnt.		0,004688	U	1,414	0,003316
Tracking	0,001588	9,68E-06	R	1,732	5,59E-06
Linearity	3,62E-05	2,21E-07	R	1,732	1,27E-07
System Rep	0,000348	2,12E-06	G	2	1,06E-06
Cable fix	0,000323	1,97E-06	G	2	9,84E-07
Amb.condn	0,002	1,22E-05	R	1,732	7,04E-06
Conn. Rep.	0,000927	0,000927	t	3,16	0,000293
C.S.Unc.					0,003329

Matched load at 2 GHz

Contribution	Estimate	Uncertainty	Distribution	Divisor	Std. Unc.
Effective Dir.	0,007732	0,007732	U	1,414	
Eff.TPmtch	0,0329	2,37E-05	U	1,414	
Sum Corr.Qnt.		0,007756	U	1,414	0,005485
Tracking	0,008214	0,000221	R	1,732	0,000127
Linearity	4,52E-05	1,21E-06	R	1,732	7E-07
System Rep	0,000195	5,23E-06	G	2	2,61E-06
Cable fix	0,000395	1,06E-05	G	2	5,3E-06
Amb.condn	0,002	5,37E-05	R	1,732	3,1E-05
Conn. Rep.	0,001519	0,001519	t	3,16	0,000481
C.S.Unc.					0,005508

Matched load at 9 GHz

Contribution	Estimate	Uncertainty	Distribution	Divisor	Std. Unc.
Effective Dir.	0,008164	0,008164	U	1,414	
Eff.TPmtch	0,0435	0,000197	U	1,414	
Sum Corr.Qnt.		0,008361	U	1,414	0,005913
Tracking	0,00279	0,000188	R	1,732	0,000108
Linearity	5,41E-05	3,64E-06	R	1,732	2,1E-06
System Rep	0,001589	0,000107	G	2	5,35E-05
Cable fix	0,001473	9,91E-05	G	2	4,96E-05
Amb.condn	0,002	0,000135	R	1,732	7,77E-05
Conn. Rep.	0,003322	0,003322	t	3,16	0,001051
C.S.Unc.					0,006008

Matched load at 18 GHz

Contribution	Estimate	Uncertainty	Distribution	Divisor	Std. Unc.
Effective Dir.	0,004687	0,004687	U	1,414	
Eff.TPmtch	0,0312	0,003506325	U	1,414	
Sum Corr.Qnt.		0,008193325	U	1,414	0,0057944
Tracking	0,001587703	0,000532253	R	1,732	0,0003073
Linearity	0,000727304	0,000243817	R	1,732	0,0001408
System Rep	0,000348341	0,000116776	G	2	5,839E-05
Cable fix	0,000322723	0,000108188	G	2	5,409E-05
Amb.condn	0,002	0,000670469	R	1,732	0,0003871
Conn. Rep.	0,000683317	0,000683317	t	3,16	0,0002162
C.S.Unc.					0,0058217

Mismatched load at 2 GHz

Contribution	Estimate	Uncertainty	Distribution	Divisor	Std. Unc.
Effective Dir.	0,007732	0,007732	U	1,414	
Eff.TPmtch	0,0329	0,004433728	U	1,414	
Sum Corr.Qnt.		0,012165728	U	1,414	0,0086038
Tracking	0,008213906	0,00301534	R	1,732	0,001741
Linearity	0,000908868	0,000333647	R	1,732	0,0001926
System Rep	0,000194736	7,14879E-05	G	2	3,574E-05
Cable fix	0,00039492	0,000144976	G	2	7,249E-05
Amb.condn	0,002	0,000734204	R	1,732	0,0004239
Conn. Rep.	0,001667015	0,001667015	t	3,16	0,0005275
C.S.Unc.					0,0088067

Mismatched load at 9 GHz

Contribution	Estimate	Uncertainty	Distribution	Divisor	Std. Unc.
Effective Dir.	0,008164	0,008164	U	1,414	
Eff.TPmtch	0,0435	0,004196884	U	1,414	
Sum Corr.Qnt.		0,012360884	U	1,414	0,0087418
Tracking	0,002789687	0,000866511	R	1,732	0,0005003
Linearity	0,001090328	0,000338669	R	1,732	0,0001955
System Rep	0,001588579	0,000493432	G	2	0,0002467
Cable fix	0,001472931	0,000457511	G	2	0,0002288
Amb.condn	0,002	0,000621225	R	1,732	0,0003587
Conn. Rep.	0,002468228	0,002468228	t	3,16	0,0007811
C.S.Unc.					0,0088068

Mismatched load at 18 GHz

B.5.2 Transmission measurements

Contribution	Estimate	Uncertainty	Distribution	Divisor	Std. Unc.
Linearity	0,000459	0,000459	G	2	0,00023
TPmtch(M*S11)	0,032305	0,001064			
LDmtch(GAMA-L*S22)	0,00631	0,000206			
TP_LM(M*GAMA-L)	0,000204	0,000204			
Mmtch		0,001372	U	1,414	0,00097
CrossTlk	3,16E-06	3,16E-06	R	1,732	1,83E-06
System Rep	0,000184	0,000184	G	2	9,21E-05
Noise	4,08E-05	4,08E-05	G	2	2,04E-05
Cable fix	0,0003	0,0003	G	2	0,00015
Amb.condn	0,000244	0,000244	R	1,732	0,000141
Conn. Rep.	0,002072	0,002072	t	3,16	0,000656
C.S.Unc.					0,001215

3 dB Attenuator S_{21} at 2 GHz

Contribution	Estimate	Uncertainty	Distribution	Divisor	Std. Unc.
Linearity	0,000574	0,000574	G	2	0,000287
TPmtch(M*S11)	0,033951	0,001828			
LDmtch(GAMA-L*S22)	0,007943	0,000421			
TP_LM(M*GAMA-L)	0,00027	0,00027			
Mmtch		0,002388	U	1,414	0,001689
CrossTlk	4,47E-06	4,47E-06	R	1,732	2,58E-06
System Rep	0,001557	0,001557	G	2	0,000778
Noise	4,08E-05	4,08E-05	G	2	2,04E-05
Cable fix	0,0003	0,0003	G	2	0,00015
Amb.condn	0,000244	0,000244	R	1,732	0,000141
Conn. Rep.	0,004255	0,004255	t	3,16	0,001346
C.S.Unc.					0,002323

3 dB Attenuator S_{21} at 9 GHz

Contribution	Estimate	Uncertainty	Distribution	Divisor	Std. Unc.
Linearity	0,000688	0,000688	G	2	0,000344
TPmtch(M*S11)	0,052631	0,003062			
LDmtch(GAMA-L*S22)	0,009772	0,001127			
TP_LM(M*GAMA-L)	0,000526	0,000526			
Mmtch		0,004461	U	1,414	0,003155
CrossTlk	5,62E-06	5,62E-06	R	1,732	3,25E-06
System Rep	0,001109	0,001109	G	2	0,000554
Noise	4,08E-05	4,08E-05	G	2	2,04E-05
Cable fix	0,0003	0,0003	G	2	0,00015
Amb.condn	0,000244	0,000244	R	1,732	0,000141
Conn. Rep.	0,004447	0,004447	t	3,16	0,001407
C.S.Unc.					0,003522

3 dB Attenuator S_{21} at 18 GHz

Contribution	Estimate	Uncertainty	Distribution	Divisor	Std. Unc.
Linearity	0,000196	0,000196	G	2	0,000098
TPmtch(M*S11)	0,032305	0,000288			
LDmtch(GAMA-L*S22)	0,00631	3,9E-05			
TP_LM(M*GAMA-L)	0,000204	0,000204			
Mmtch		0,00033	U	1,414	0,000233
CrossTlk	2,24E-05	2,24E-05	R	1,732	1,29E-05
System Rep	0,000184	0,000184	G	2	9,21E-05
Noise	5,75E-05	5,75E-05	G	2	2,88E-05
Cable fix	0,0003	0,0003	G	2	0,00015
Amb.condn	3,45E-05	3,45E-05	R	1,732	1,99E-05
Conn. Rep.	0,000623	0,000623	t	3,16	0,000197
C.S.Unc.					0,000368

20 dB Attenuator S_{21} at 2 GHz

Contribution	Estimate	Uncertainty	Distribution	Divisor	Std. Unc.
Linearity	0,00023	0,00023	G	2	0,000115
TPmtch(M*S11)	0,033951	0,000472			
LDmtch(GAMA-L*S22)	0,007943	0,000136			
TP_LM(M*GAMA-L)	0,00027	0,00027			
Mmtch		0,00061	U	1,414	0,000432
CrossTlk	3,16E-05	3,16E-05	R	1,732	1,83E-05
System Rep	0,001557	0,001557	G	2	0,000778
Noise	5,75E-05	5,75E-05	G	2	2,88E-05
Cable fix	0,0003	0,0003	G	2	0,00015
Amb.condn	3,45E-05	3,45E-05	R	1,732	1,99E-05
Conn. Rep.	0,00113	0,00113	t	3,16	0,000358
C.S.Unc.					0,000979

20 dB Attenuator S_{21} at 9 GHz

Contribution	Estimate	Uncertainty	Distribution	Divisor	Std. Unc.
Linearity	0,000264	0,000264	G	2	0,000132
TPmtch(M*S11)	0,052631	0,004805			
LDmtch(GAMA-L*S22)	0,009772	0,000419			
TP_LM(M*GAMA-L)	0,000514	0,000514			
Mmtch		0,005234	G	1,414	0,003702
CrossTlk	3,98E-05	3,98E-05	R	1,732	2,3E-05
System Rep	0,001109	0,001109	G	2	0,000554
Noise	5,75E-05	5,75E-05	G	2	2,88E-05
Cable fix	0,0003	0,0003	G	2	0,00015
Amb.condn	3,45E-05	3,45E-05	R	1,732	1,99E-05
Conn. Rep.	0,001314	0,001314	t	3,16	0,000416
C.S.Unc.					0,003771

20 dB Attenuator S_{21} at 18 GHz

Annex C: Participants reports

C.1 INTI Report

Previous check

The traveling standards pin-depth were measured and connectors were carefully inspected to ensure a good mechanical condition.

Hardware

The measurements were performed using a Rohde & Schwarz ZVK Vector Network Analyzer which covers a frequency range up to 40 GHz.

A 12-term model was solved to find the error terms of the VNA based setup. The calibration of the VNA was performed with the SOLT method. An Agilent 85054B calibration kit was used for high reflection calibration standards and a R&S ZV-Z21 calibration kit for low reflection calibration standards. Both kits have Type-N connectors. In addition, 2 Type-N sliding loads from Maury up to 18 GHz were used.

Measurements

The measured values were error corrected with the VNA firmware. In addition, all the raw data were taken from the VNA and processed with a software implemented by INTI, which gave the same results.

Reported results are obtained as the mean of ten measurements, performing a new calibration of the VNA among them. The mean value includes both system and connector repeatability. After calibration, a set of verification devices traced to PTB were measured to verify the calibration accuracy.

According to the technical protocol, the S-parameters of each device in the real and imaginary form with its associated combined uncertainty were reported.

The ambient laboratory temperature during the measurements was $(23 \pm 1)^\circ\text{C}$.

Uncertainty and traceability

Uncertainties of S-parameters were calculated assuming equal real and imaginary components.

The uncertainties of the VNA were calculated based on EURAMET cg-12 [14].

The SOLT method uses definitions of the standards obtained by a TRL method which has better uncertainties.

Our traceability in S-parameters depends on dimensional characteristics of a set of coaxial air lines. Our air lines were measured at the Dimensional Metrology Laboratory at INTI to obtain traceability to the SI base unit of length (m).

Linearity of the system was measured with a step attenuator calibrated by INTI at 1 GHz.

C.2 NIST Report

We used a commercial vector network analyzer (VNA) for the measurements. We calibrated the VNA using our own multical LRL software which utilizes multiple airline standards (we used 5) to give the best possible combination of airlines at each frequency. The calibration was verified with in-house check standards. We then measured the devices using a pattern for one-ports of three connects on port #1 and three connects on port #2. The final result for each device is an average of all connects. For two-ports, we made three connects in the “forward” direction, reversed the device and made three more connects. The final results for the two-port S-parameters are the averages of all connects accounting for forward and reverse directions.

C.3 NRC Report

METHOD

The measurement was performed on a PNA Agilent model E8364C (10 MHz to 50 GHz) network analyzer. This instrument has two (2.4 mm) ports on the front panel. This instrument is a regular production unit that has NO special option such as extended dynamic range or extra power amplifier etc... However, it is equipped with external loop cables, allowing the replacement of the couplers by external ones. No computer was attached to the instrument and the instrument firmware was used for the zeroing and measurement.

The zeroing standards are taken from a HP calibration kit model 85054D plus some other standards. This kit is a regular production unit with no special option. No sliding load was available to perform this measurement. Instead we used a set of air-lines from Maury Microwave. The lines are 3 cm, 4.28 cm, 5 cm, and 7.5 cm. These zeroing standards are currently used in our laboratory.

Several zeroing/measurement cycles were performed in different configuration/operating conditions. The reason for doing this was that we wanted to ensure that the results are reproducible, and that no obvious “mistake” was done. We did not use any “check/verification standards”, such as a previously measured attenuator of the same type, in order to check or correct our results. However we performed the obvious tests such as checking the phase of a short, the insertion loss of the THRU, etc.

Although we performed many zeroing/measurement cycles, we did not average or modify the output results from the network analyzer.

C.4 CENAM Report

CENAM (México) Measurements

1. Measurements method

The measurements were performed on a commercial Vector Network Analyzer (VNA). The VNA used for this set of measurements was an Agilent E8363C. The calibration of the VNA was performed with the TRL method using precision coaxial airlines and with the SOLT method using a Hewlett Packard 85054B calibration kit.

As it is known, the TRL method consists of three fundamental measurement steps:

- 1.- THRU- A standard transmission line is inserted between test port 1 and test port 2 of the network analyzer. The Thru used is a 5 cm airline.
- 2.- REFLECT- One-port and high reflective identical devices are connected to each of the two test ports of the network analyzer.
- 2.- LINE- Two standard transmission lines are inserted between test port 1 and test port 2 of the network analyzer, with a different length to that used in the THRU connection. One of the airlines used has 6 cm of length and the other has 7.5 cm of length.

The SOLT method (Short-Open-Load-Thru) requires a 50Ω Load, the ones used are a lowband load up to 2 GHz and a sliding load for higher frequencies.

2. Traceability

The set of beadless precision air-lines in Type-N connector used are measured dimensionally, traceable to the SI base unit of length (m) realized at CENAM. The electrical characteristics of the transmission lines are calculated from the physical dimensions. The precision air-lines are used as primary calculable standards.

The coaxial terminations from the 85054B calibration kit were characterized prior by means of a TRL method. The calibration coefficients of the sets of coaxial terminations are obtained from the reflection coefficient measurements and whose values are applied automatically in the Vector Network Analyzer. The coaxial terminations are used as working standards.

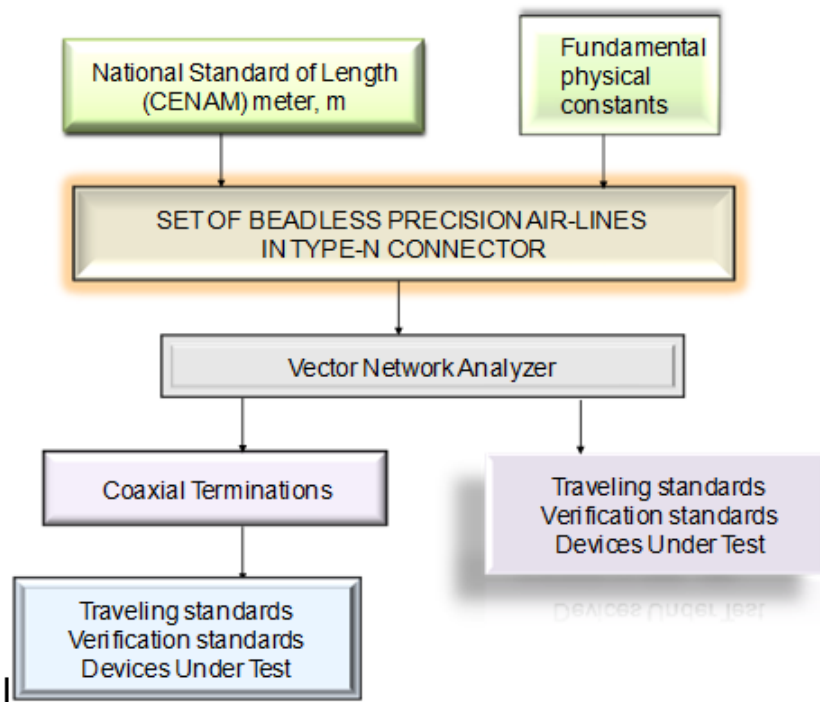


Figure 1. Structure of traceability

3. Measurements

The measurements were performed using a VNA system, the setup and configuration is summarized in the following tables:

Type of VNA:	E8363C
Type of calibration kit:	Reference airline kit –precision N 85054B Type N Calibration kit
Method of VNA calibration:	TRL, Short-Open-Load/Sliding load-Thru (two ports measurements), Short-Open-Load/Sliding load (one port measurements)
Sweep type:	Frequency list From 2 GHz to 18 GHz in step of 1 GHz
Averaging Factor:	20
IF Bandwidth:	10 Hz
Power level:	-17 dBm
Other:	<ul style="list-style-type: none"> • Adapter NMD 2.4 mm (female) to Type N (male), Manufacturer: MMC • Adapter NMD 2.4 mm (female) to Type N (female), Manufacturer: MMC • Test Port Cable 8946C25, Manufacturer: Maury Microwave

Table 1. VNA measurement system at CENAM

<p>One port measurement setup</p> <p>Note: The one port devices with male connectors were connected to port 2 of the Vector Network Analyzer and an S22 measurement carried out , this is equivalent to measuring S11.</p>	<p>A test port adapter NMD 2.4 mm to Type N (female) was connected to port 2 of the VNA.</p> <p>The VNA was calibrated with this configuration using the TRL method. After that, the Matched load and Mismatched load were measured. These measurements were repeated to get 5 sets of measurements for each frequency and for each device. The standard was disconnected, rotated by about 120° and reconnected for each measurement. The VNA was re-calibrated, the standard was disconnected, rotated by about 180° and reconnected.</p> <p>The VNA was calibrated using SOL (Short-Open-Load/Load sliding) method. After the calibration, the measurements of reflection coefficient were performed. These measurements were repeated to get 4 sets of measurements at each frequency for each device. The standard was disconnected, rotated by about 180° and reconnected for each measurement. The VNA was re-calibrated, the standard was disconnected, rotated by about 180° and reconnected.</p>
<p>Two port measurement setup</p>	<p>A single test port cable was connected to port 1 of VNA and on the other end a test port adapter NMD 2.4 mm to Type N (male) was connected.</p> <p>A test port adapter NMD 2.4 mm to Type N (female) is connected to port 2 of VNA.</p> <p>The VNA was calibrated with this configuration using the TRL method. After the calibration, the S-parameters of the 3 dB and 20 dB attenuators were measured. The S-parameters measurements were repeated to get a total of 6 sets data for each frequency and for each attenuator. The standard was disconnected, rotated by about 120° and reconnected for each measurement. The VNA was re-calibrated, the standard was disconnected, rotated by about 120° and reconnected.</p> <p>The VNA was calibrated using SOLT (Short-Open-Load/Load sliding-Thru) method. After the calibration the attenuators were measured. These measurements were repeated to get 4 sets of measurements for each frequency and for each device. The standard was disconnected, rotated by about 180° and reconnected for each measurement. The VNA was re-calibrated, the standard was disconnected, rotated by about 180° and reconnected.</p>
<p>DUT orientation:</p>	<p>Port 1 Type-N (male) Port 2 Type-N (female)</p>

Table 2. VNA measurement setup at CENAM

Laboratory temperature	23 °C with variations not larger than ± 1 °C
Laboratory relative humidity	35 % with variations not larger than ± 15 %

Table 4. Environment conditions at CENAM

4. Measurement Uncertainties

The Type B uncertainty for the reflection coefficient measurements for one port devices, U_{VRC1_port} , has been calculated using the following formula:

$$U_{VRC1_port} = \sqrt{\frac{(D + M\Gamma)^2}{2} + \frac{(T\Gamma)^2}{3} + \frac{(L\Gamma)^2}{3} + \frac{(A)^2}{3} + \frac{(R_{VRC})^2}{3}} \quad (1)$$

where:

D Effective directivity of VNA

M Effective source match of VNA

T Effective reflection tracking of VNA

L System derivation from linearity

A Airline reflection

R_{VRC} represents all the Random contributions: system repeatability, connector repeatability, effects of ambient conditions.

Γ Magnitude of the reflection coefficient of the 1-port DUT

The Type B uncertainty on U_{VRC2_port} reflection coefficient for two port devices has been calculated using the formula:

$$U_{VRC2_port} = \sqrt{\frac{(D + M\Gamma)^2}{2} + \frac{(T\Gamma)^2}{3} + \frac{(L\Gamma)^2}{3} + \frac{(A)^2}{3} + \frac{(\Gamma_L S_{21}^2)^2}{2} + \frac{(2\Gamma M \Gamma_L S_{21}^2)^2}{2} + \frac{(R_{VRC})^2}{3}} \quad (2)$$

where:

Γ_L Effective load match

S_{21} Magnitude of the forward transmission coefficient of the two port device under calibration

R_{VRC} represents all the Random contributions: system repeatability, connector repeatability, effects of ambient conditions and effects of the cable flexure.

For the transmission measurements uncertainty:

$$U_{TM} = \sqrt{\frac{(LS_{21})^2}{3} + \frac{(I)^2}{3} + \frac{(T_{TM})^2}{3} + \frac{(M_{TM})^2}{2} + \frac{(R_{dB})^2}{3}} \quad (3)$$

where:

I is the estimated/measured cross-talk

M_{TM} is the calculated error term due to mismatch

T_{TM} Effective transmission tracking of VNA

R_{dB} represents all the random contributions: system repeatability, connector repeatability, effects of ambient conditions and effects of the cable flexure.

The Type A uncertainty is the dispersion of the experimental data. Therefore, the combined uncertainty U_c has been calculated as square sum between Type B and Type A

The combined uncertainty for the phase of reflection coefficient measurements of one port devices has been evaluated with the following equation:

$$u(\arg(\Gamma)) = \sqrt{\frac{\left(\arcsin\left(\frac{U_{c\Gamma}}{|\Gamma|}\right) \times \frac{180}{\pi}\right)^2}{1} + \frac{(CT_{\text{phase}})^2}{3} + \frac{(R_{\text{phase}})^2}{n}} \quad (4)$$

where:

$U_{c\Gamma}$ combined uncertainty on reflection coefficient for one port devices

CT_{phase} Thermal coefficient in phase

R_{phase} repeat measurements in phase

n number of measurements

The combined uncertainty for the phase of reflection coefficient measurements of two port devices has been evaluated with the following equation:

$$u(\arg(S_{11})) = \sqrt{\frac{\left(\arcsin\left(\frac{U_{cS_{11}}}{|S_{11}|}\right) \times \frac{180}{\pi}\right)^2}{1} + \frac{(CT_{\text{phase}})^2}{3} + \frac{(\text{Cable})^2}{3} + \frac{(R_{\text{phase}})^2}{n}} \quad (5)$$

where:

$U_{cS_{11}}$ combined uncertainty on reflection coefficient for two port devices

Cable represent the cable flexure

$$u(\arg(S_{21})) = \sqrt{\frac{\left(\arcsin\left(10^{\frac{U_{cdB}}{20}} - 1\right) \times \frac{180}{\pi}\right)^2}{1} + \frac{(CT_{\text{phase}})^2}{3} + \frac{(\text{Cable})^2}{3} + \frac{(R_{\text{phase}})^2}{n}} \quad (6)$$

where:

U_{cdB} combined uncertainty on transmission coefficient

The results are in magnitude and phase format. To evaluate the uncertainties in real and imaginary format the following method was used:

The vector of input quantities: $X = (r, \phi)$

The vector of output quantities: $Y = (r \cos \phi, r \sin \phi)$

Two transformations f_1 and f_2 are defined as:

$$\begin{aligned} f_1(r, \phi) &= r \cos \phi \\ f_2(r, \phi) &= r \sin \phi \end{aligned}$$

The Jacobian matrix of the transformations is:

$$J = \begin{bmatrix} \frac{\partial f_1}{\partial r} & \frac{\partial f_1}{\partial \phi} \\ \frac{\partial f_2}{\partial r} & \frac{\partial f_2}{\partial \phi} \end{bmatrix}$$

where:

$$\frac{\partial f_1}{\partial r} = \cos \phi \quad \frac{\partial f_1}{\partial \phi} = -r \sin \phi \quad \frac{\partial f_2}{\partial r} = \sin \phi \quad \frac{\partial f_2}{\partial \phi} = r \cos \phi$$

In matrix form, the law of propagation of uncertainty states that:

$$J = \begin{bmatrix} \cos \phi & -r \sin \phi \\ \sin \phi & r \cos \phi \end{bmatrix}$$

Where $V(X)$ is the covariance matrix of the input and $V(Y)$ is the covariance matrix of the output

$$V(X) = \begin{bmatrix} u^2(x_1) & u(x_1, x_2) \\ u(x_2, x_1) & u^2(x_2) \end{bmatrix}$$

$u(x_1)$ is the uncertainty in magnitude

$u(x_2)$ is the uncertainty in phase

$u(x_1, x_2) = u(x_1) u(x_2) r(x_1, x_2)$

$r(x_1, x_2)$ is the correlation coefficient

The covariance matrix of the output has been calculated as follows:

$$V(Y) = \begin{bmatrix} u^2(y_1) & u(y_1, y_2) \\ u(y_2, y_1) & u^2(y_2) \end{bmatrix}$$

$$V(Y) = \begin{bmatrix} \cos \phi & -r \sin \phi \\ \sin \phi & r \cos \phi \end{bmatrix} \begin{bmatrix} u^2(x_1) & u(x_1, x_2) \\ u(x_2, x_1) & u^2(x_2) \end{bmatrix} \begin{bmatrix} \cos \phi & \sin \phi \\ -r \sin \phi & r \cos \phi \end{bmatrix}$$

where:

$$u^2(y_1) = \cos \phi [(\cos \phi)(u^2(x_1)) + (-r \sin \phi)(u(x_2, x_1))] - r \sin \phi [(\cos \phi)(u(x_1, x_2)) + (-r \sin \phi)(u^2(x_2))]$$

$$u^2(y_2) = \sin \phi [(\sin \phi)(u^2(x_1)) + (r \cos \phi)(u(x_2, x_1))] + r \cos \phi [(\sin \phi)(u(x_1, x_2)) + (r \cos \phi)(u^2(x_2))]$$

$$u(y_1, y_2) = \sin \phi [(\cos \phi)(u^2(x_1)) + (-r \sin \phi)(u(x_2, x_1))] + r \cos \phi [(\cos \phi)(u(x_1, x_2)) + (-r \sin \phi)(u^2(x_2))]$$

$$u(y_2, y_1) = \cos \phi [(\sin \phi)(u^2(x_1)) + (r \cos \phi)(u(x_2, x_1))] - r \sin \phi [(\sin \phi)(u(x_1, x_2)) + (r \cos \phi)(u^2(x_2))]$$

$u(y_1)$ is the uncertainty of real part

$u(y_2)$ is the uncertainty of imaginary part

The correlation coefficient of the output variables has been calculated using the following formula:

$$r(y_1, y_2) = \frac{u(y_1, y_2)}{u(y_1) \times u(y_2)}$$

C.5 NPLI Report

Scattering Coefficients by Broad-Band Methods

SIM.EM.RF-K5b.CL

NPLI(India) Measurements

Environmental conditions:

Temperature: $(23 \pm 1)^\circ\text{C}$

Relative Humidity: $(50 \pm 10) \% \text{RH}$

Measurement description:

The traveling standards received for the comparison were checked for their pin depths. The S-parameters of the traveling standards have been measured using a Vector Network Analyser (WILTRON VNA 37247B) System, which has been calibrated using a Type N Calibration kit, Model no.3653 and the precision coaxial airline for full 12-term, 1601 data points. The calibration method used was the SOLT one in Type-N connector for the desired 17 frequencies points from 2 to 18 GHz. The respective S-parameters of one port and two port components have been recorded in the real and imaginary form, $S_{ab} = x + jy$. The S-parameters of each traveling standard have been measured ten times by connect-disconnect at the desired frequencies points. The mean value of the real and imaginary components of S-parameter has been reported for each standard. The combined standard uncertainty for the real and imaginary components i.e. $u(x)$ and $u(y)$ and the correlation coefficient $r(x, y)$ have been calculated and reported accordingly [1, 2 & 3].

Traceability route:

The S parameter measurement (S_{21}/S_{12}) is traceable to the 30 MHz WBCO attenuator of NPL India through transfer standard coaxial attenuators and (S_{11}/S_{22}) measurement is traceable to the Dimension metrology at NPL India through transfer standards coaxial airlines and calibration kit components.

References:

1. "Guidelines on the Evaluation of Vector Network Analyzers(VNA)", Calibration Guide Euramet cg-12 Version 2.0 (03/2011).
2. N.M.Ridler and M.J.Salter, "An approach to the treatment of uncertainty in complex S-parameter measurements", Metrologia, 2002, 39, pp 295-302.
3. Song Meng and Yueyan Shan, "Measurement uncertainty of complex valued microwave quantities", Progress in Electromagnetics Research, Vol. 136, 421-433, 2013.

Annex D: Pin Depth measurements

The following tables show the reported values of pin depth in the order they were measured.

Some participants reported the pin depth as a delta measurement together with the reference depth used to zero the connector gage. In one case, a different offset from the rest was used, so in order to compare the reported values, depths were converted to absolute values (pin depth definition) based on the reference depth provided by each laboratory which expressed the pin depth as a delta value.

Not all laboratories reported pin depth measurements.

Device: 3 dB Attenuator	Pin depth [mm] Male port	Pin depth [mm] Female port
INTI (1st measurement)	5,284	5,226
NIST	-	-
NRC	5,281	5,238
CENAM	5,284	5,229
INTI (1st control)	5,283	5,232
NPLI	5,292	5,238
INTI (2nd control)	5,283	5,239

Table 91: *Pin depth measurements - 3 dB Attenuator*

Device: 20 dB Attenuator	Pin depth [mm] Male port	Pin depth [mm] Female port
INTI (1st measurement)	5,284	5,232
NIST	-	-
NRC	5,288	5,238
CENAM	5,289	5,232
INTI (1st control)	5,290	5,239
NPLI	5,301	5,250
INTI (2nd control)	5,286	5,239

Table 92: *Pin depth measurements - 20 dB Attenuator*

Device: Matched Load	Pin depth [mm]
INTI (1st measurement)	5,273
NIST	-
NRC	5,270
CENAM	5,272
INTI (1st control)	5,271
NPLI	5,283
INTI (2nd control)	5,264

Table 93: *Pin depth measurements - Matched Load*

Device: Mismatched Load	Pin depth [mm]
INTI (1st measurement)	5,264
NIST	-
NRC	5,264
CENAM	5,266
INTI (1st control)	5,264
NPLI	5,276
INTI (2nd control)	5,264

Table 94: *Pin depth measurements - Mismatched Load*

Annex E: Electrical stability of standards

The following figures show the measurements of each device made by the pilot laboratory, along with the expanded uncertainty associated with the measurement, normalized to the mean value of the measurements obtained at the beginning and at two control measurements at the respective frequencies.

Each measurement is offset slightly in the figures for ease of viewing.

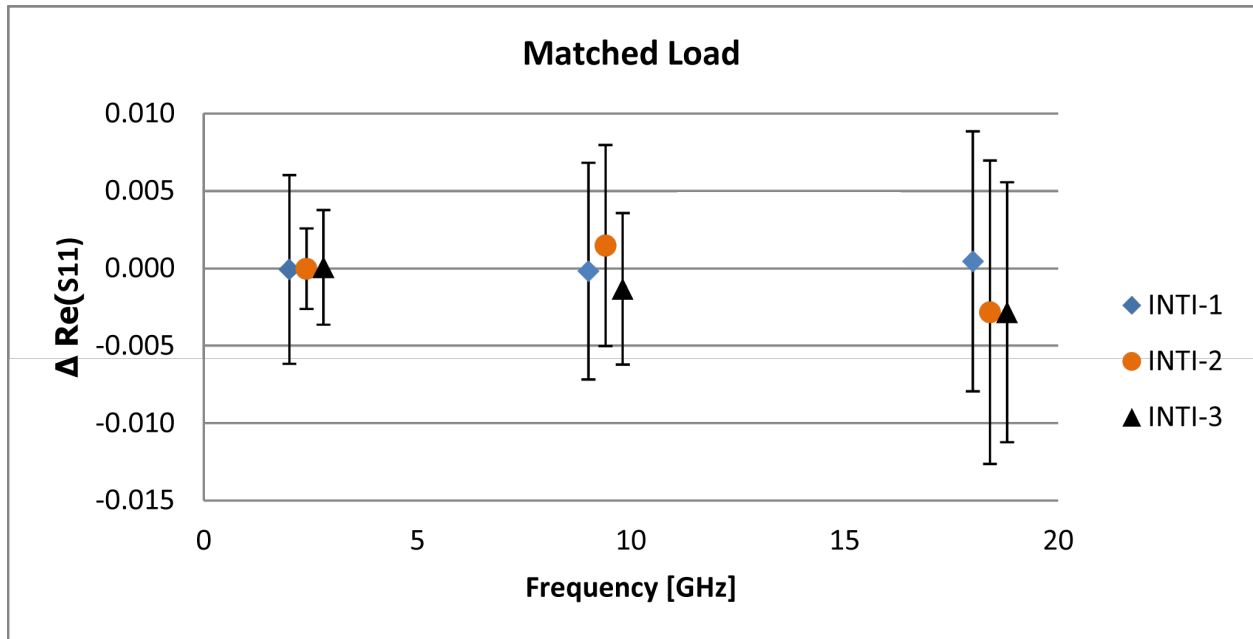


Figure 27: Matched Load. Real part of S_{11} measured at INTI.

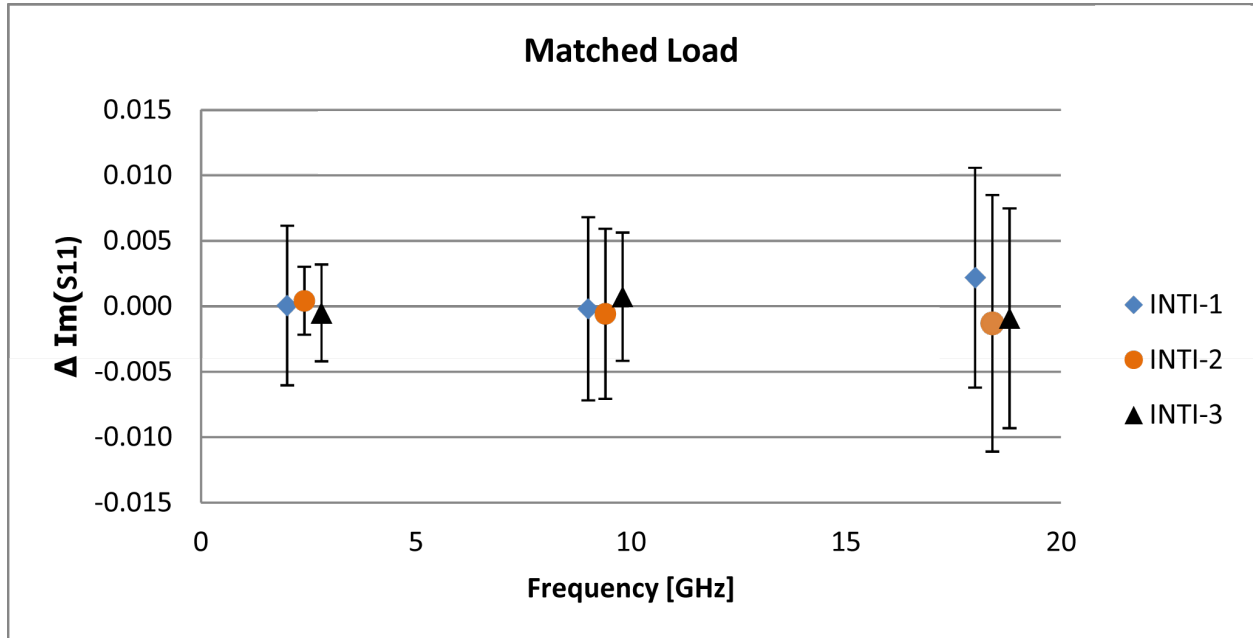


Figure 28: Matched Load. Imaginary part of S_{11} measured at INTI.

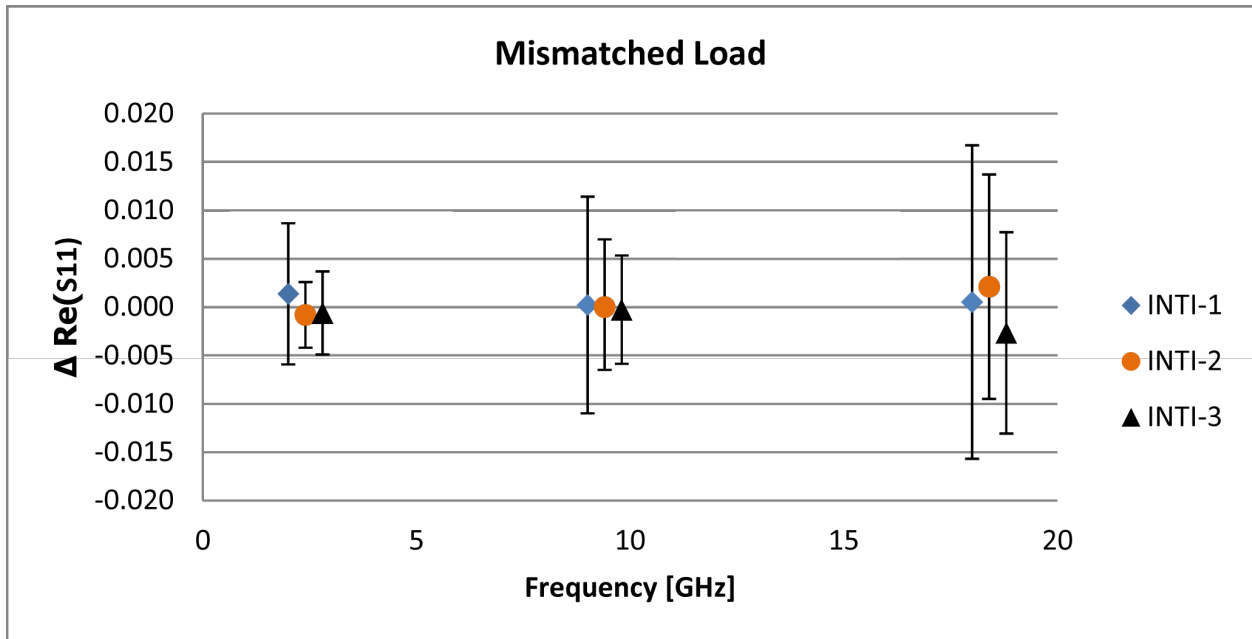


Figure 29: *Mismatched Load. Real part of S_{11} measured at INTI.*

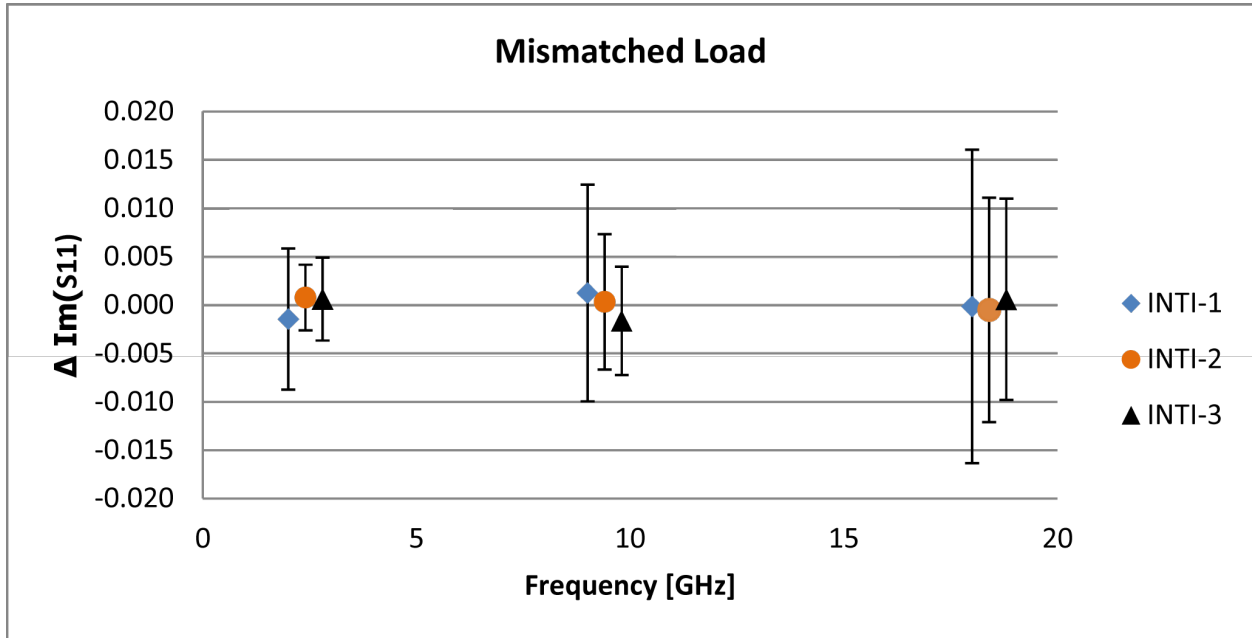


Figure 30: *Mismatched Load. Imaginary part of S_{11} measured at INTI.*

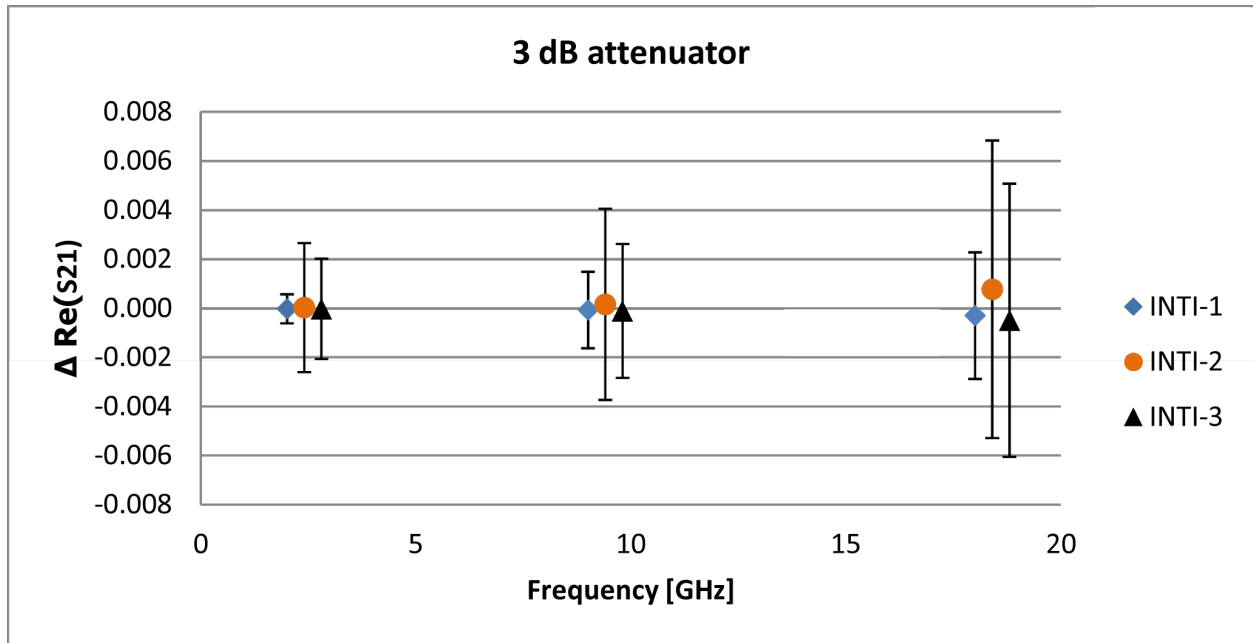


Figure 31: 3 dB attenuator. Real part of S_{21} measured at INTI.

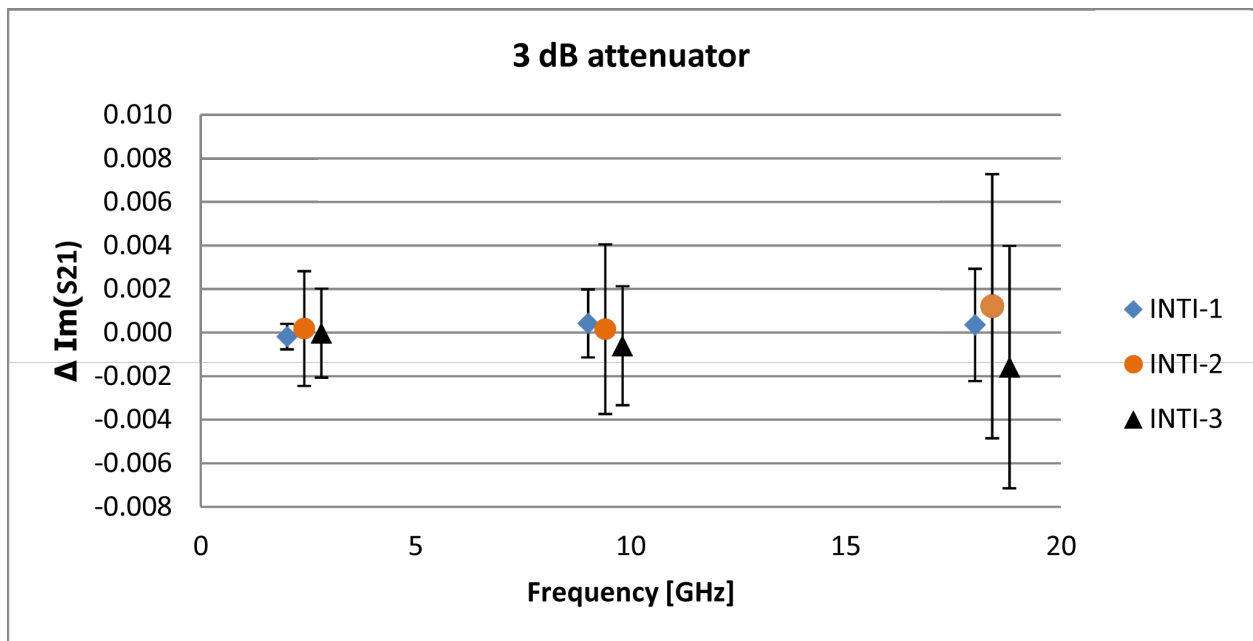


Figure 32: 3 dB attenuator. Imaginary part of S_{21} measured at INTI.

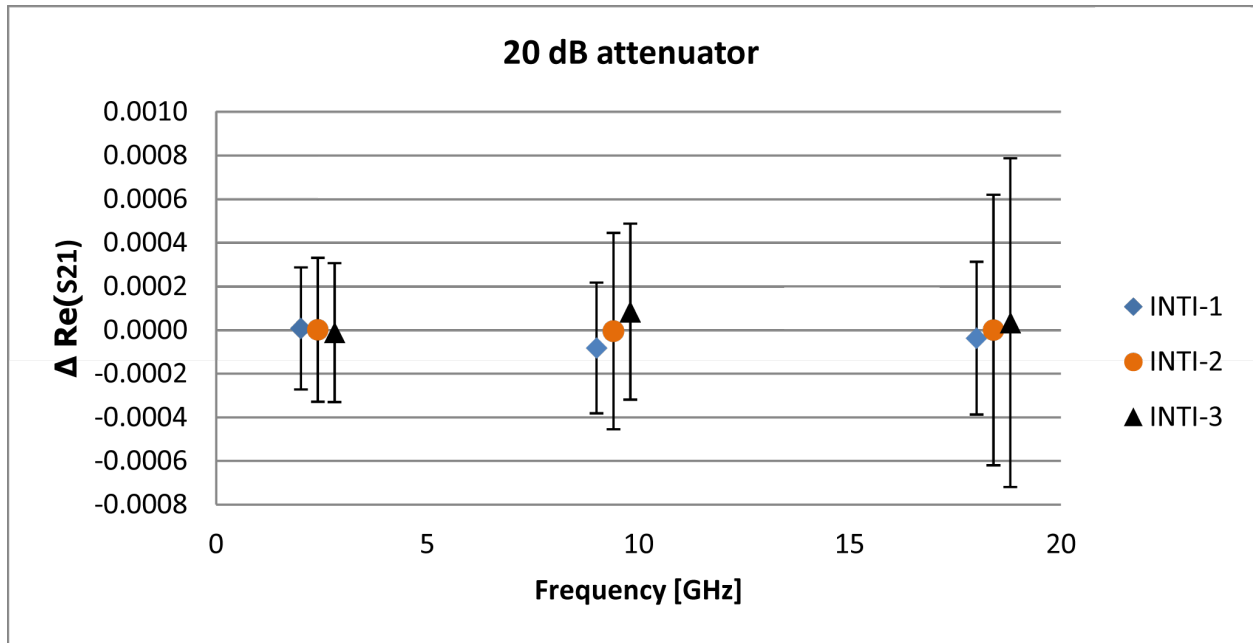


Figure 33: 20 dB attenuator. Real part of S_{21} measured at INTI.

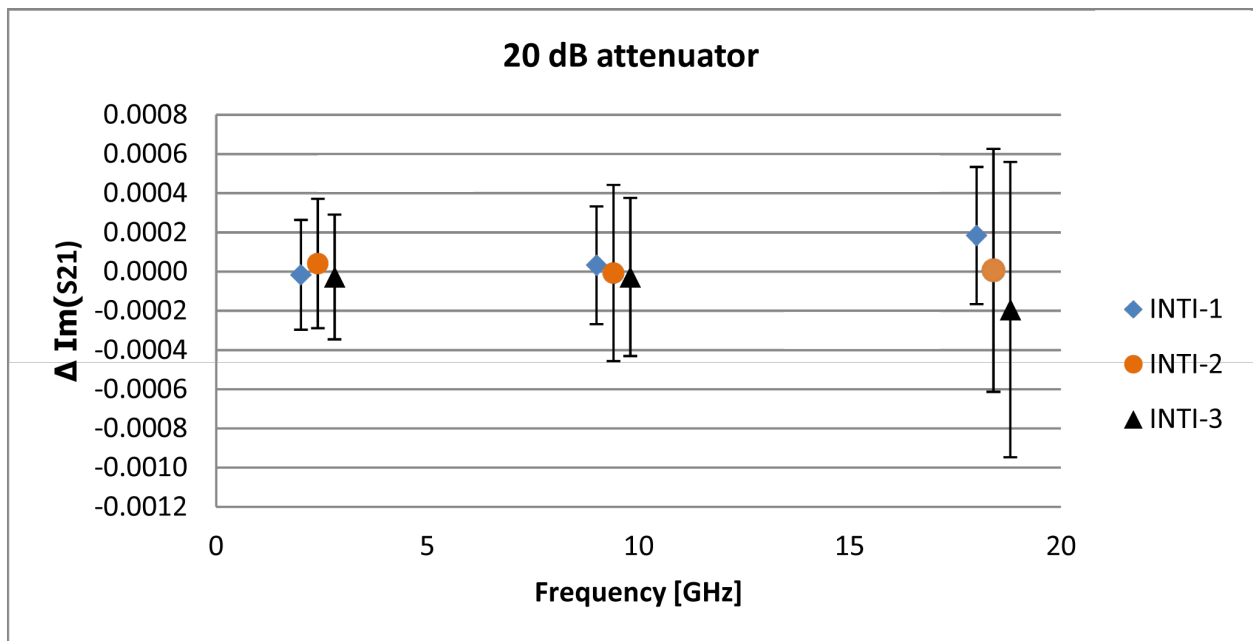


Figure 34: 20 dB attenuator. Imaginary part of S_{21} measured at INTI.